Kaunas University of Technology

Faculty of Mechanical Engineering and Design (MIDF)

Conceptual Design of a Blended Wing Body Aircraft for Urban Air Mobility Operation

Master's Final Degree Project

Sathvik Sathyanarayana Rao

Project author

Professor, doc. dr. Vaidas Lukoševičius
Supervisor

Kaunas, 2019

Kaunas University of Technology

Mechanical Engineering and Design

Conceptual Design of a Blended Wing Body Aircraft for Urban Air Mobility Operation

Master's Final Degree Project

Aeronautical Engineering (6211EX024)

Sathvik Sathyanarayana Rao

Project author

Professor, Vaidas Lukoševičius

Supervisor

Associate Professor, Robertas Keršys

Reviewer

Kaunas, 2019

Kaunas University of Technology

Faculty of Mechanical Engineering and Design

Sathvik Sathyanarayana Rao

Conceptual Design of a Blended Wing Body Aircraft for Urban Air Mobility operation

Declaration of Academic Integrity

I confirm that the final project of mine, Sathvik Sathyanarayana Rao, on the topic „Conceptual Design of a Blended Wing Body Aircraft for Urban Air Mobility Operation "is written completely by myself; all the provided data and research results are correct and have been obtained honestly. None of the parts of this thesis have been plagiarised from any printed, Internet-based or otherwise recorded sources. All direct and indirect quotations from external resources are indicated in the list of references. No monetary funds (unless required by Law) have been paid to anyone for any contribution to this project.

I fully and completely understand that any discovery of any manifestations/case/facts of dishonesty inevitably results in me incurring a penalty according to the procedure(s) effective at Kaunas University of Technology.

(name and surname filled in by hand) (signature)

Kaunas University of Technology

Faculty of Mechanical Engineering and Design

Study Programme – Aeronautical Engineering 6211EX024

Task Assignment for Final Degree Project of Master Studies

Student Sathvik *Sathyanarayana Rao*

1. Title of the Final Project:

Conceptual Design of a Blended Wing Aircraft for Urban Air Mobility Operation.

Vientisos sparno-liemens konstrukcijos orlaivio, skirto judėjimui mieste, koncepcijos kūrimas ir tyrimas

2. Aim of the Final Project:

The Aim of this project is to Design and Analyse the aerodynamics of Blended wing aircraft for the concept of Urban Air Mobility

3. Tasks of the Final Project:

a) Market research, Scope and Trade studies;
b) Understanding of General Aviation regulations;
c) Aircraft Initial Sizing;
d) Constrain analysis;
e) Aircraft geometric calculations;
f) Analysis of various aerofoils;
g) Initial Aircraft Analysis;
h) Aircraft CAD modelling and CFD;

4. Structure of the Text Part:

a) A brief study of UAM scope with Market analysis and GA regulation are presented
b) The project methodology is explained and trade off studies are analysed for best aerodynamic solution
c) The aircraft initial sizing and geometric parameters are calculated, and Required Aerofoils are analysed.
d) Initial aircraft aerodynamic analysis is carried out and later CAD model is designed for CFD analysis.
e) All the results and values obtained are analysed and concluded

5. Consultants of the Final Project:

-

Author of the Final Project Sathvik Sathyanarayana Rao,
(Name, Surname, Signature, date)

Supervisor of the Final Project Vaidas Lukoševičius,
(Name, Surname, Signature, date)

Head of Study Programme Janina Jablonskytė,
(Name, Surname, Signature, date)

RAO, Sathvik Sathyanarayana. Conceptual Design of a Blended Wing Body Aircraft for Urban Air Mobility operation. Professor doc. dr. Vaidas Lukoševičius; Faculty of Mechanical Engineering and Design, Kaunas University of Technology.

Study field and area (study field group): Aeronautical Engineering (E 14), Engineering Sciences.

Keywords: Urban Air mobility; Blended Wing Body; Constrain Diagram; XFLR5; Aircraft;

Kaunas, 2019. 81p.

Summary

The project is mainly focused on design of an aircraft for the purpose of urban air mobility which requires aircraft to take off from a small distance or vertically. The concept of urban air mobility is new in the aviation industry and a platform for advancements in modern aerodynamics. Since most of the concepts have already been under research and development, the blending wing aircrafts which are widely proposed for future of air transportation are being researched for large commercial aircrafts only. No research suggesting the use of Blended wing aircrafts for the general aviation was found in the literature. Also, most of the concepts for urban air mobility requires aircraft with numerous complex capabilities to meet the future requirements.

In this project a brief study of the market and scope for the UAM concept is investigated. Since the UAM concept is very new and no regulations have been formed by the aviation regulatory bodies, the project includes certification and regulation study as well. Since most of the design features of UAM concept studied in literature meet the GA requirements, the basic aircraft designed in this project is also a design for GA variant. The general aircraft design methodology is followed for this project. The main tasks of the conceptual design consist of aircraft initial sizing where the initial weight estimations, performance parameter estimations and other relevant requirements are calculated, studied and listed for performing constrain analysis.

In order to perform constrain analysis a constrain diagram is generated using MATLAB software which consists of a plot bearing thrust loading, wing loading, required lift coefficient and stall speeds. The data are analysed from this and then an optimum design point is used for further aircraft geometric calculations where all the dimensional parameters are finalised. In order to meet the requirements, various aerofoils have been analysed and selected for various cross section of the aircraft. Initial modelling and characteristic analysis of the aircraft is done in XFLR5 software. Finally, a CAD model for CFD purpose is modelled and analysed in Solidworks software. In the end, basic inner structure of the aircraft is modelled for UAM concept representation.

The results obtained from the sizing was successfully designed and analysed in various digital software. The aerodynamic characteristics of the designed aircraft had many advantages compare to the conventional configurations. The results obtained for the geometric calculations were aerodynamically stable and had high lift to drag ratio with low induced drag properties.

The designed aircraft was found to be aerodynamically stable and most efficient at cruise height of 1000m with a lift to drag ratio of 29.697 at 3 Degree AOA for a design Cruise speed of 81 m/s. The aircraft’s ability to generate most of the lift from centre body resulted in reduced wing loading on the outboard sections of the aircraft geometry.

RAO, Sathvik Sathyanarayana. Vientisos sparno-liemens konstrukcijos orlaivio, skirto judėjimui mieste, koncepcijos kūrimas ir tyrimas. Profesorius doc. dr. Vaidas Lukoševičius; Kauno technologijos universitetas, Mechanikos inžinerijos ir dizaino fakultetas.

Studijų kryptis ir sritis (studijų krypčių grupė): Aeronautikos inžinerija (E 14), Inžinerijos mokslai

Reikšminiai žodžiai: Miesto oro judumas; Apibūdinkite diagramą; XFLR5; Orlaiviai;

Kaunas, 2019. Puslapių sk. 81p.

Santrauka

Baigiamąjame darbe išnagrinėtas vientisos liemens-sparno orlaivio konceptualus projektavimas. Orlaivis bus eksploatuojamas miesto judumo tikslais. Miesto oro judumo koncepcija yra nauja aviacijos pramonėje. Kadangi dauguma idėjų jau buvo tiriamos ir plėtojamos ir šiuo metu pritaikomos dideliems komerciniams orlaiviams, vientisos liemens-sparno konstrukcijos orlaiviai siūlomi oro transporto ateičiai. Apžvelgus literatūrą, pasigęsta tyrimų, rodančių vientisos liemens-sparno konstrukcijos panaudojimą bendroje aviacijoje. Be to, daugumai miesto oro judėjimo koncepcijų reikia daugybės sudėtingų pajėgumų turinčių orlaivių, kurie atitiktų keliamus aukštus reikalavimus.

Darbe atlikta vientisos liemens-sparno konstrukcijos koncepcijos orlaivių rinkos apžvalga. Kadangi vientisos liemens-sparno konstrukcijos koncepcija labai nauja, aviacijos reglamantavimo institucijos nėra numačiusios taisykles, projektas apima sertifikavimo bei reguliavimo tyrimus. Konceptualiam projektui taikoma bendra orlaivių projektavimo metodika. Pagrindiniai koncepcinio projekto uždaviniai yra orlaivio dydis, apskaičiuoti, ištirti ir pirminiai masės parametrai, atlikta eksploatacinių parametrų analizė ir kiti atitinkami reikalavimai.

Siekiant atlikti orlaivio analizę, naudojantis MATLAB programine įranga, sukurta programa, įvertinanti sparno apkrovas, reikiamo kėlimo koeficientą ir stabdymo greitį. Išanalizuoti duomenys leidžia atlikti tolimesnius orlaivių geometrinius skaičiavimus. Taip pat, buvo išanalizuoti ir atrinkti įvairūs vientisos liemens-sparno konstrukcijos orlaivio skerspjūviai. Pradinis orlaivio modeliavimas ir aerodinaminės charakteristikos išanalizuotos XFLR5 programinės įrangos pagalba.

Suprojektuoto vientisos liemens-sparno konstrukcijos orlaivio aerodinaminės savybės daug pranašesnės, lyginant su įprastos konfigūracijos orlaiviais. Skaičiavimų rezultatai stabilūs aerodinaminiu požiūriu ir turi aukštą kėlimo ir pasipriešinimo jegų santykį. Sukurtas vientisos liemens-sparno konstrukcijos orlaivis aerodinaminiu požiūriu stabilus ir efektyviausias 1000 m skridimo aukštyje, apskaičiuotas kėlimo ir pasipriešinimo jėgos santykis 29,697, esant 3° laipsnių atakos kampui ir 81 m/s gričiui. Suprojektuotas vientisos liemens-sparno konstrukcijos orlaivis geba didžiausią kėlimo jėgos dalį generuoti liemens pagalba, tai sumažina sparno perkrovas orlaivio išorėje.

Table of Contents

List of Figures

List of Tables

List of abbreviations and terms

Abbreviations:

UAM – Urban Air Mobility;

BWB – Blended Wing Body;

KTAS – Knots True Airspeed;

AOA – Angle of attack;

VLM – Vortex Lattice Method;

MGC – Mean Geometric Chord;

GA – General Aviation;

AOI – Angle of Incidence;

eVTOL – Electric Vertical Take Off and Landing;

LE – Leading Edge;

TE – Trailing Edge;

Nomenclature:

W – Weight;

S – Wing Area;

V_C – Cruise Velocity;

V_A – Manoeuvring Speed;

n – limit load factor;

(t/c) – aerofoil thickness to chord ratio;

(L/D) – Lift force to drag force ratio;

C_L – Wing Coefficient of Lift;

C_D – Wing coefficient of Drag;

C_M – Wing Coefficient of pitching moment;

V_V – Climb Speed;

ROC – Rate of Climb;

V_{TO} – Take off speed;

V_S – Stall speed;

S_g – Take off ground run;

V_C – Cruise Velocity;

V_H – Maximum aircraft speed;

$C_{D_{min}}$ – Minimum drag coefficient;

ρ – Density;

(T/W) – Thrust loading;

(W/S) – Wing Loading;

q – Dynamic pressure;

k – Lift Induced drag constant;

$C_{D_{TO}}$ – Take off Drag Coefficient;

$C_{L_{TO}}$ – Take off Lift Coefficient;

AR – Aspect Ratio;

e – Oswald's Span efficiency;

b – Wingspan;

λ – Taper ratio;

C_r – Wing Root chord;

C_t – Wing tip Chord;

C_{avg} - Average Chord;

R_e – Reynold's number;

μ – Dynamic Viscosity;

C_P – Coefficient of pressure;

α – Angle of Attack;

Φ – Bank Angle;

C_{MGC} – Mean Geometric Chord;

Y_{MGC} – Location of MGC along the wing semi-span;

C_{Di} – Coefficient of induced drag

Introduction

As the developed part of the world sees towards an eco-friendlier future, Hybrid technological developments are on the rise and a significant growth in the electric propulsion systems across various field is the new necessity. Although the fully electric propulsion system was extensively tested and implemented on tesla cars in the United States of America and in recent days by other Automobile manufactures, time has come for the same to be done in the aeronautical sector. Many aeronautical Multi-National Companies (MNCs) have already started with their experimentation, research and implementation of various concepts. The idea of hybrid propulsion in aeronautics is not new, but it is still in the infant stages of its lifecycle.

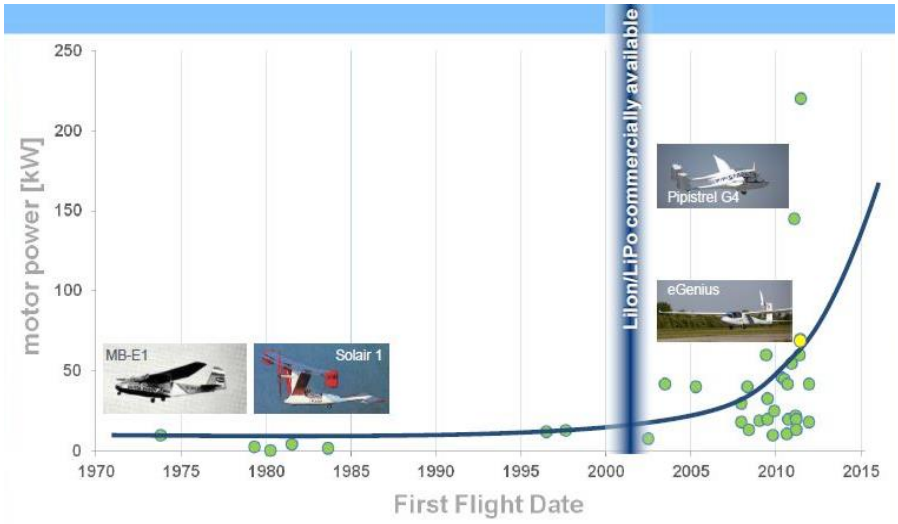

Fig. 1. Growth in R&D of hybrid propulsion in general aviation. (1)

From the above graph we can see that the earliest electric aircraft flight took place in mid 1970s. Although it appears to have been developed quite a long time ago, this technology is still in its development process. We can clearly see the evolution of technology and the first class of aircraft to be powered by fully electric or hybrid propulsion system is the general aviation category. With the success of the technology in this category, the application is later expected to extend among larger transport category aircrafts. In the upcoming trade studies, we can see some of the already tested, proven and flown fully electric general aviation aircrafts which have been widely tested for a current technological development known as Urban Air Mobility (UAM).

This project (Thesis) will focus on developing an eco-friendly aircraft to meet the growing demand of transport requirements in populated cities across the world. The more aerodynamic designs are, the more efficient becomes the travel and hence reduction in cost. In the 21st century, the global warming has become a major concern. The developed and developing countries are taking strong steps to reduce it.

Over the years the hybrid aircraft development has seen multiple experimental flights, this includes testing of fixed wing as well as rotary wing aircrafts. The recent developments of research and implementation in hybrid aircrafts has taken place with hybrid aerodynamic designs with modern and futuristic aerodynamic concepts. Also, in the literature studies we can see a modern transition in the hybrid aircrafts design considerations.

Most of the developments for a hybrid aircraft have taken place for small aircrafts with distributed electric propulsion which includes both propeller aircraft as well as ducted fan aircrafts. All these experimentation with different source of propulsion has been made on the light aircraft category. From the below graph we can see that the light aircraft category has a lower take-off mass and wide range of empty mass/take-off mass ratio which allows it to be considered for the research of scope for urban air mobility concept.

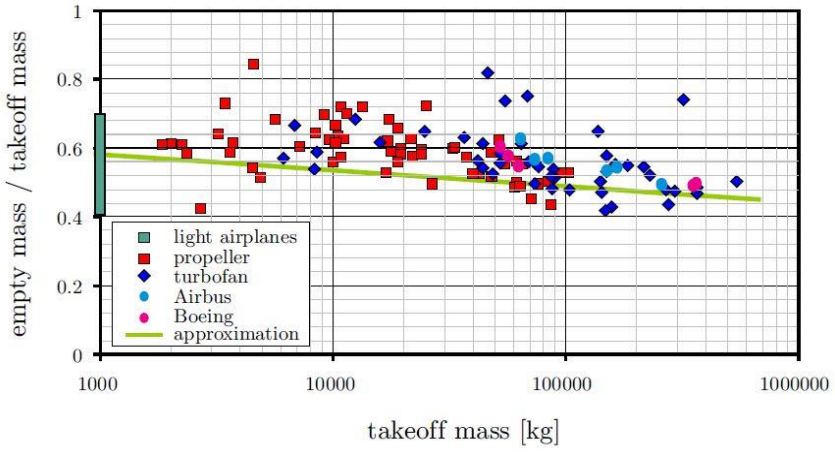

Fig. 2. Various aircraft category and their total mass to take off mass ratio. (2)

In a new multi-disciplinary approach, this project focuses on development of a General Aviation (GA) aircraft in accordance with the possible CS 23 regulations. The GA hybrid aircraft is being formulated for market potential urban air mobility concept and to come up with a state-of-the-art aircraft in the aeronautical Industry.

This project has been focused on urban air mobility and will involve the use of Blended Wing Body (BWB) aircraft which is widely in discussion amongst the major aircraft manufacturers and research establishments for large aircraft categories. The idea of proposing a conceptual design of BWB to UAM is to make the concept more efficient and cost effective in longer run. In the future chapters various studies have been considered where a comparison has been presented about the aerodynamics, propulsion, market potential and other relevant technical and non-technical parameters for conventional and non-conventional aircrafts.

Novelty.

Although similar technology exists, it was noted that no such planned type or technique was found in the public open source which was relatively cheap, small, convenient and comfortable to be used in various multi-disciplinary sectors.

Aim and Tasks.

The Aim of this project is to Design and Analyse the aerodynamics of Blended wing aircraft for the concept of Urban Air Mobility. To achieve this project, it is necessary to complete a series of Tasks such as:

1. Market research, Scope and Trade studies;
2. Understanding of General Aviation regulations;
3. Aircraft Initial Sizing;
4. Constrain analysis;
5. Aircraft geometric calculations;
6. Analysis of various aerofoils;
7. Initial Aircraft Analysis;
8. Aircraft CAD modelling and CFD;

1. Scope and Market Research

The scope of this project extends to urban transportation, emergency medical services, instant firefighting capabilities and possible defence purposes. When it comes to the population of various growing cities, it is clear from the statistics below obtained from oxford economics that it is a huge increase forecasted for top 50 populated cities up to the year 2030 (3).

Table 1. Population (change 2013-2030) in the Indian Subcontinent (3)

Rank	Country	City	Population (in millions)
2	Bangladesh	Dhaka	8.4
3	Pakistan	Karachi	7.5
8	India	Delhi	5.9
9	India	Mumbai	5.1
12	India	Bangalore	4.5
14	Pakistan	Lahore	4.2
17	India	Chennai	3.7
18	India	Hyderabad (India)	3.6
20	India	Ahmadabad	3.4
23	India	Surat	3.1
27	Bangladesh	Chittagong	2.6
30	India	Pune	2.5
41	India	Ghaziabad	2.1

In the above list of top 50 population change of cities between 2013-2030 referred from oxford economics (3) we see that, most of the population increase is in the Indian subcontinent region and the traffic congestion with growing demand for cars will be a big challenge for the regional government. As more and more companies are investing in the concept of urban air mobility, India is one of the major centres of forecast for demand in urban air taxi as a solution to most of the metropolitan cities. Although here in this study India is taken as a reference for where the technology can be used, it is not new in the western part of the world and has been developed to a larger extent. This is clearly studied and explained in the literature survey.

The scope of the project is extensively high with many companies investing in the concept of urban air mobility. It is important to note that in a market study presented to NASA by Booz Allen Hamilton (BAH) (4) which is an information technology consulting company, clearly mentions that not all markets are viable for the urban air mobility concept. The study considers most of the densely populated and modern cities of the USA (4).

The air shuttle and air taxi markets were considered as viable for UAM (4). It is obvious that in densely populated Indian subcontinent cities as listed in table above, UAM as air shuttle would serve as a fast means to transport air travellers to the airport saving time and money in the longer run. The air taxi is something which will have to be investigated deep further before implementation of UAM as a structured layout for overall operations needs to be planned effectively.

The non-viable markets of UAM are the emergency services such as ambulance, firefighting and any other similar operations. Such operations are non-viable market only due to the technology constrain as of now and may be viable with evolution of UAM technology down the line (4).

It was noted from the study presented by Booz Allen Hamilton Inc that the challenges of the urban air mobility concept go beyond technology (4). The study emphasized on short term and long-term challenges, possible whether variations, passenger and on ground passer-by's safety requirements, other technological and non-technological challenges which also includes certification and regulation barriers (4).

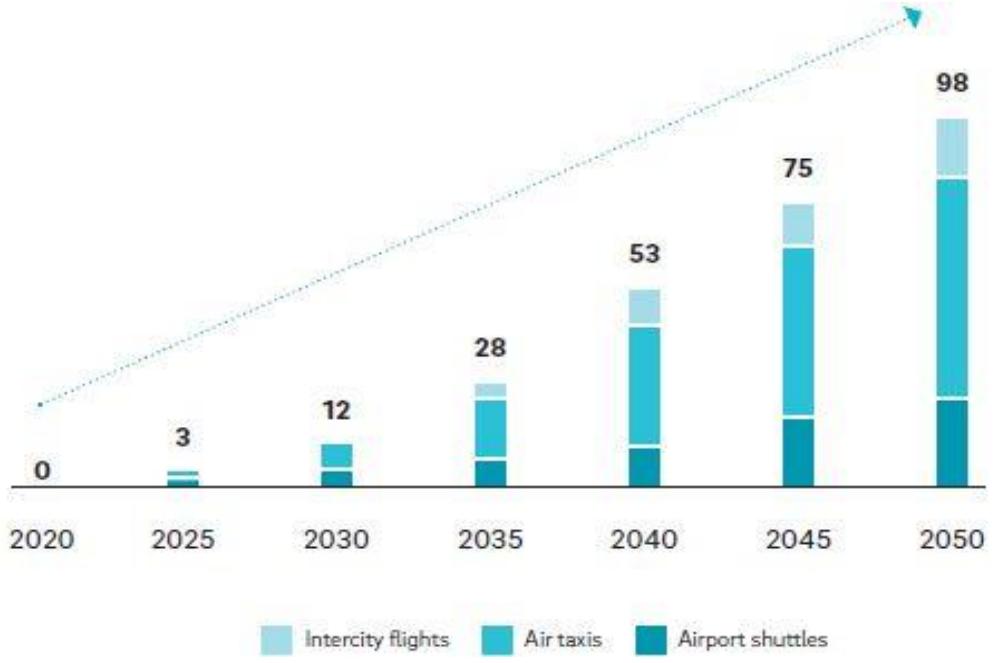

Fig. 3. Forecast of number of cities that will have UAM operations by the year 2050 (5)

In another market study published by Roland Berger GmbH which is a European consulting company based in Germany gives us an idea about the European progress in the field of urban air mobility. According to the company in the above figure we see that it is estimated about 100 cities by 2050 approximately around the world will have UAM operations which includes intercity flights, air taxis and airport shuttle operations (5). It is very well known that the aviation industry comes with a huge cost of investment, but it is also optimized to provide the best service in the cheapest possible way. The American and European market study considered have other technological surveys which has been considered in relevant chapters.

In this scope and market study presented, the American and European scenarios were considered and studied with the help of market forecast presented by Booz Allen Hamilton Inc and Roland Berger GmbH respectively. What is important to note is that the Asian market for UAM is void and with reference to (table 1) obtained from oxford economics, we can clearly see that the population increase is highest in the south Asian region or the Indian subcontinent. It is worth to mention here that one of the world's leading urban transportation giant Uber listed India as one of the potential countries were UAM can be implemented as a solution for traffic congestion in one of the White papers published by Uber Elevate (6).

Fig. 4. Uber Elevate route forecast for UAM operation in India (6)

In the above picture we see that the Uber Elevate program from Uber technologies Inc clearly represents that there is a huge saving on time consumed during the travel with respect to on road transportation and air transportation for the same distance. When it comes to the cost, we see that only long-term forecast reduces the cost of air transportation. This is same as what was mentioned in market forecasts predicted for American and European scenarios. In a recent survey done by Oxford economics listed and forecasted the GDP growth as well as fastest growing smart cities around the world. It was noted from the survey that between 2019-2035 the south Indian cities particularly Bengaluru which dominates the aerospace investments and establishments in India along with Hyderabad and Chennai being major financial and business destinations for various MNCs are strong performers with respect to GDP growth and 85% of top 20 fastest growing cities will be Indian. (7)

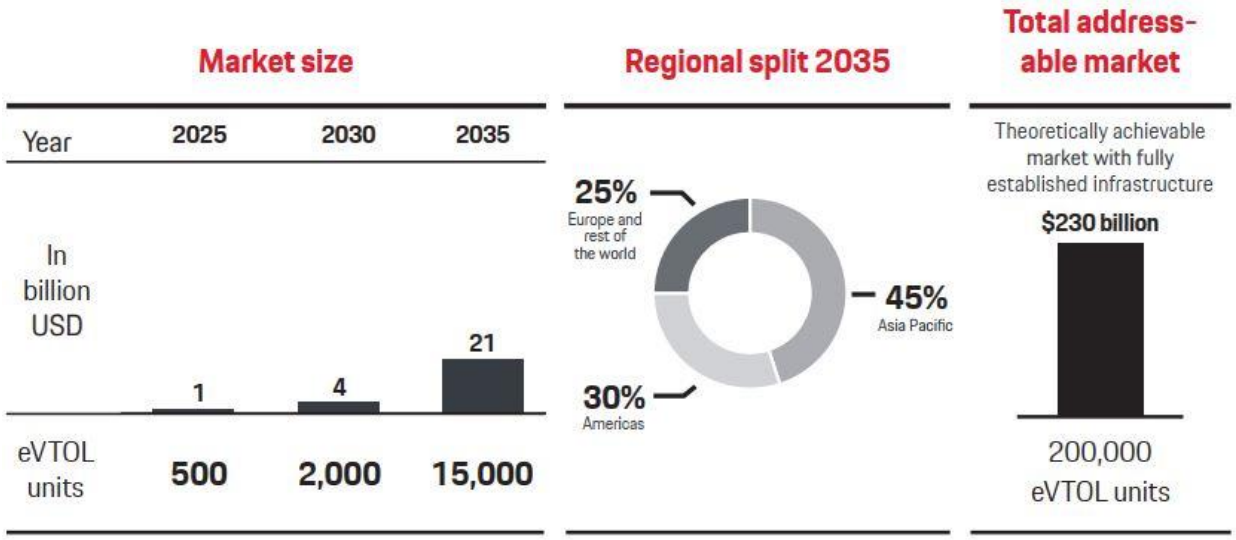

Fig. 5. Passenger drone market sizing forecast (8)

As we see from (Figure 5) region wise split of market forecast of passenger drones up to 2035 shows that 45% of market is expected to be consumed by Asia pacific region. This percentage of share forecasted from the Porsche Consulting GmbH company falls in line with the population growth in the south Asian region, especially in the Indian subcontinent mentioned in (table 1) and coincidently all the top 10 fastest growing cities around the world belong to the Asia Pacific region as well with all being Indian cities.

Table 2. The fastest growing cities of the world between 2019-35 (7)

Rank	**Growth (%y/y, 2019-35)**	**City**	**GDP 2018 ($ trillion, constant 2018 prices)**	**GDP 2035 ($ trn, constant 2018 prices)**
1	9.17	Surat	28.5	126.8
2	8.58	Agra	3.9	15.6
3	8.50	Bengaluru	70.8	283.3
4	8.47	Hyderabad	50.6	201.4
5	8.41	Nagpur	12.3	48.6
6	8.36	Tiruppur	4.3	17.0
7	8.33	Rajkot	6.8	26.7
8	8.29	Tiruchirappalli	4.9	19.0
9	8.17	Chennai	36.0	136.8
10	8.16	Vijayawada	5.6	21.3

Few of the major factors with which affect the market of urban air mobility are as follows:

- Infrastructure available or needed in the city of operation;
- type of technology under trials and which is best feasible;
- stakeholders Interests: The government, citizens, environmentalist etc.

In order to be certified and fly, it is required for an institution or organization to consider all the above-mentioned factors as well as other relevant parameters. The regulation and certification of aircraft of such a kind is discussed in the next chapter.

2. Regulations and Certification

When the scope and market analysis of urban air mobility were studied, one of the major barriers of UAM implementation and operation observed was the regulations to be followed and the process of certification involved. This is also clearly stated in the 3 different market studies cited in the earlier section 2. During the studies it was noted that, a dedicated regulation for the concept of Urban air mobility does not exist. Nevertheless, just like how various aviation regulation bodies around the world are making amendments for Unmanned Aircraft Systems (UASs) based on experiences from testing to deployment, the same will have to be employed for urban air transportation. One of the ideas and representation of how the UAM operation would take place is depicted below:

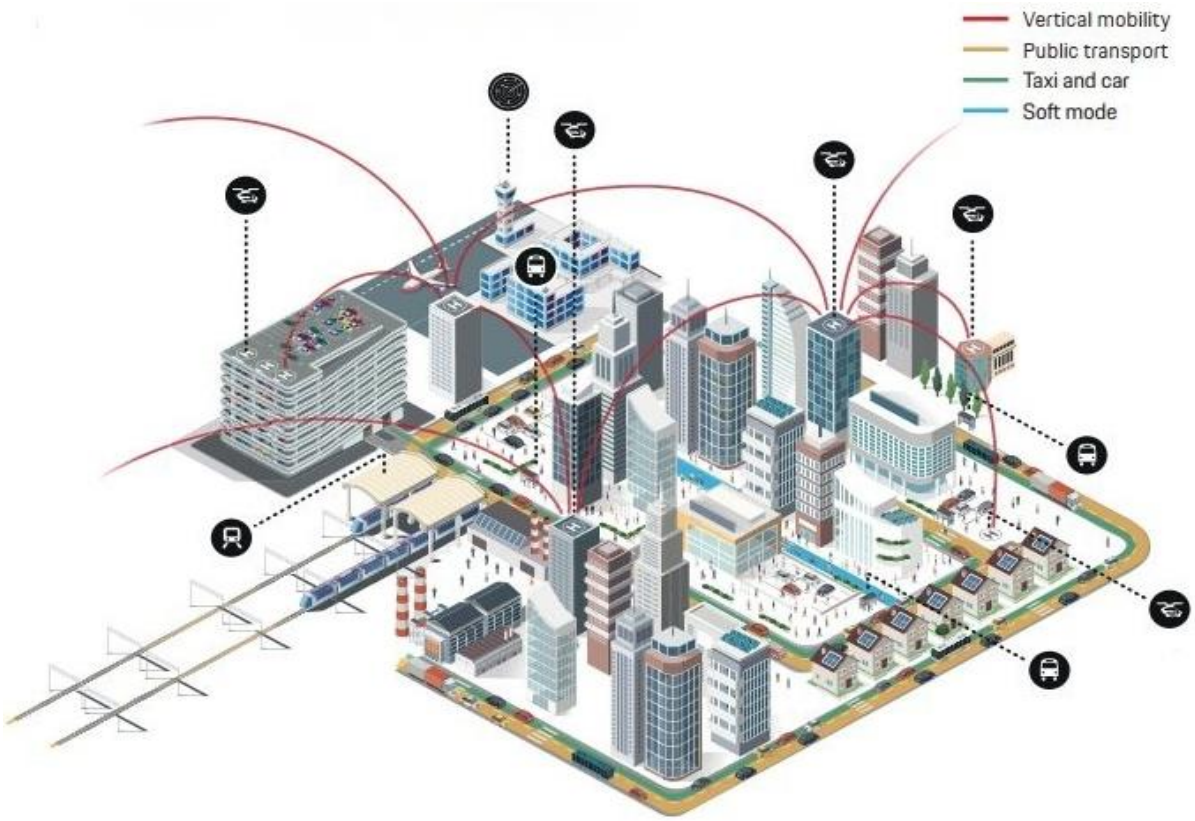

Fig. 6. VTOL concept representation for UAM operations in a City (8)

In the above picture we can see how complex the operation of urban air mobility is. Since the mobility is mainly targeted for urban environment safety becomes a paramount importance. With reference to (Table 1) and (Table 2), 4 of the top 10 fastest growing cities are expected to have high population density. Although none of the market forecasts mentions these cities as potential target for UAM operation, with respect to the rate of growth and GDP, they can be potential cities for UAM operations anytime down the line in future. There has been some credible survey done by experienced scientific and other consulting companies which suggest the kind of regulations which can be followed for UAM operations given the reasonable inputs and experience available. In this Project (Thesis), all possible basic regulation procedures will be followed which are found applicable respectively for the design of aircraft.

From the studies made for UAM operation, many technologies and infrastructure were suggested like vertiports for Vertical Take Off and Landing (VTOL) aircrafts, Passenger drones, Manned and unmanned modes, semi-autonomous and fully autonomous systems etc. (8).

It is very hard to agree on a system when such variety of designs are under considerations for the same concept of operation. Other most significant factor to be considered in this project is the eco-friendly electric aircraft engines being implemented. Almost all the regulatory procedures from Federal Aviation Administration (FAA) for the United States of America (USA) and European Aviation Safety Agency (EASA) for European Union (EU) have certain set of rules to be followed for Combustion engines and electric engines in case of UAVs. Below table gives a clear idea about the various options of regulations which can be considered in order to implement the concept of UAM.

Table 3. Comparisons of different type certifications (4)

Regulatory Body	**Fixed Wing**	**Rotary**	**Hybrid or Special**	**Engines**	**Propellers**
FAA	Part 21 Part 23 Part 25	Part 27	Part 21.17(b)	Part 33	Part 35
EASA	CS-22 CS-23 CS-25	CS-27 CS-29	CS-VLA CS-VLR	CS-E	CS-P
NATO	STANAG 4671 STANAG 4703	STANAG 4702	Draft STANAG 4746	STANAG 4703 STANAG 3372	STANAG 4703

The main goal of this project is to design an aircraft which would be beneficial for general aviation market and as a concept of advanced development for urban air mobility operations. Hence, It is better to meet all the possible basic CS 23 regulations which are the certification specifications including the codes for confirming the aircraft flightworthiness of normal, utility, aerobatic and commuter class aeroplanes (9). In the next section the design methodology that is followed for the project is mentioned which is then followed by the aircraft design and later to CFD simulations.

The following are the few CS 23 regulations followed for this project:

- CS 23.49 Stalling speed: The stall speed requirement for general aviation aircraft is 61 KTAS or 113 km/h (9).
- CS 23.1 Applicability (a): Aircraft weight less than 5670 kg (9)
- CS 23.53 Take-off performance:
- CS 23.57 Take-off path: Take off path extends from a position where the aircraft is in starting point to a point where the aircraft is 457 meter or 1500 feet above the ground surface (9).
- CS 23.63 Climb: general, for aircraft weight less than or equal to 2 722 kg (9)
- CS 23.25 Weight limits: Passenger weight suggested is 77 kg for commuter aircraft and 86 kg for utility type aircraft (9).
- CS 23.333 Flight Envelope: Subpart (b) is followed.
- CS 23.335 Design Speeds: V_C not less than $33 * \sqrt{\frac{W}{S}}$, V_A not less than $V_S * \sqrt{n}$ (9)
- CS 23.337 Limit Manoeuvring Load Factor: given by, $n = 2.1 + \frac{24000}{W+10000}$ (9)

Where: W is MTOW in lb, S in ft^2 and the n need not be more than 3.8 (9).

3. Project Methodology

The design methodology to be followed in this project is based on the same process followed for any aircraft development. The design involved here is to facilitate further developments over a period. The project is hence split into multiple phases of development. The first Phase includes the conceptual design phase where a basic design is developed according to initial specifications. For this project (thesis) the basic design will be analysed using Computational Fluid Dynamics (CFD) and made feasible for future trials, upgradation and development. The below flowchart gives a clear idea about the aircraft design process.

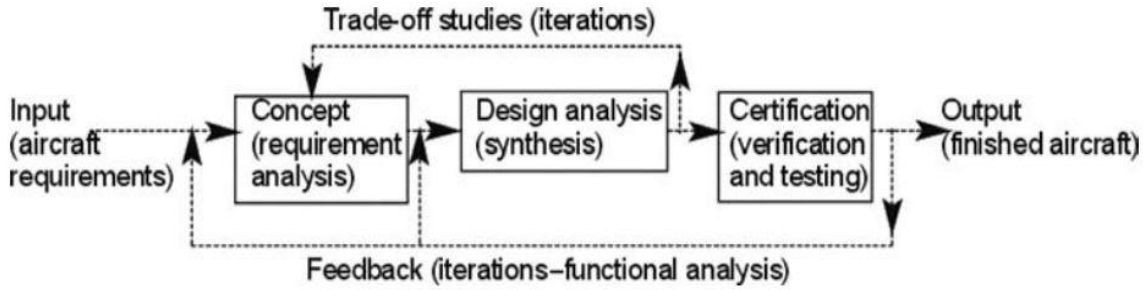

Fig. 7. Aircraft design process (10)

As seen from above figure, the overall flow process of an aircraft design involves multiple iterations before it can be finalized. The initial input is the aircraft requirements. This is strongly dependent on customer needs. In this project's case, from the market potential analysis it is understood that the aircraft in need is for urban air mobility operations. The demand for the capacity of aircraft and mission requirements is known here. Concept (requirement analysis) is made from multiple trade off studies made from available literature data studied. The Aircraft Transport Association (ATA) suggest a common design process for a commercial transport aircraft and this is represented in the (Figure 7). When a new aircraft is being conceived, designed, built, and certified, as multidisciplinary approach it is essential for the aircraft to follow all the 4 phases involved in development. Usually the effectiveness of a newly designed aircraft is tested on a scaled down prototype and multiple iterations are carried out in order to optimize and arrive at a convincing design (10). As mentioned by the author of book in reference (11) Fundamental phases of aircraft design process and the tasks involved in achieving them are:

1 *Requirement Phase*: Mission definition, required targets like speed, distance, altitude, passengers and payload are set; (11)
2 *Conceptual Design phase*: Initial aircraft configuration, aerodynamics, such parameters are defined; (11)
3 *Preliminary design phase*: Detailed geometry development, performance parameter estimations, weight and balance calculations, stability and control are defined; (11)
4 *Detail design phase*: Detailed design of structural, mechanical, avionics, environmental control systems and many more sub systems are finalized; (11)
5 *Proof-of-concept aircraft construction and testing phase*: Prototyping, testing and validation of scaled down model are analysed, optimization technics are used to improve the design if necessary. (11)

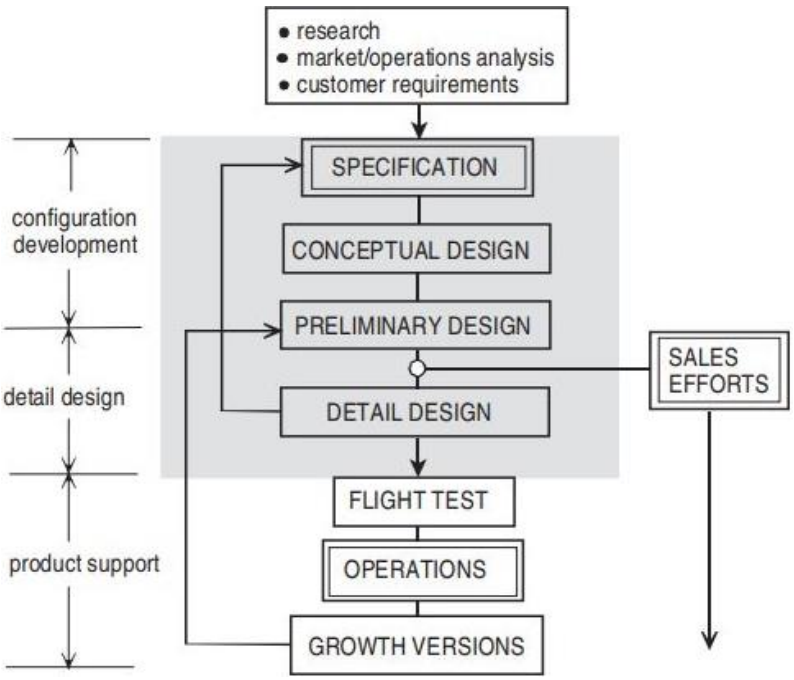

Fig. 8. Design flowchart of the civil aeroplane development process (12)

In the above figure, we see that the initial start of a design depends on the type and kind of research done for the project. In the earlier chapters the market potential survey and operation analysis including the discussion on the regulation and certification procedures were mentioned. The customer requirement which follows next is dependent on some statistics. In this project, the quantities like number of passenger travel, type of route such as intercity, air shuttle or other emergency services were discussed. In the above represented flow chart, we see that one of the major requirements before moving to the conceptual design of the aircraft is the specifications. This is clearly dependent on the literature studies and trade-offs made with other factors to be taken as reference such as the type of regulation to be employed. Once the studies are made with reference to already existing similar projects in the market, the designer gets a clear idea of some values which can be convincing. Once such specifications are in hand, the designer moves to the Conceptual design phase which lays the foundation for the overall development and optimization of the project based on various results and needs.

The following are the algorithm steps that will be followed in the conceptual design of the aircraft for UAM operation:

1. Gather the requirements, know the type of mission and regulation which can be followed;
2. Based on the needs and requirements of aircraft a constrain diagram is created;
3. From the values obtained in constrain diagram, other relating aircraft geometric parameters are calculated;
4. Various air foil analysis is carried out in order to select the best aerofoil;
5. A preliminary analysis of the aircraft is modelled in XFLR5 in order to compare the design polar with constrain analysis;
6. A 3D surface CAD surface model is developed for performing CFD analysis.

4. Trade Studies

Trade studies is defined as an element of system engineering which helps to arrive at a technical solution by studying the various alternatives available. The main objective of trade studies is to highlight the potential problem-solving solution and the best choice is to be opted on justified academic basis. Some of the aircrafts under development and testing for the concept of urban air mobility is listed below with all the possible fact sheet data collected:

Table 4. Existing aircraft designs for UAM concept

Sl. No	**Aircraft**	**Type**	**Wingspan (m)**	**MTOW (Kg)**	**Passenger Capacity**	**Cruise Velocity (Km/h)**
1	Aurora	3 surfaces	8	800	2	180
2	Cora	Multi Rotor with wing	11	181 + empty weight	2	180
*3	Vahana (Beta)	Tandem wing	6.25 +	815	2	230
4	Bell Nexus	Multi rotor with 3 surface design	-	-	4	-
5	Lilium	Wing with canard	10	-	5	300
*6	Opener Blackfly	Tandem wing	4.17 +	232.693	1	128.748
7	Ehang experimental	Milti rotor	-	360	-	100 Max
8	Volvocopter	Multi rotor	-	450	2	70
**9	Flynano	Box Wing	4.8	170	1	120
**10	X-57 Maxwell	Fixed wing		1360	4	280
11	Pipistrel Vertical Solution	Blended Wing	-	-	-	-
12	EVA X01	Wing	-	250	2	300

*Consists of 2 different full span wings on the same aircraft
**Not a VTOL aircraft: used as reference for comparison.

From the above table we see that a variety of aircraft configuration has been used with different modes of propulsion and aerodynamics. A brief study of different configurations and other aircraft systems used in UAM are studied below.

4.1. Aerodynamics:

The aircrafts listed in (Table 1) consists of conventional and unconventional aerodynamic designs. This includes various configurations such as:

1. Tube and Wing (TAW)
    a) Conventional with Distributed Electric Propulsion wing (DEP wing);
    b) Tailless canard wing;
    c) 3 surface aircraft (Tri-surface);
2. Tandem wing;
3. Box wing: Also known as closed wing;
4. Rotary wing: a) pure multi rotor design, b) hybrid multi rotor design;
5. Blended Wing Body (BWB).

The above aircrafts are classified based on their lift generating mechanism, wing design and Other structural appearances. A discussion of the different aerodynamic configuration is given below:

4.1.1. Tube and Wing (TAW):

The tube and wing configuration are most widely used in conventional aircraft designs which consist of a wing, fuselage and a tail which constitutes Horizontal and Vertical stabilisers. With the modern technological developments, Tube and wing design configuration has undergone additions and the different types of designs are studied below.

4.1.1.1. Conventional with DEP:

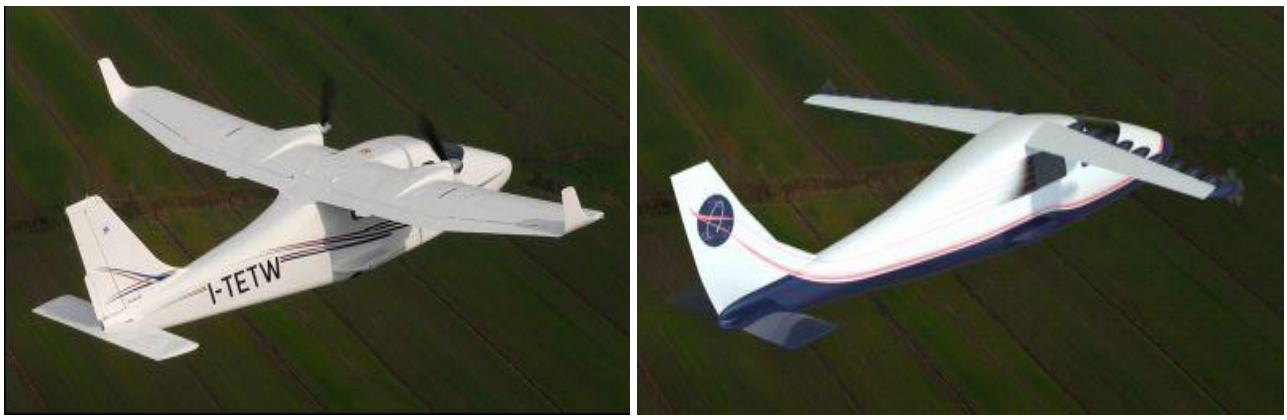

(a) (b)

Fig. 9. (a) Tecnam P2006T, (b) X-57 Maxwell experimental aircraft. (13)

In the above figure we see the typical tube and wing configuration. The X-57 Maxwell aircraft is an experimental aircraft developed by NASA for testing the distributed electric propulsion concept. From (Figure 9a and 9b) we see that the X-57 aircraft fuselage and tail configuration are same as of the Italian general aviation aircraft Tecnam P2006T. The Tecnam P2006T was used as a base line model with only modification to the wing. The Distributed Electric Propulsion (DEP) wing of the X-57 Maxwell was installed on the base line model P2006T with the DEP wing optimized for cruise conditions (14). It is projected that the all-electric X-57 Maxwell aeroplane will achieve 5 times lower energy use than the original P2006T (14).

There is a lot of reduction in the wing area of X-57 for the same lifting capability as that of P2006T aircraft. This is expected to be achieved by the help of distributed electric propulsion wing. The DEP wing for X-57 Maxwell experimental aircraft was chosen as a part of NASA's Scalable Convergent Electric Propulsion Technology Operations Research (SCEPTOR) project (15).

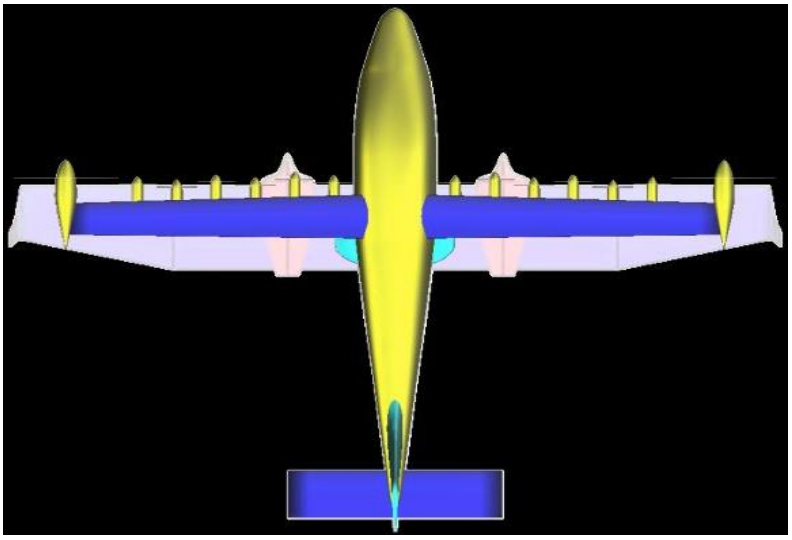

Fig. 10. Comparison of X-57 Maxwell to Baseline Tecnam P2006T aircraft (13)

Above figure gives clear representation of the advantages of DEP wing. Compared to the original wing of Tecnam P2006T which has a loading and area of 16.365 lb/ft^2 (7.423 Kg/m^2) and 158.88 ft^2 (14.76 m^2) respectively, the X-57 aircraft has a wing loading of 45 lb/ft^2 (20.41 Kg/m^2) and wing area being 66.67ft^2 (6.19 m^2) (14). The concept of distributed electric propulsion is studied in detail under propulsion as sub section.

One of the major concerns for a light aircraft designer is low speed performance of the aircraft. This is also a major factor for aircraft sizing considering the take-off and landing scenarios. It is very likely at times that the aircraft designers come up with an oversized wing in order to meet the desired cruise requirements as the oversized wing tends to fly at lower speeds and in the same time has a high lift to drag ratio to fly in cruise conditions. This problem is solved using distributed electric propulsion (DEP) which includes small propellers installed along the span of the aircraft and there by increases the dynamic pressure on the aircraft wings during lower speed requirements and facilitates higher cruise velocities in cruise condition (Figure 11a and 11b). This in turn helps to accommodate a smaller wing without any loss in low or high-speed performance efficiency (15).

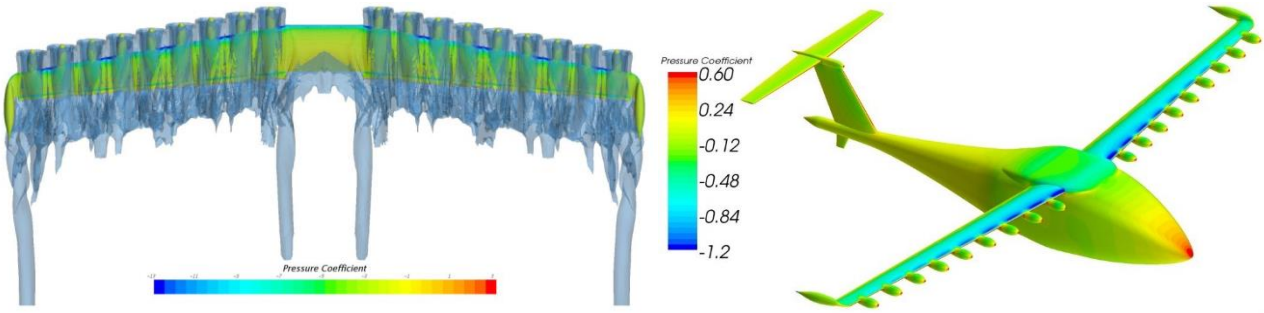

(a) (b)

Fig. 11. (a) DEP wing landing condition (slow speed), (b) DEP wing cruise condition (16).

4.1.1.2. Tailless Canard Aircraft

The term tailless wing is widely referred to the flying wing and blended wing concepts. Here it has been studied as a system referring to modern design of aircrafts for UAM concept listed above in (table 4). As the name itself reflects, the tailless wing aircraft doesn't have an active tail design. The functions of the conventional tail of aircraft is compensated by the aircraft unconventional control surfaces and wing designs.

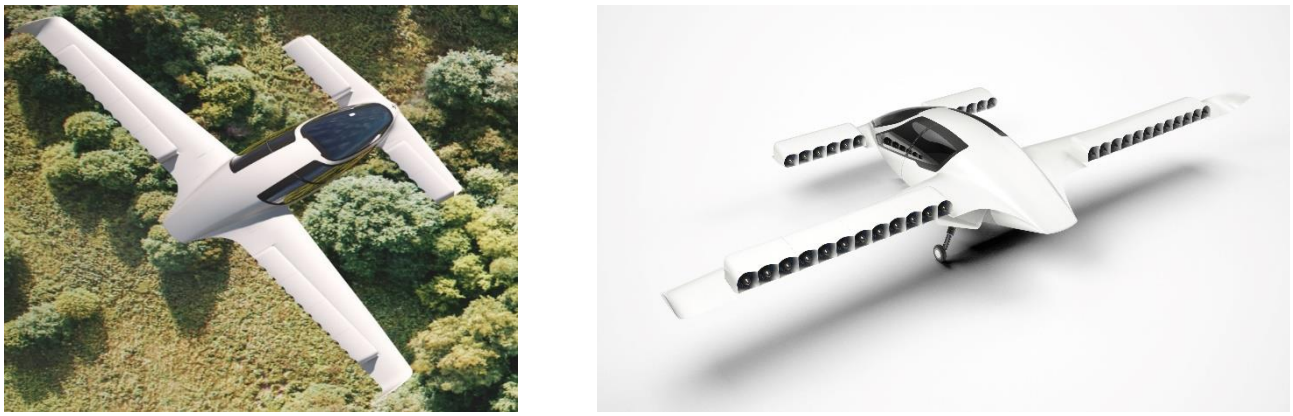

Fig. 12. eVTOL jet from Lilium GmbH (17)

Lilium jet is one of the currently very well know eVTOL company which is focused on urban air mobility. It is important to note that there are no scientific publications available for the study of this aircraft. The data and information used here are in private website of the company and other open sources. The company has had a prototype testing completed and is committed to the development of 5 seat eVTOL aircraft. The aircraft specifications are listed in (Table 4). The aircraft designed by lilium can be configured as a Canard and tailless aircraft.

According to Lilium GmbH, it claims to have designed a low noise, simple, high speed, emission free and a low operating cost VTOL aircraft. The aircraft is powered by 36 ducted fan brushless motors. One of the notable features of the aircraft is its modernistic and innovative control system which involves 12 Ducted fans on each main wing which also serves as the main propulsion system for the aircraft. During the take-off, all the engines are in vertical position allowing the aircraft take off vertically and a transition towards the horizontal direction helps in achieving the forward acceleration of aircraft resulting in airflow over the wings and the conventional lift generation. The engines are used for providing differential thrust in the cruise phase which enables the aircraft to manoeuvre without the presence of a Tail (18).

As studied in the X-57 configuration earlier, the propulsion system of Lilium jet is also based on the principle of distributed electric propulsion. The electric engines of the lilium jet are configured to generate low drag at cruise conditions which has resulted in the aircraft being able to achieve higher speeds and range. The company claims that, because of the above system of design and arrangements, the aircraft's energy consumption per seat becomes comparable to that of an electric car and this in turn offers 3 times faster travel (18).

The Lilium jet consists of an integrated high lift system, in conventional terms this is known as high lift device. The main purpose of integrating such a high lift system is to achieve lift at low speeds consuming less power. This is achieved by the dynamic flow of air over the wings (18).

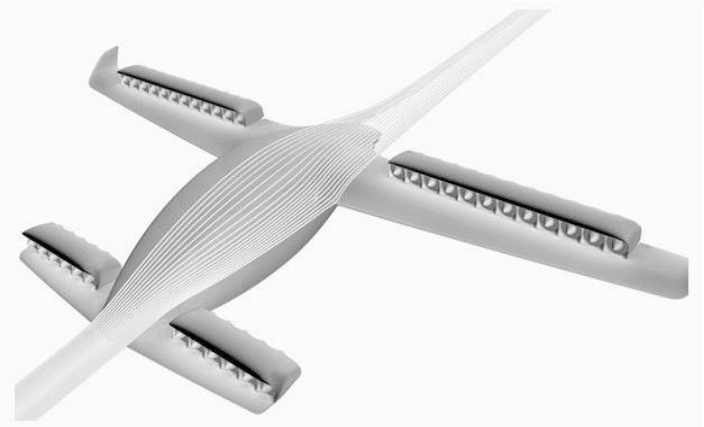

Fig. 13. Laminar flow over the Lilium jet fuselage (18)

The type of design used here once again a tube and wing configuration. The figure depicts a laminar and streamline flow over the fuselage. We can see that the lilium jet consist of a forward stub wing with integrated high lift system which also adds addition thrust to the aircraft. The stub wing at the front is generally known as a canard in general aviation terms. It adds additional area and helps in creating small scale lift and acts as a control system for multiple manoeuvres during cruise flight.

Fig. 14. Airflow comparison of integrated and conventional high lift device (18)

In the above (figure 14) we can observe in the left picture; the trailing edge of the wing is fitted with the ducted fan propulsion system powered by the brushless motor which is embedded to the wing to act as an integrated high lift device. We can observe that in the flap deflected position the flow is more laminar and streamlined over the wings and the flow separation is nothing but the engine exhaust which is also streamlined. This is not the case in conventional flap system where the flow separation takes place and the air becomes turbulent leaving the high lift device. Hence the integrated system proves to be aerodynamically more efficient than the conventional high lift system.

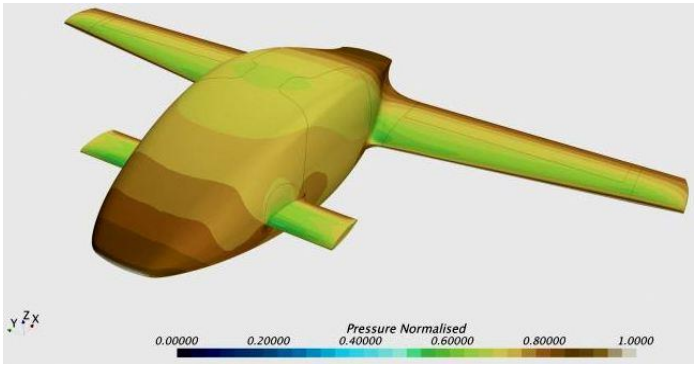

Fig. 15. Lilium jet normalised pressure distribution at 5^0 AOA (19)

4.1.1.3. 3 surface aircraft

The introduction of 3 surface aircraft came into existence during the early 1970s energy crisis. There was need to minimize energy loses and design a more efficient aircraft. The idea of canard aircraft derives its inspiration from triplane design where induced drag generating from the tail apart from main wing were not considered. According to E.R Kendall (20), 3 surface aircraft with use of canards have high stability which is inherited by the design itself and results in low induced drag of the aircraft compared to the conventional 2 surface design which consists of wing and tail only (20).

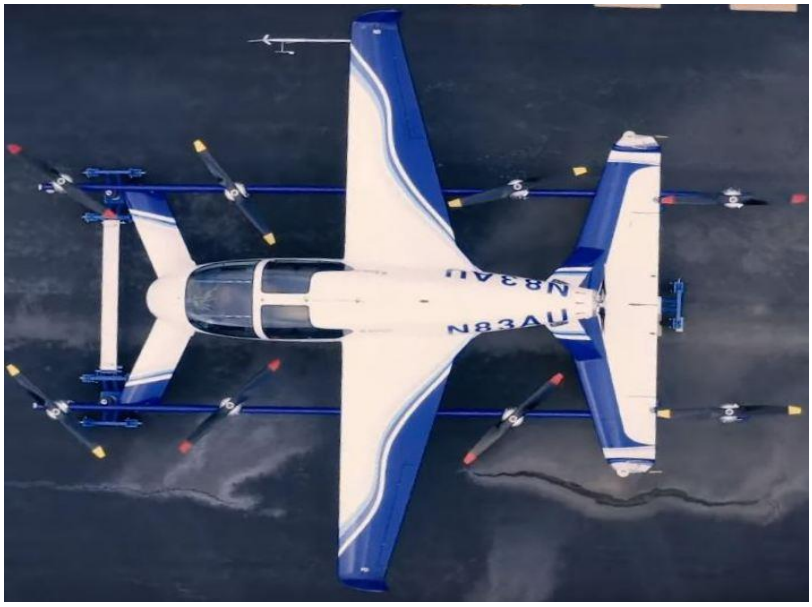

Fig. 16. Aurora Flight Sciences PAV eVTOL with 3 surface configurations (21)

Aurora Flight sciences is a US based company who are involved modern aircraft design. The picture above is an experimental electric Vertical Take-off and Landing (eVTOL) Passenger Air Vehicle (PAV) designed and developed by the aurora flight sciences. The configuration uses an open rotor distributed electric propulsion. This type of configuration where separate and combination of propulsion systems are used for lift and cruise phases are studied in propulsion as sub section. Compared to Lilium jet, which is a pure canard aircraft, the PAV is a 3-surface configuration. From earlier literature we saw that X-57 was a pure conventional wing aircraft, Lilium Jet was a pure canard and wing configuration and Aurora PAV is a 3-surface configuration. In one of the aerodynamic trade-off study conducted by Bruce and Kamran (22) which included comparison of conventional, Canard and Tri-surface designs concluded that in high aspect ratio aircrafts, the canard configuration were expected to perform better and in low values the 3 surface or tri-surface design proved to be superior (22).

One of the important use of 3 surface aircraft with canards is to maintain the longitudinal trim of the aircraft for a series of Centre of Gravity positions (CG) with reduced Induced drag (20). In stability and control theory, static margin (11) is expressed as:

$$S.M = \frac{h - h_n}{C_{MGC}} \quad (1)$$

Where: *S.M* is the Static margin, h is the neutral point, h_n is the Centre of gravity, and C_{MAC} is the Mean Aerodynamic Chord.

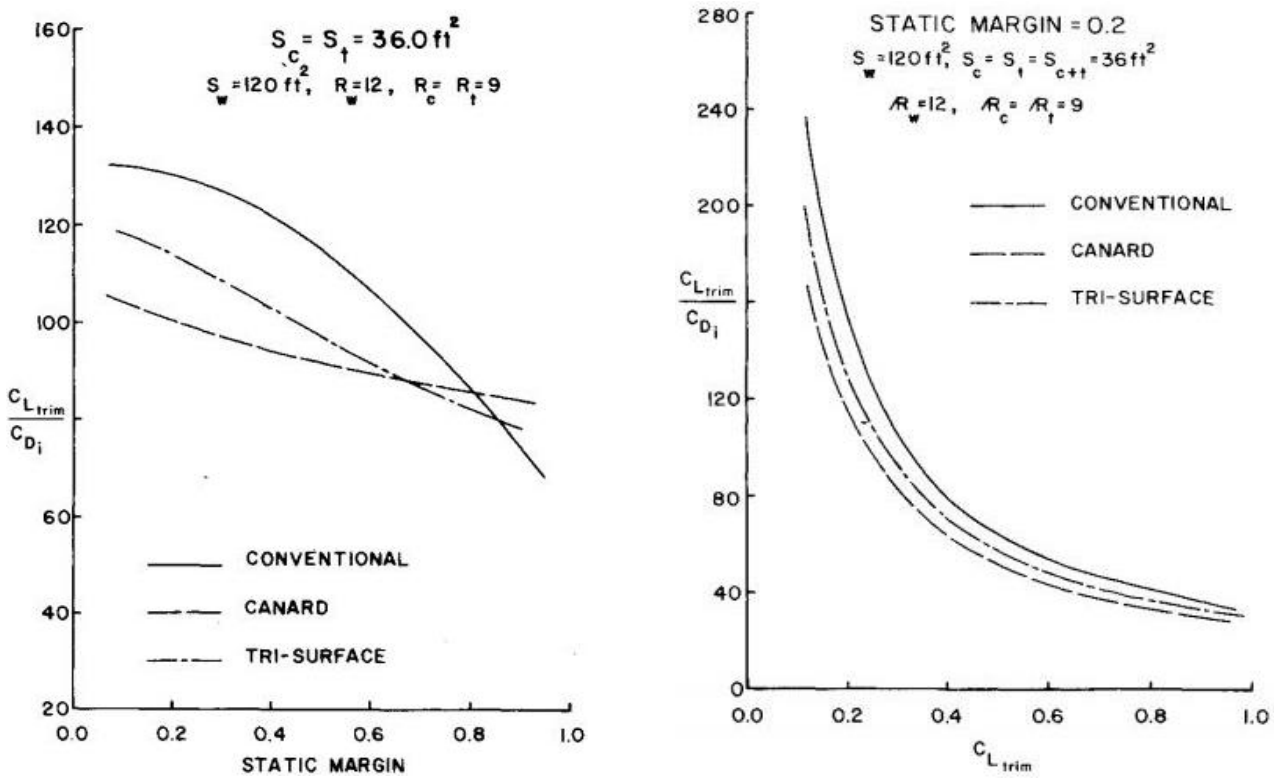

(a) (b)

Fig. 17. (a) Induced Drag vs static margin, (b) Induced Drag change vs Trim lift coefficient (22)

In the aerodynamic trade off study done by Bruce and Kamran (22), A six seat passenger aircraft with a MTOW of 1200 lb and 120ft^2 wing area was considered. The same aircraft was analysed for different configurations such as Wing/tail (Conventional), Canard/wing and Canard/wing/tail (3 surface or tri surface) (22). The above graph in (figure 17) shows the comparison of results obtained for all the 3 configurations. In (figure 17a) we can observe that the induced drag in Tri-surface tends to decrease with high static margin after 0.85 but it is less effective before it compared to conventional and canard configuration. The Tri surface configuration appears to be 2nd best at a static margin of 0.2 considering various velocities and altitudes with respect to reduced induced drag (22). This is evident from the graph in (figure 17b).

One of the major importance of the 3-surface aircraft design is it allows the aircraft to operate with very less drag but without any greater changes in longitudinal static stability of the aircraft. The lift generated by the canard has considerable effect on the neutral point of the airplane which tends to move ahead towards the aircraft's nose. This induces a considerable amount of pitching moment and instability in the aircraft which is countered by the addition of a horizontal tail. With proper trims of the added horizontal surface can help reduce the aircraft drag further down and in-turn give rise to better stability to the aircraft (23).

The tri surface configuration, if properly designed will result in allowing the aircraft to operate at a minimum drag condition for a wide range of trimmed lift coefficients. This allows the aircraft to operate at less power requirement for a mission. One of the concerns of 3 surface aircrafts are the vortex generation and interaction which breaks down at high angles of attack are not an important drawback. The other factors of this configuration are studied in further chapters (23).

4.1.2. Tandem Wing Aircraft:

One of the notable advantages of tandem wing is higher lifting surface area compared to the wingspan. Since 2 full wings are placed one behind the other, there is a lot of space which is saved, and this is one of the major priorities for UAM operations. Many companies are investing in tandem wing designs for multiples purposes which are studied here.

(a) (b)

Fig. 18. (a) Tandem wing Opener Blackfly (24), (b) Tandem wing Airbus Vahana (25)

The aircrafts seen in (figure 18a and 18b) are one of the very extensively tested UAM concepts designed and developed by Opener Inc and Airbus respectively. Both these configurations consist of a transition lift system for VTOL and cruise condition. This type of propulsion and aerodynamics can be categorised as tilt wing as well. This is studied under propulsion as subsection further in this report.

Some of the important parameters which influence the aerodynamics and stability of the tandem wing aircraft configurations are the vertical distance, spacing and angle at which the forward and aft wings are positioned respectively. When these parameters are optimised for best possible combinations, the tandem wing aircraft aerodynamic stability is expected to be better than conventional configuration (26).

According to Jinbin Fu et.al (26), The investigation done by Mueller, T. J. and Michelsen, M. D. resulted in conclusions where the wake created by the forward wing caused downwash and interferences on the aft wing due to less gap between the 2 lift generating surfaces (26).

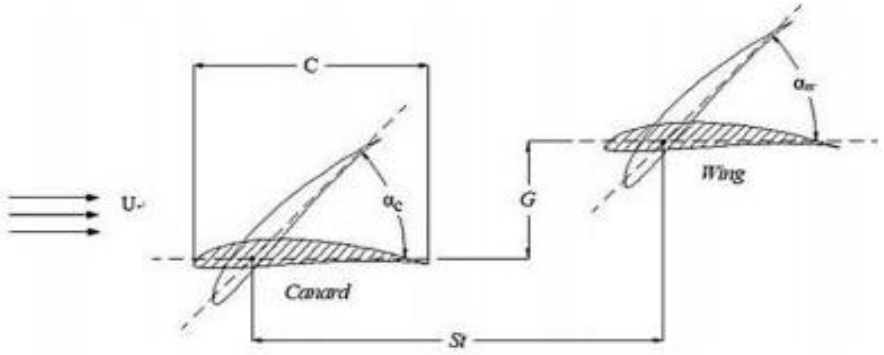

Fig. 19. Flow configuration in tandem wings (26)

In the above figure: G is the vertical distance or gap between the 2 lifting surfaces, St is the distance between 25% mean aerodynamic chord of both surfaces which is known as stagger, D is the decalage angle which is the angle relative to AOA or α of 2 wings and also this is equal to the difference in incidence of the 2 wings with Decalage being negative if incidence of aft wing is higher than incidence of forward wing (26).

According to Kamran Rokhsaz and Bruce P. Selberg investigations (27), the dual wing configuration proved to have higher lift to drag ratio compared to a single wing design and other investigations have showed reduction in induced drag compared to the conventional designs (27). The below figure 20 shows a series of aerodynamic analysis done by Jinbin Fu et.al (26) for different vertical spacings between the 2 wings.

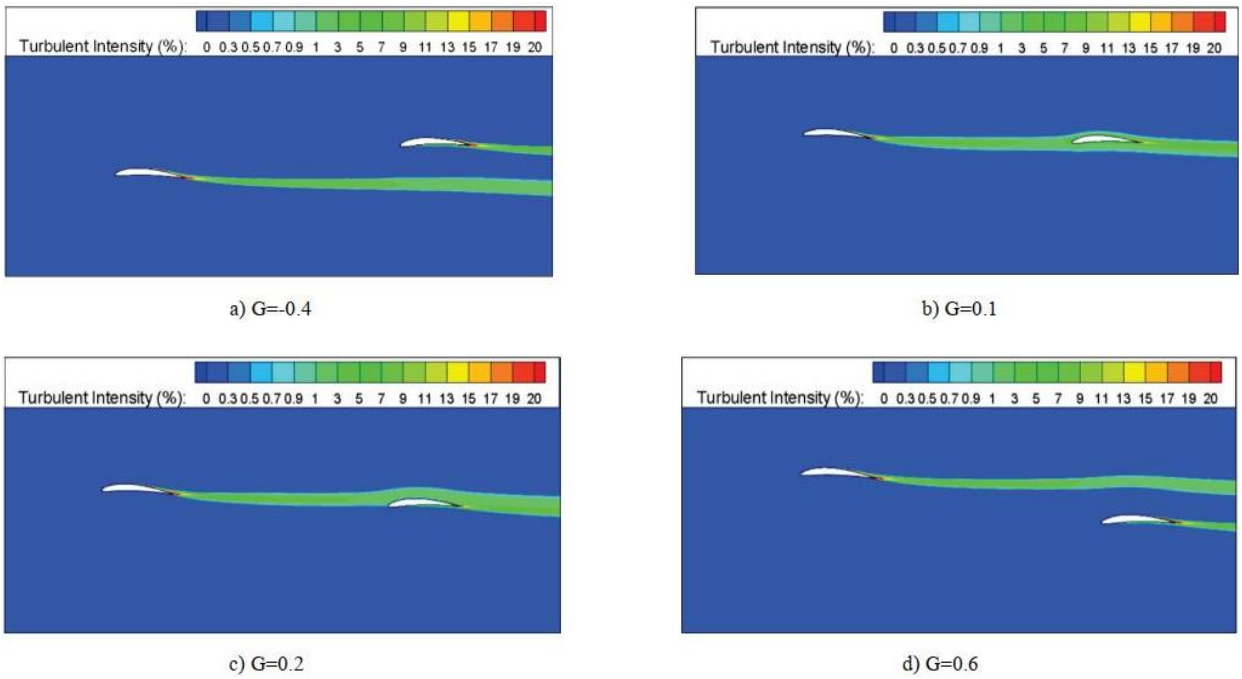

Fig. 20. Effect of wake due to forward wing on aft wing at different vertical spacing (26)

In the above figure we see that with the gap reduced to positive 0.1 and 0.2, the wake interferences created by the forward wing engulfs the aft wing. This creates a huge loss in lift and increased drag resulting in reduced aerodynamic efficiency. The negative gap at -0.4 and positive gap at 0.6 results in wake avoidance which was see with lower G (Gap or vertical spacing of the tandem wings) values (26). Even though the configurations in (Figure 18) are designed and developed to have higher negative gaps, it was surprising to note that the author in reference (26) mentions about an observation where the tandem aerofoil with positive gap configuration has slightly higher lift and lower drag compared to same gap values in negative region (26). The St or stagger which refers to the spacing of tandem wings along the horizontal plane also has major impacts on the aerodynamics. It was observed that as the stagger increases, there is a significant increase in the aerodynamic efficiency as there is enough time for the dissipation of wake or turbulence generated from the forward wing. This in turn results in increased total lift and reduced drag (26). The Decalage has the most adverse effect on the tandem wing aerodynamics. In the analysis done by Jinbin et.al (26), it was noted that there was an increase in lift to drag ratio with increase in decalage angles. It was observed that tandem wing aircrafts with higher angles of decalage were aerodynamically more stable, but stall angles were quite lower (26).

It was noted that after certain decalage angle the lift to drag ratios start decreasing and there is a significant increase in aircraft drag. This is clear from the graph below in the (figure 21) and CFD simulations in (figure 22).

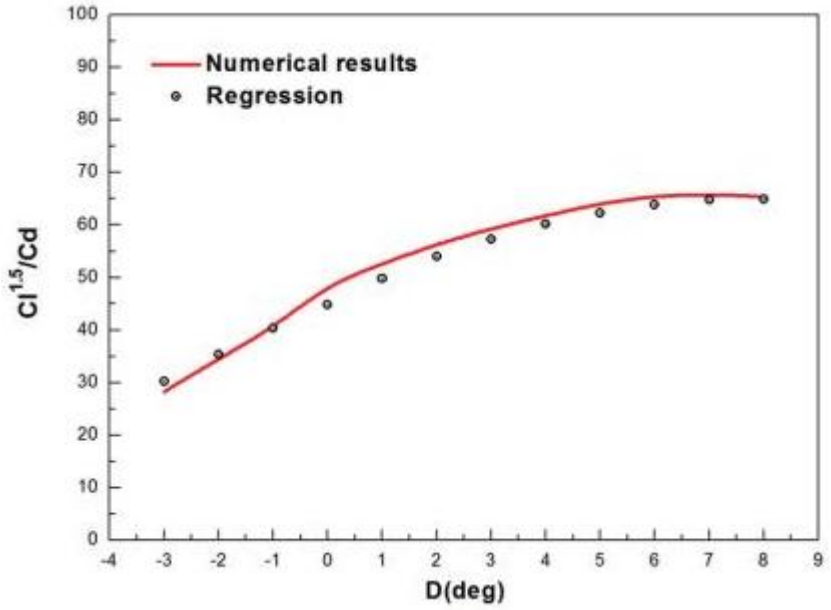

Fig. 21. L/D ratio changes vs Decalage angle (26)

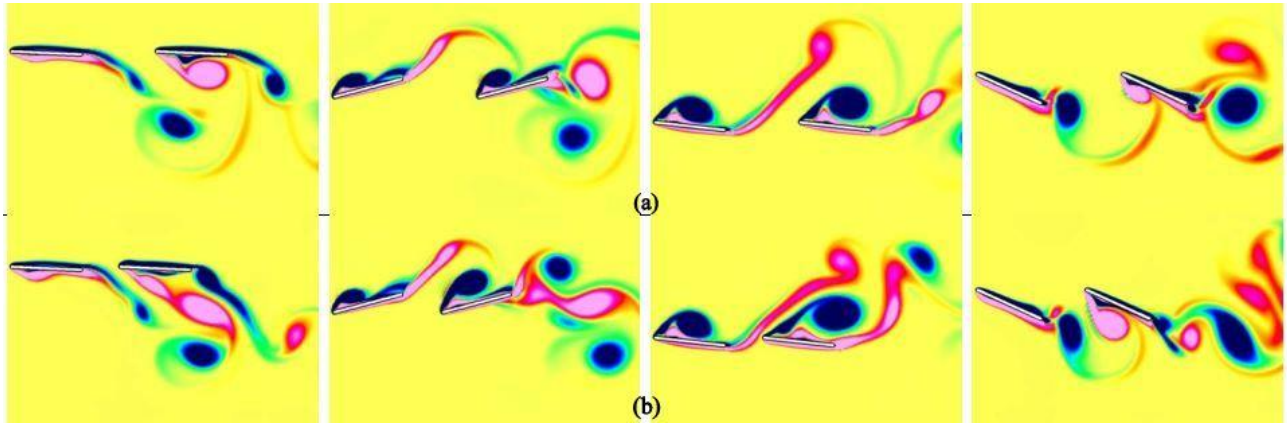

Fig. 22. Air flow at different stagger length and decalage angle of a tandem wing design (28)

4.1.3. Box Wing aircraft

In above section it was clear that modern unconventional aircraft designs are more focused on increasing the lift to drag ratio with less induced drag in order to save fuel and increase efficiency of flight time. These technologies are also driven by the 21st century aviation requirements to cut down the harmful emissions from burning of fossil fuel. As mentioned in the introduction, this has further pushed for development of hybrid and electric propulsion systems and in turn an approach towards modern unconventional design are under consideration. One such consideration is the concept of Box wing aircraft. As seen in tandem wings design, the box wing aircraft also has potential to improve the total lift of the aircraft with reduced wingspan length (29). According to the research investigated by A. Somerville et al (29), Prandtl (1924) put forward that the induced drag tends to reduce in multi wing planes offset vertically and joined at the wing tip (29). The wing tip vortices are circular flow around the wing tips, combined with the free-stream flow (29). The wing tip vortices are generated due to the span wise flow and difference in air flow at wing tips. The larger the span wise flow, the bigger the vortex is (29). In other terms aircraft with large wing areas are more likely to generate large vortex at wing tips. The modern aircrafts have multiple solutions like usage of different types of winglets to reduce the magnitude of vortex generated at the wing tips. The history of wing studies differentiates between finite and infinite wing, where infinite wing refers to aircrafts with no wing tips and hence no wing tip vortices and ideal lift without losses. One of the techniques to achieve the advantage of infinite wing in real time aircrafts which have finite wing with wing tips is the implementation of closed wing or box wing design where the tips are closed with a horizontal surface like shown in below figure 23.

Fig. 23. Box wing design single seat aircraft from Flynano Oy (30)

In the research study published by A. Somerville et al (29), it was observed that the box wing aircraft had a reduction of 32% in induced drag compared to the conventional aircraft which had around 2.9% (29). The Box wing aircraft is categorised as a non-planar wing design. This comes with the evolution of winglets at wing tips. Generally like in any other aircraft design, the interference drag causes reduction in efficiency of the lower wing of box wing configuration, but the rear wing experiences enhanced lift characteristics (31) since it is freely exposed to free stream air relative to its boundary condition. The best suited design of box wing aircraft is when the front wings are designed to stall only when the rear wing is generating enough lift to keep the aircraft stable (31). The CFD analysis in (figure 24) shows a clear difference in the vortex generation and progression on a conventional aircraft compared to Box wing aircraft configuration.

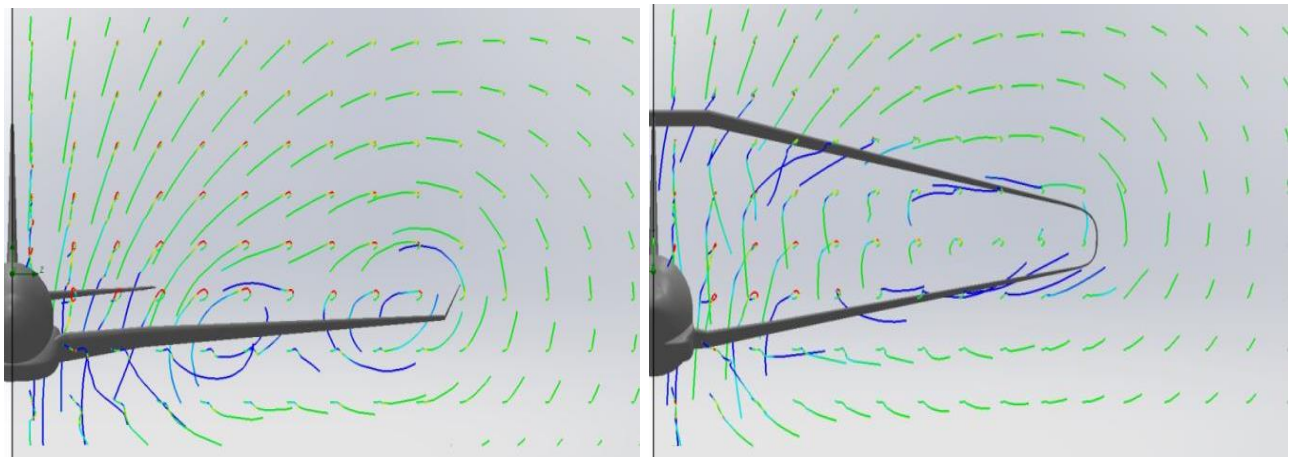

(a) (b)

Fig. 24. (a) Conventional wing vortex, (b) Box wing vortex (31)

In order to reduce the wing tip vortex generated in conventional cantilever wing as seen in figure 24a, the wing tip of the Box wing are closed to form non planner closed wing configuration as shown in figure 24b. It is very evident from the above figure the vortex progression along the span of the cantilever wing combines to form a bigger vortex with winglets being a factor of minimum possible reduction. According to Adeel Kalidh et. al (31), the closed wing design results in reduced vortex which results up to 40% reduction on induced drag compared to cantilever wing configuration (31).

If observed carefully in the figure 23, we can observe a reduced chord length of the aircraft wings. This is due to the lifting surface area being split across 2 wings. One of the disadvantage of this configuration is higher parasite drag compared to the conventional wings and the reduced chord length results in lower operational Reynolds number, high viscous flow and increased skin friction drag (31).

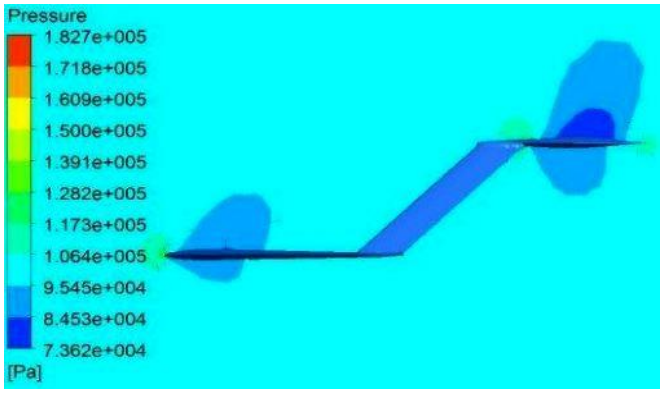

h/b	*e*
0	1
0,05	1,15178
0,1	1,26814
0,15	1,37327
0,2	1,47189
0,25	1,56610

(a) (b)

Fig. 25. (a) Pressure contour for h/b = 0.75 (32), (b) Span efficiency factor vs h/b ratio (33)

In a box wing, Cant angle is angle at which the winglet is placed with respect to main wing. The height to span ratio (h/b) dominates the prominence in Box wing design configuration. A cant angle tilted outward from the wing at the tips with an optimum h/b ratio can significantly reduce the overall induced drag and increase the effective lift across the span of the wings (32).

4.1.4. Multi rotors.

Rotary wing refers to generation of lift by the thrust produced by rotating propellers or blades which work on the principle of aerodynamic lift generation as well. In (table 4) we see that multiple multirotor aircrafts are under development and testing for the concept of UAM. Unlike in previous sections where distributed electric propulsion also consisted of thrust generation through multiple rotors, here the whole principle of lift and cruise system has no usage of aerodynamic wings. A separate lift and cruise system like seen in Aurora eVTOL consists of hybrid configuration. This type of configuration and propulsion system is studied in propulsion as sub section.

(a) (b)

Fig. 26. (a) Ehang 184 (34), (b) Volocopter 2X (35)

In the above figure we see typical multi rotor design configurations which are developed for Urban air mobility. Similar designs are under consideration from different companies for UAM operations. The use of distributed electric propulsion has resulted in usage of small rotors. One of the major advantages of multi rotor configuration is the large payload capability compared to fixed wing aircrafts. The Ehang 184 and Volocopter 2X are single and two seat aircrafts. The Nexus from Bell helicopter is designed to carry 5 passengers in total for UAM operation across various cities. The disadvantage of such configurations is huge power requirements. With innovations in technologies such designs have become economically more feasible but still lack efficiency in parameters like speed, aerodynamics and power requirements. This has led to innovations in Multi-rotor passenger flights in recent times and has found application in UAM operations. The performance of a multi rotor aircraft is influenced by multiple factors. The system design, fuselage and propulsion interface. Fluid flow and interaction is an important parameter to be considered as the multi rotor configuration tend to generate high aerodynamic drag compared to fixed wing system and have low aerodynamic efficiencies in both hover and cruise mode (36).

Fig. 27. 4+1 seat configuration Bell Helicopter Nexus (37)

The above aircraft is a multi-rotor configuration with tilt rotor system. Also, this aircraft consists of 3 surface aircraft design. Nexus has vertical and horizontal control surfaces with a small fixed wing helping to generate small lift assisting the multi rotor system and maintaining the efficiency. This type of tilting propulsion system is discussed in propulsion as sub chapter.

The complications in aerodynamics of a multi rotor or a configuration involving rotor propulsion is that of vortex generated by blade tips and vortex generated by the whole rotor system consisting of multiple blades (36). The spacing of these rotors and fuselage has great impact on the overall system design. The acoustics in aviation industry is a major concern especially with rotor propulsion. The use of multi rotor configuration requires optimisation of the noise levels before it can be proven feasible for the urban air mobility operations. One of most important parameters influencing the sound levels is airflow around the design configuration. This in turn is dependent on separation distances between rotors, interaction of airflow between the fuselage and wings (arms) of propulsion system (36).

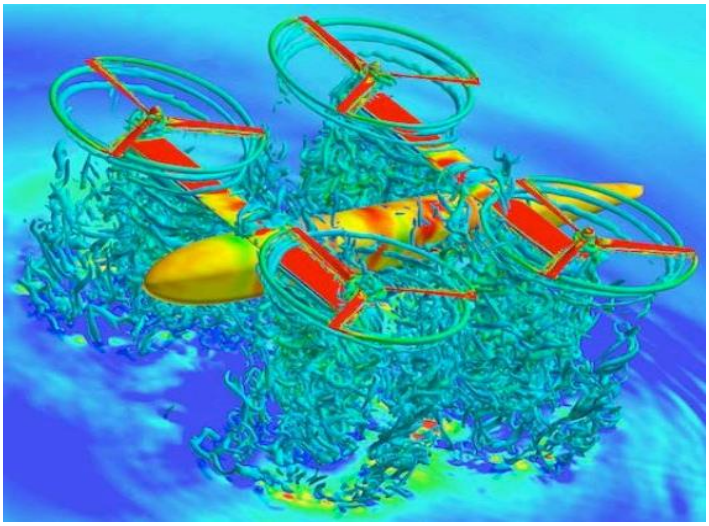

Fig. 28. Q-Criterion and pressure for a generic quad tiltrotor in hover mode (36)

In a research conducted by Seokkwan Yoon et.al (36), The influence of rotor spacing on aerodynamic efficiency and noise levels were studied with the help of Q-criterion method which is a vortex identification method used in CFD. According to the result obtain from this study, the quad rotor system generated 3% higher thrust compared with thrust produced by 4 individual rotors. Also the total net vertical force generated in the VTOL system consisted of high positive contribution from the rotors but considerably more negative vertical force from the wings (arms) and little from the fuselage (36). It was noted from the study that as the distance between the rotos increases, the overall aerodynamic efficiency reduces. The fuselage adds to the stability of the system by helping reduce the interaction of different rotor flows or vortices (36). Although this configuration has some added advantages compared to the fixed wing system, the noise and power requirements remain a concern.

4.1.5. Blended Wing Body (BWB) aircraft

Unlike the other aircraft studied above, the concept of blended wing aircraft is recent. Although not completely new since the idea of flying wing was tested which dates to post wold war ear and has been extensively tested and flown for various military purposes. Blended wing body design does not have a distinguishable fuselage and wing. The absence of tail is not a distinguishable feature in BWB design as many concepts with it were also noted during the research. The primary control surfaces are embedded in the structural design itself. Unlike the conventional designs were the lift is generated only by the wing mainly or rotor blades in case of rotary wing, here the whole design configuration of the aircraft contributes to lift including the fuselage, unlike in classical configuration its purpose is to house and carry the payload. The term blended wing is different from flying wing. In the Blended wing aircraft multiple sweep angles are merged to form a blended aerodynamic design (38).

In Blended wing aircraft system lift is generated both by the central body and by lateral wings. This produces an outcome of enhanced L/D ratio compared to the conventional design (38). The Blended wing design of aircrafts offers multiple advantages with respect to engine placement which in turn can help reduce the noise levels because of shielding effect produced by the central body (38).

Fig. 29. Proposed VTOL blended wing concept for UAM by Pipistrel vertical solutions (39)

Although a large amount of research and publications are available for the application of BWB in large transport aircrafts. Very less or none were found for small aircraft designs. The BWB aircraft has the potential to be more efficient and less fuel consumption compared to the conventional design with same capabilities (40).

Some of the aerodynamic advantages of BWB compared to other configurations mentioned above are (40):

- Reduced wetted area;
- reduced Skin friction drag;
- reduced wing loading as the centre body contributes to lift;
- reduced Interference drag as there is less or no structural assemblies.

The lift generated by the central body of blended wing body aircraft results in lower wing loading (Figure 30). This in turn helps the aircraft to achieve excellent low speed characteristics. This type of configuration also comes with challenges like, absence of tail requires to maintain controllability and trims facilitated in the centre body and wings. In order to accommodate payload, the aircraft's centre portion requires usage of thick aerofoil shapes which might create more profile drag (40).

Ideally BWB aircraft is trimmed to cruise condition. Reflex aerofoils are also used in order to achieve the trim characteristics. Ideally the typical values for thickness of aerofoils for the centre section is 16-18% (t/c) (38).

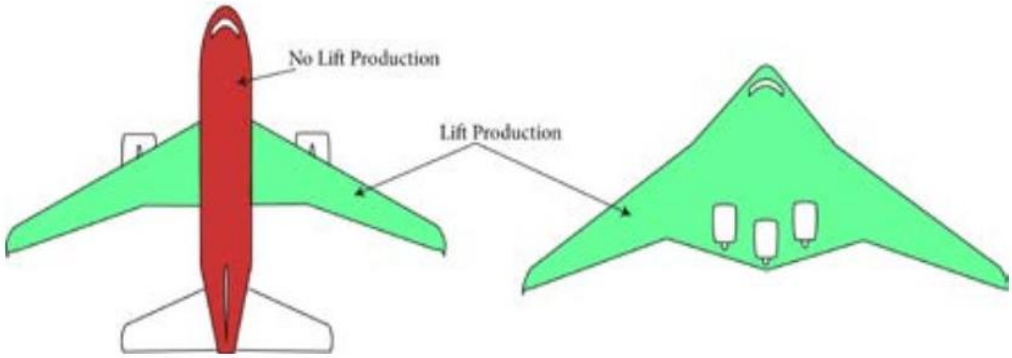

Fig. 30. Lift production comparison between the BWB and a conventional airliner (41)

The complications of the blended wing design are that, the conventional control surfaces are absent or are more complexly embedded to the BWB design configuration. The elevons which act as the control surface for the pitch and roll movement are used. Combination of active and passive control surfaces are used for efficient control and stability of the aircraft (41). As we see from above figure 30, The BWB configuration consists of a non-circular cross section. The urban air mobility concept does not require operation of the aircraft at high altitudes. This eliminates the need for pressurization of aircrafts where cylindrical fuselage is efficient. Hence, the non-cylindrical cross section is not of a concern here.

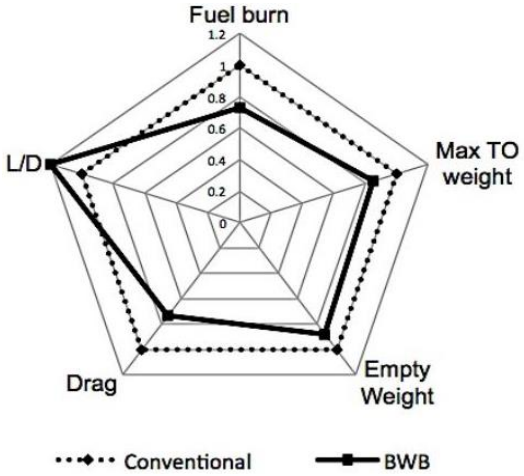

Fig. 31. Performance comparison between a conventional and BWB configuration (41)

A study done by Marino et al (41), which consisted of comparison between a conventional aircraft design and BWB aircraft design. Some of the observation were made (41) in which BWB design had:

- 27% less fuel burn;
- 15% weight savings;
- 12% reduced empty weight;
- 27% reduced thrust requirement;
- 20% more L/D ratio;
- expected 50% less emission in commercial airline operation by 2050 (Large aircrafts).

Table 5. Pros and cons of BWB aircraft design

Sl. No	Pros	Cons
1	Even Weight distribution	Cabin structure and configuration
2	Noise reduction	Hybrid Control surface
3	Enhanced L/D ratio	Low Static Margin scope
4	efficient MTOW capability	Very new concept in the aviation industry
5	Scope for exploring applications	Very less data available for General aviation

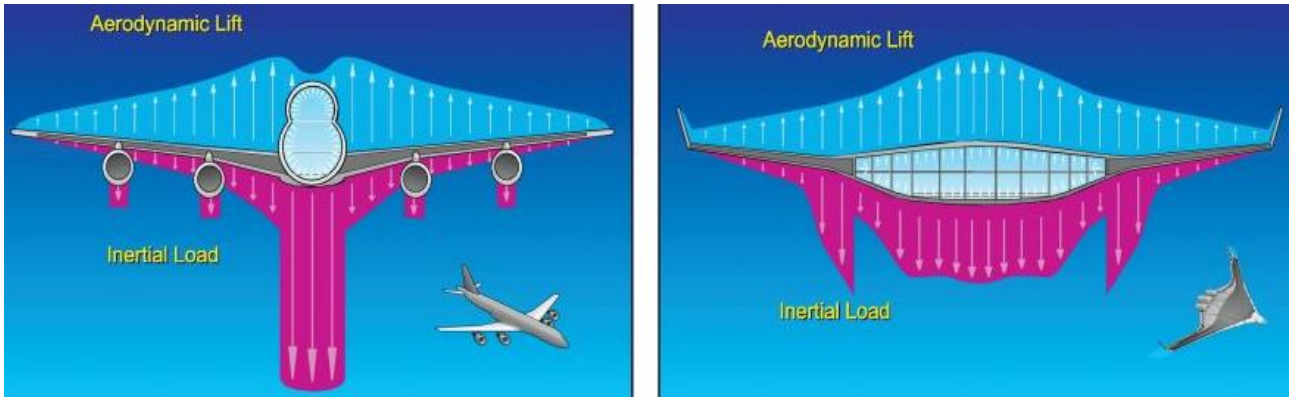

(a) (b)

Fig. 32. (a) TAW (b) BWB; Comparison of aerodynamic, inertial, and cabin pressure loads (42).

Above figure gives a clear idea about the aerodynamic lift distribution on the blended wing body aircraft design. High lift is generated from the central body reducing the loading on the wings. The inertial load is evenly distributed making the static stability of the aircraft better compared to conventional design. The pressure distribution is efficient in the TAW configuration, but a lot of scope is available in BWB as well. The T/W ratio requirement is reduced in case of BWB compared to the TAW configuration which turns to be more economical in the airline industry involving large transport aircrafts.

Table 6. Comparison of BWB design variants L/D ratio for similar Wetted area and volume (43)

Design Type	$(L/D)_{MAX}$	C_L cruise	L/D cruise
Conventional (TAW)	20.6	0.47	19.7
All wing	25.7	0.24	23.2
Blended wing Body (BWB)	*26.1*	*0.28*	*24.4*
Hybrid Flying wing	24.5	0.36	22.1

4.2. Brief overview of Aerodynamics trade study:

In above trade study presented a series of different configuration under consideration for the concept of urban air mobility was studied. The concept of UAM requires light weight, eco-friendly, and low space consumption and similar urban environmental favourable characteristics. A brief comparison of all the features of different configuration studied in aerodynamic trade-off is tabulated below. The feasibility matrix with weightage from 1 to 5 gives clear idea of the best design consideration for the concept of urban air mobility.

Note:

- Weightage ranges from 1 being the worst to 5 being the best;
- total weightage per matrix depends upon the number of variables considered for the comparison;
- combined values from all the Feasibility matrixes is analysed;
- acoustics or noise feasibility is not considered here and is studied under propulsion as sub section.

Table 7. Aerodynamics Feasibility Matrix (AFM)

Sl. No	**Aircraft type**	**Induced Drag**	**Lift**	**(L/D) Max**	**Lifting Area**	**Total**
1	TAW	2	3	3	3	11
*2	Tandem Wing	3.5	3.2	3.3	3.8	13.6
*3	Box wing	3.5	3.5	3.4	3.7	14.1
**4	Multi rotor	1.5	3	2.5	3	10
5	*BWB*	*3.8*	*4.5*	*3.8*	*4.8*	*16.9*

*Weightage given is for total combined lifting surfaces
**Efficiency factors considered

Table 8. Structural Feasibility Matrix (SFM)

Sl. No	**Aircraft Type**	**Area (square) occupied on ground**	**MTOW/Empty Weight Fraction**	****Wing loading**	**Total**
1	TAW	2	3	3	8
*2	Tandem Wing	3.4	3.2	3.5	10.1
*3	Box Wing	3.3	3.1	3.7	10.1
4	Multi Rotor	4	4	3.5	11.5
5	*BWB*	*3.8*	*3.8*	*4*	*11.6*

* Weightage given is for total combined lifting surfaces
**Disc Loading in case of a multi rotor

Table 9. Operational Feasibility Matrix (OFM)

Sl. No	**Aircraft Type**	***Power Requirements (Hybrid Propulsion)**	**Stability and Control**	**VTOL capability**	**Total**
1	TAW	3	3.5	3.2	9.7
2	Tandem Wing	3.2	3.2	3.9	10.3
3	Box Wing	3.2	3	2.5	8.7
4	*Multi Rotor*	*3*	*4*	*5*	*12*
5	BWB	3	3	2	8

*Electrical power equivalent to conventional propulsion is taken into consideration for aircrafts where Hybrid or fully electric data are not available.

The combined feasibility matrix is based on the merit. It means that the order in which the aircraft type is arranged in the table below will have the highest combined value of aircraft on the top and follows down the table in a decreasing order.

Table 10. Combined Feasibility Matrix (General) (CFM)

Sl. No	**Aircraft Type**	**Total (AFM)**	**Total (SFM)**	**Total (OFM)**	**Total (CFM)**
1	TAW	11	8	9.7	28.7
2	Tandem Wing	13.6	10.1	10.3	34
3	Box Wing	14.1	10.1	8.7	32.9
4	Multi Rotor	10	11.5	12	33.5
5	*BWB*	*16.9*	*11.6*	*8*	*36.5*

Table 11. CFM based on Merit

Aircraft Type	**Total**
BWB	*36.5*
Tandem Wing	34
Multi rotor	33.5
Box Wing	32.9
TAW	28.7

Clearly from table 11 it can be concluded that Blended wing Body aircraft is best suited for UAM concept. With proper trade-offs achieving VTOL capability is not difficult. Although other configurations look inferior, all the configurations are subjected to changes with evolution in technology.

4.3. Propulsion system:

As mentioned earlier the goal of this project to is to design a multipurpose BWB aircraft having applications in UAM but not limited to it. A brief study of the already existing propulsion systems which are proposed for UAM are mentioned below:

4.3.1. Distributed Electric Propulsion (Ducted)

As studied in earlier section, Most of the UAM concept proposed and developed uses distributed electric propulsion. The type of DEP used varies according to type of configuration used and position of placement. Since the DEP concept consists of many small propulsion units providing equivalent thrust of 1 required power plant, a significant amount of drag also is a concern. Some of the techniques are discussed below

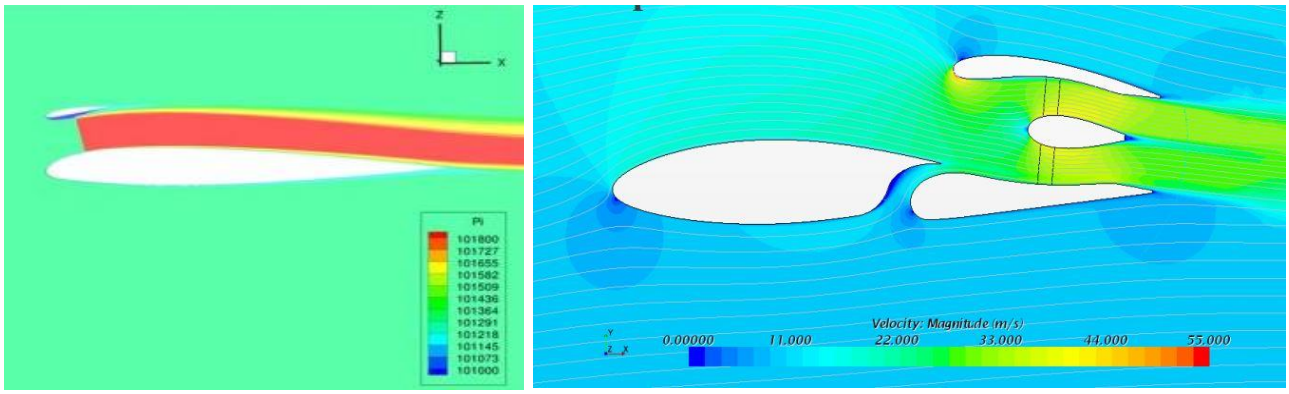

(a) (b)

Fig. 33. (a) Ducted DEP in leading edge (44), (b) Ducted DEP in trailing edge (45)

The Ducted fan propulsion system in the leading-edge lacks VTOL capability or the complexity of facilitating such a design is high. Whereas in the trailing edge it is very much feasible and widely being tested too. In both the cases the flow over the wings is more efficient and reduced induced drag properties are observed. In case of ducted fans, the thrust developed is more and resulting noise is also less. But in case of multi rotors where the lift generation required big rotors, the use of duct might increase the overall thrust by a small percentage, but the noise still will remain a significant concern.

Fig. 34. DEP components (44)

The components and configuration used in DEP is like the RC aircraft system. It consists of ducted fan or a propeller powered by a brushless motor in turn connected to the electronic speed controller (ESC) and the system is usually powered by a li-po battery.

4.3.2. Distributed electric propulsion (Open propeller)

This type of propulsion is the most widely developed and implemented in UAM concepts like Airbus vahana, Opener blackfly, Aurora eVTOL etc. The open rotor system can be classified in to 2 types:

1) Tilt Wing system;
2) Separate lift and cruise system.

In the tilt wing system like seen in opener black fly and airbus vahana, the open rotor propulsion system tilts from vertical hover position to horizontal cruise mode gradually creating a forward motion. Since such systems include the whole wing tilting, a significant amount of lift is still generated in hover mode as well. Only the use of appropriate aerofoil and design can reduce the unnecessary pitching moment created.

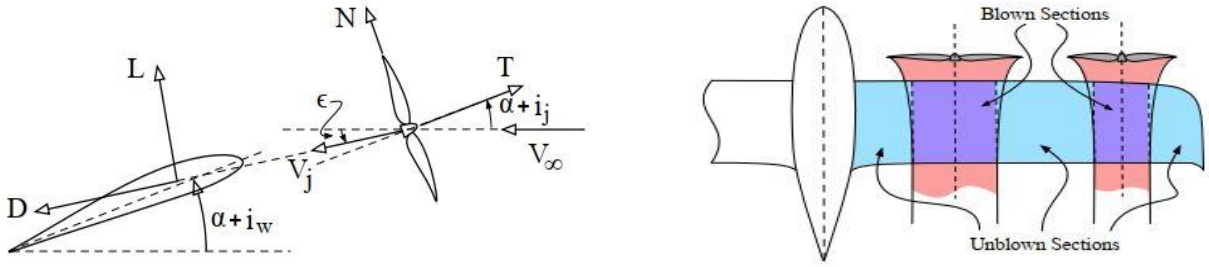

Fig. 35. Wing AOI i_w, Jet AOI i_j, Fuselage AOA α with the lift L, drag D, thrust T and normal force of the propeller N, downwash of the propeller ε, slipstream of the jet V_j (46).

In the separate lift and cruise system like seen in Aurora eVTOL and Kitty Hawk Cora, the aircraft is powered by Some rotors for the hover mode and a separate rotor in the rear for the cruise mode. Although such a system is complex, it does not have complex techniques of tilting and in case of emergency the stability of the aircraft is secured. But the major disadvantage is the total drag produced and the increased overall empty weight (47).

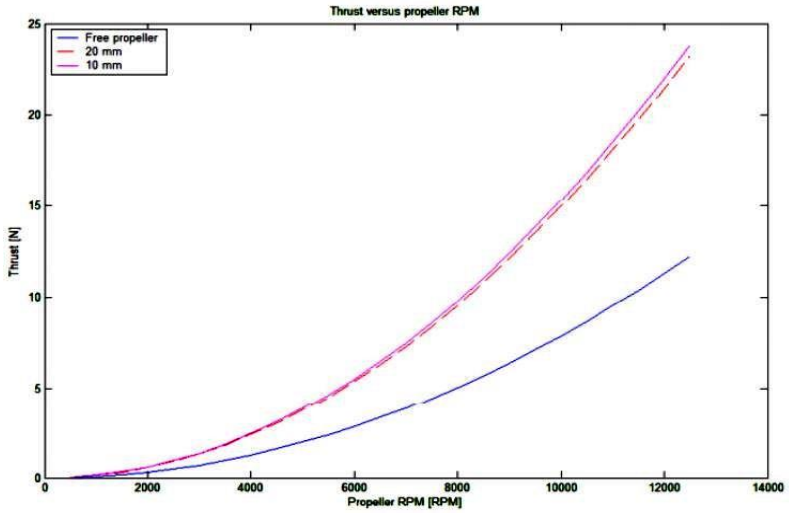

Fig. 36. Ducted vs open propeller thrust comparison (48)

The above graph clearly gives the idea about the major advantage of the ducted fan propulsion system compared to the free propeller. It can be clearly seen that the thrust generated by ducted fan is significantly higher for the same RPM compared to open propeller system.

5. Initial Sizing

5.1. Existing GA Twin engine aircraft data

Table 12. 5-6 seat GA aircraft design values

Aircraft	**Engines**	**Number of seats**	**MTOW (kg)**	**Wing Area (m^2)**	**Wing Loading (N/m^2)**
Diamond DA62	2	5-6	2300	17.10	1319.47
Cessna 310R	2	5	2087	16.258	1259.2
Beechcraft B55 Barron	2	5-6	2313	18.51	1225.8
Piper PA-23	2	5	2359	19.283	1200

The average value of wing loading is 1251.1175 N/m^2

Table 13. 5-6 seat GA aircraft performance parameters

Aircraft	**Rate of Climb (m/s)**	**Wingspan (m)**	**Aspect Ratio (AR)**	**Take off Distance (m)**
Diamond DA62	6.1	9.19	5	-
Cessna 310R	8.6	10.67	7.2	-
Beechcraft B55 Barron	8.5	11.53	7.18	511
Piper PA-23	7.1	11.341	6.67	517

The average values of the performance parameters which are considered for the design in constrain analysis are as follows:

- Rate of climb: 7.5 m/s
- Wingspan: 10.68 m
- Aspect Ratio: 6.5
- Take off Distance: 514 m

5.2. Weight Estimation

An aircraft weight builds up process is one of the most important estimations to be made before the initial sizing is considered. The MTOW of an aircraft is the ultimate load that an aircraft can carry on take-off. In order to determine this several weights contributing factors are to be considered. A broad classification of weights to be considered according to author of (49) is as follows (49)

a) *Payload Weight (W_P)*: In this project. The aircraft is being developed for multipurpose. Hence, Passengers, Firefighting capabilities, Emergency services are considered as different operation scenarios.
b) *Crew Weight (W_C)*: Single pilot is considered.
c) *Battery Weight (W_B)*: (Since the aircraft is planned to be electrically powered, battery weight is considered)
d) *Empty Weight (W_E)*: It is obtained from statistical data for initial calculations
e) *Maximum Take-off weight (W_{MTOW})*

$$W_{MTOW} = W_P + W_C + W_B + W_E \quad (2)$$

- W_P is estimated as follows:

According to CS 23 regulations, the weight of each passenger to be considered is 77 kg to 86 kg. Hence an average weight of 81.5 kg is considered. Since the aircraft to be designed is for a 5-seat configuration the total passenger weight for the aircraft is 407.5 kg

Since the aircraft is being designed for multipurpose usage like intercity or airport shuttle, an additional baggage allowance of 23 kg·2 = 46 kg per passenger is considered. Hence, for 5 passengers the total baggage allowance is 230 kg

Hence the total Payload weight is approximately:

$$W_P = Total\ Passenger\ weight + Total\ baggage\ weight$$

$$Wp = 640 \text{ kg}$$

This means the aircraft is capable of also transporting replaceable payload up to 640 kg in case of firefighting, medical emergency or similar mission purposes.

- W_C is estimated as follows:

According to CS 23 regulation, the weight of the crew member, pilot in the case of the aircraft in consideration here is 77 kg. Assuming an allowable baggage of 23 kg, the total crew weight is:

$$W_C = 100\ kg$$

- W_B refers to the weight of the battery system. Unlike in conventional aircrafts the electric propulsion mode is powered by strong battery packs. The weight of these battery packs also increases with the total weight of the aircraft.

In order to arrive at an approximate battery weight for a 5-seat aircraft statically data's and approximations are considered. In the specification of Pipistrel Taurus G4 published by Tine Tomažič et. al (50), The weight of the battery packs for a 4-seat aircraft was calculated to be 500 kg. Hence for the 5+1 seat configuration using mathematical approximations, the weight of the battery packs can be approximated as:

$$W_B = 750\ kg$$

- Although there are Empty weight approximation methods, for better and accurate outcome the statistical data are used. Keeping the Pipistrel Taurus G4 as the base of reference whose empty weight was calculated to be 632 kg. Hence; using mathematical approximations we can estimate the Empty weight of a 5+1 seat aircraft to be:

$$W_E = 948\ kg$$

Therefore,

The total MTOW of the aircraft be calculated by substituting all the values in above equation:

$$W_{MTOW} = 640 + 100 + 750 + 948$$

$$W_{MTOW} = 2438\ kg$$

$$W_{MTOW} = 2440\ kg \text{ or (5380 lb)}$$

According to CS 23 weight regulations for aircrafts, the estimated 2440 kg aircraft comes under single engine or twin-engine aircrafts under 2722 kg (6000 lb) (9)

The about weight is the Maximum take of weight which has been considered for the initial sizing of the aircraft. In S.I units, the MTOW is:

$$W_{MTOW} = 23936.4 \text{ N}$$

5.3. Performance Parameter estimations

The next important step after the weight estimation is to estimate the required wing area and thrust output. Considering the UAM concept with requires VTOL design capabilities, a special case is considered at the end the constrain analysis. Here the aircraft is considered as a CS 23 category aircraft and the design process is carried out.

In order to arrive at the wing area and thrust approximations, several parameters are considered based on the statistical data and other aeronautical relations.

a) *Number of crew and passengers*: 1+5
b) *Engines*: 2 for general purpose and DEP for UAM concept with VTOL capability.
c) *MTOW*: 2440 kg, in S.I units: 23937 N
d) *Turn Load/Speed/Height*: The speed and height are the cruise speed and height which is 290 km/h and 3280 feet respectively. In S.I units: 81 m/s and 1000 m respectively.

The turn load is related to roll and according to CS 23.157 the recommended bank angle is:

$$\Phi = 60°$$

Hence the Turn load can be calculated as (11):

$$\Phi = \cos^{-1}\left(\frac{1}{n}\right) \tag{3}$$

$$n = \frac{1}{\cos \Phi} = \frac{1}{\cos 60} = 2$$

Therefore, the turn load is:

$$n = 2g$$

e) *Rate of Climb at sea level (ROC)*:

According to CS 23 requirements, suggested climb gradient is 4% and a climb speed not less than $1.3V_S$, Therefore:

Climb speed is V_V = 40 m/s and ROC at sea level is 7.5 m/s

f) Take off run/speed:

Take off speed is considered slightly higher than the Stall speed (49), that is:

$$V_{TO} = 1.2V_S$$

For CS 23 aircraft the stall speed suggested is not more than 61Knots or 113 Km/h. in S.I units 31 m/s. Hence;

V_{TO} is 37 m/s

The aircraft is also designed to meet short take-off and landing requirement to make it feasible to operate from small airports. Hence take off run is:

$$S_g = 400 \text{ m}$$

g) Cruise Speed/Height: 81 m/s and 1000 m
h) Service ceiling: 10000 ft, in S.I units: 3048 m
i) Aspect ratio of the Wing: 6.5
j) The Author in reference (49) suggests the maximum aircraft velocity as:

$$V_{MAX} = 1.25V_C$$

As obtained from the trade studies, the cruise velocity is 81 m/s. hence the maximum velocity of the aircraft can be estimated as:

$$V_H = V_{MAX} = 101.25 \text{ m/s}$$

According to CS 23.335 regulation, the V_C need not be more than 0.9 V_H (9). This results in V_C = 91 m/s. Also, the V_C considered in this project is 81 m/s. Hence; it can be considered as an acceptable value for the initial design.

k) Assuming the aircraft to take off from a concrete runway: The rolling friction coefficient is taken to be:

$$\mu = 0.04$$

Few other important aerodynamic factors like $C_{D_{min}}$, $C_{D_{TO}}$, $C_{L_{TO}}$,and other similar parameter are estimated by preliminary analysis for similar aerofoils and conditions.

Based on BWB aircraft data for large aircrafts, the following aerodynamic coefficients were taken as reference for preliminary design from other similar concepts.

l) Maximum lift coefficient: C_L for take-off: 1.6
m) Drag coefficient at take-off: C_D for take-off: 0.04
n) Minimum drag coefficient: C_{Dmin} is 0.009

The sweep angles are another parameter of the aircraft to be considered. High sweep angles reduce the lift in the wing tips but also provides scope for distributed CG across the aircraft. Hence;

o) Wing sweep from the root to Average chord of the aircraft: 30°
p) Wing sweep from the Average chord to wing tips: 48°

5.4. Wing Area and thrust requirement estimation

The wing area and thrust sizing is done with the help of constrain diagram. The Constrain analysis is done with the help of MATLAB programme (Appendix 1). Before plotting, the sizing parameters listed in above section is applied to various (T/W) sizing formulas given by the author of reference (11).

The sizing parameters are considered for different aircraft requirements such as:

- Stall requirements
- Take-off requirements
- Climb requirements
- Cruise requirements
- Turn requirements

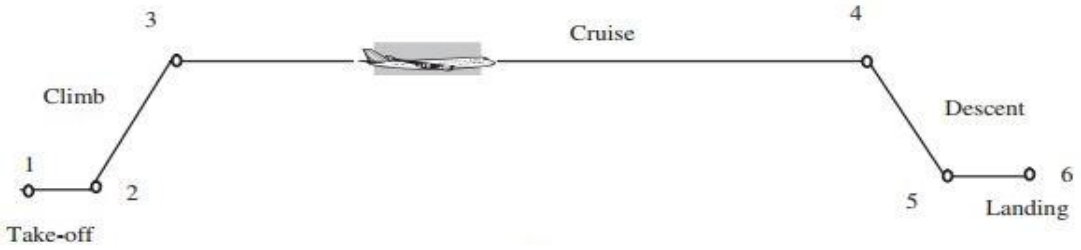

Fig. 37 Various phase of aircraft flight

The equations used for the wing area sizing of various requirements are modified form of lift equation. The wing loading is defined as the ratio of MTOW to planform area given by:

$$Wing\ Loading = \frac{Weight\ of\ the\ Aircraft}{Total\ Wing\ Area} \tag{4}$$

In modified terms of lift equation:

$$\frac{W}{S} = \frac{1}{2}\rho V^2 C_L \tag{5}$$

Ever variable in the above equation changes based on the type of phase the aircraft is considered for the design. For example, the stall requirement of wing loading for above equation can be written as:

$$\left(\frac{W}{S}\right)_{Stall} = \frac{1}{2}\rho_{Stall} \cdot (V^2)_{Stall} \cdot (C_L)_{Stall} \tag{6}$$

In the methodology mention by author in reference (11), with the help of simplified drag model, the aircraft performance characteristics are transformed into relation where thrust to weight ratio is a function of wing loading in the form of:

$$\left(\frac{T}{W}\right) = f\left(\frac{W}{S}\right) \tag{7}$$

The sizing parameter approximations have been substituted in the below equations with respect to the different requirements mentioned above. The equations have been referred from reference (11) and is incorporated in MATLAB program for a range of wing loading values.

- Thrust to weight ratio for turn requirements is given by (11):

$$\frac{T}{W} = q \cdot \left[\frac{C_{D_{min}}}{\frac{W}{S}} + k \cdot \left(\frac{n}{q}\right)^2 \cdot \frac{W}{S} \right] \tag{8}$$

- Thrust to weight ratio for climb requirements is given by (11):

$$\frac{T}{W} = \frac{V_V}{V} + \frac{q}{\frac{W}{S}} \cdot C_{D_{min}} + \frac{k}{q} \cdot \frac{W}{S} \tag{9}$$

- Thrust to weight ratio for Take-off requirements is given by (11):

$$\frac{T}{W} = \frac{{V_{TO}}^2}{2g \cdot S_G} + \frac{q \cdot C_{D_{TO}}}{\frac{W}{S}} + \mu \cdot \left(1 - \frac{q \cdot C_{L_{TO}}}{\frac{W}{S}} \right) \tag{10}$$

- Thrust to weight ratio for cruise requirements is given by (11):

$$\frac{T}{W} = q \cdot C_{D_{min}} \cdot \left(\frac{1}{\frac{W}{S}} \right) + k \cdot \left(\frac{1}{q}\right) \cdot \left(\frac{W}{S}\right) \tag{11}$$

- Thrust to weight ratio for service Ceiling is given by (11):

$$\frac{T}{W} = \frac{V_V}{\sqrt{\frac{2}{\rho} \cdot \frac{W}{S} \cdot \sqrt{\frac{k}{3 \cdot C_{D_{min}}}}}} + 4 \cdot \sqrt{\frac{k \cdot C_{D_{min}}}{3}} \tag{12}$$

The dynamic pressure in each case above is calculated for different altitude, speed and density, given by the equation:

$$q = \frac{1}{2} \cdot \rho \cdot V^2 \tag{13}$$

The inviscid or induced factor is given by (11):

$$k = \frac{1}{\pi \cdot AR \cdot e} \tag{14}$$

$$k = 0.067$$

The Oswald's span efficiency is given by (11):

$$e = 1.78 \cdot (1 - 0.045 \cdot AR^{0.68}) - 0.64 \tag{15}$$

$$e = 0.85$$

Lower the aspect ratio, higher is the span efficiency.

5.5. Constrain Analysis:

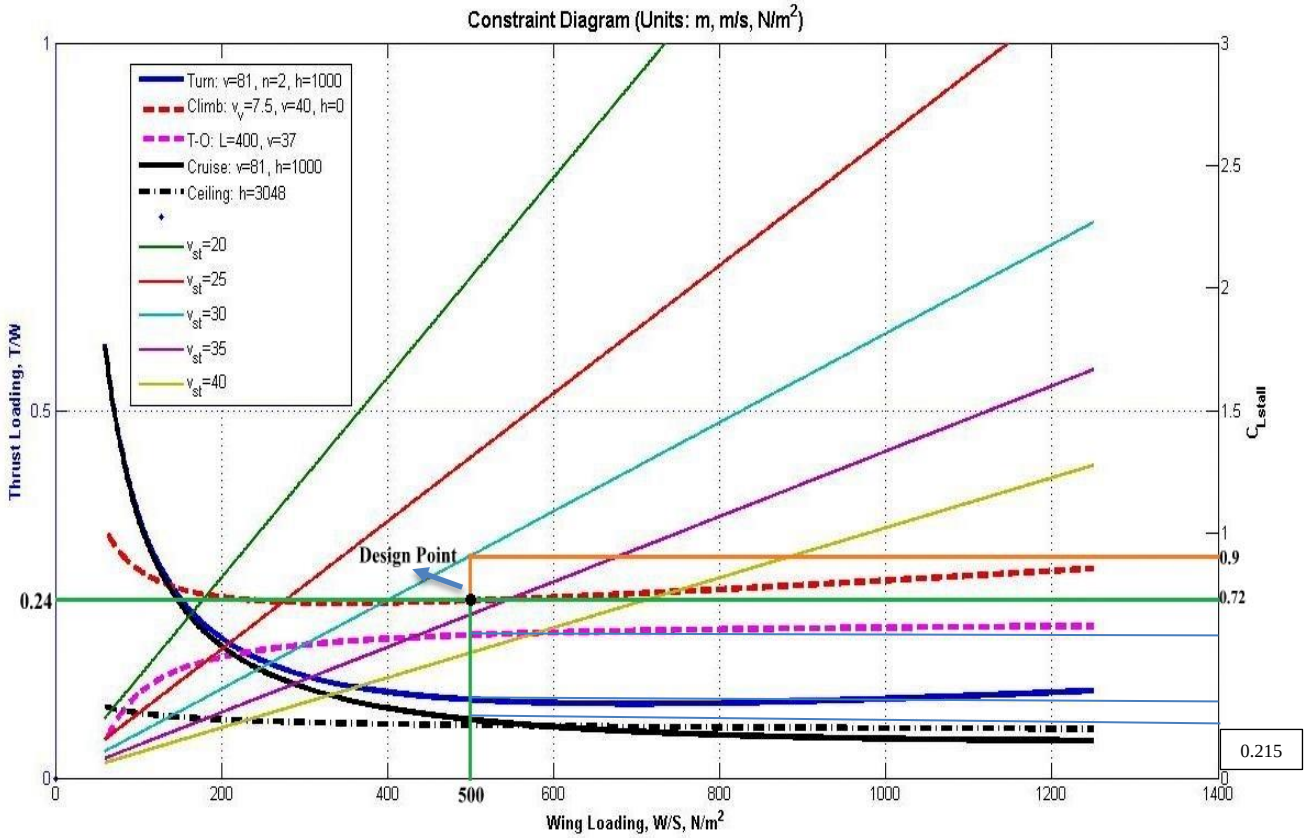

Fig. 38. Aircraft Constrain diagram

From the above figure we can see that the optimum design point which meets all the requirements within the recommended stall speed of 31.40 m/s according to CS 23 regulation is at wing loading equal to 500 N/m^2. The corresponding other parameter is:

- T/W = 0.24 (For GA purpose only). In case of UAM concept, T/W is equal to 1 or 1.3 in order to facilitate VTOL capabilities.
- C_{Lmax} Clean = 0.72 for climb requirements and C_{Lmax} with high lift device = 0.9 to achieve lower stall speeds

It is clear from the constrain analysis that with the use of high lift device or with better lifting aerofoils the aircraft can operate in lower stalling speeds as well. From the above constrain analysis the following conditions are obtained for the operation of the aircraft at different altitudes and phases:

- With a wing loading of 500 N/m^2 for the aircraft's cruise at 1000 m and ceiling at 3048 m requires a lift coefficient of 0.215
- To meet the turn requirement at 1000 m with 2g loading and a velocity of 81 m/s, the lift coefficient requirement is 0.317
- To meet the take-off requirements at 37 m/s, the lift required for the aircraft is 0.571.
- The highest thrust and lift requirements was found to be in the climb phase with lift needed up to 0.72

5.5.1. Aircraft initial geometric sizing:

From the Constrain diagram:

$$Wing\ Loading = \frac{MTOW}{S} \tag{16}$$

Therefore, wing area is:

$$S = 47.872\ m^2$$

For an AR of 6.5 used in constrain analysis, The Span of wing is given by:

$$AR = \frac{b^2}{S} \tag{17}$$

$$b = 17.64\ m$$

In order to facilitate easy VTOL capabilities, it is necessary to house the engines using DEP concept in trailing edges of the wing. The aircraft is being designed for 2 configurations. One is for it operate as general Aviation aircraft and other is to facilitate UAM operation feasibility.

Hence from table 9-5 in reference (11), the taper ratio is taken to be:

$$\lambda = 0.3$$

The root chord or the centre lifting body is calculated as:

$$C_r = \frac{2 \cdot b}{(1 + \lambda) \cdot AR} \tag{18}$$

$$Cr = 4.175\ m$$

For the ease of design, the Final Root chord used in design is:

$$C_r = 4.2\ m$$

The Tip chord can be calculated as:

$$\lambda = \frac{C_t}{C_r} \tag{19}$$

$$C_t = 1.26\ m$$

Average chord length is given by:

$$C_{avg} = \frac{C_r + C_t}{2} \tag{20}$$

$$C_{avg} = 2.73\ m$$

The Mean Geometric chord is given by:

$$C_{MGC} = \frac{2}{3} \cdot C_r \cdot \left(\frac{1+\lambda+\lambda^2}{1+\lambda}\right) \quad (21)$$

C_{MGC} = 2.993 m

C_{MGC} = 3 m

The location of Mean Geometric chord from the Root of the wing is given by:

$$Y_{MGC} = \left(\frac{b}{6}\right) \cdot \left(\frac{1+2\lambda}{1+\lambda}\right) \quad (22)$$

Y_{MGC} = 3.618 m

Some of the other important parameter which influence the aerodynamic design are listed below. Since no small aircraft with Blended wing Body design were found

In order to prevent extreme stall, the inboard section was given less sweep with 30 degrees and a higher sweep angle for the outboard section

- Wing Sweep root chord to Average chord: 30°
- Wing Sweep Average chord to Tip chord: 48°

The sweep has direct effects on lift characteristics being reduced. The tips with small chord length are expected stall quicker than the rest of the wing. The sweep gives a maximum advantage of overall span length is decreased and allows more space for operation

Reynold's number in cruise condition:

- ρ = 1.225 kg/m3
- V=81 m/s
- Length of Chord in root: 4.2 m
- Dynamic viscosity $1.7045 \cdot 10^{-5}$ Kg/m-s

$$Re_{Root} = \frac{\rho \cdot V \cdot L}{\mu} \quad (23)$$

$Re_{Root} = 24 \cdot 10^6$

- Length of chord at the tip: 1.26 m

Hence;

$Re_{Tip} = 7 \cdot 10^6$

The Reynolds number in cruise condition from tip to root ranges between 7 to 24 million.

6. Aerofoil analysis and Selection

The lift to drag ratio is one of the most important parameters of any aircraft design configuration. As seen in the trade studies all the different configuration deal with increasing the L/D ratio and minimising the induced drag generated from the lift generating surfaces. The lift to drag ratio equation is given by (49):

$$\frac{L}{D} = \frac{Lift}{Drag} = \frac{\frac{1}{2} \cdot \rho \cdot V^2 \cdot S \cdot C_L}{\frac{1}{2} \cdot \rho \cdot V^2 \cdot S \cdot C_D} = \frac{C_L}{C_D} \tag{24}$$

With lift coefficient comes pitching moment which is a natural force in the vertical axis given by:

$$M = \frac{1}{2} \cdot \rho \cdot V^2 \cdot S \cdot C_M \tag{25}$$

In the design of blended wing body aircraft, the centre body also contributes to most of the lift while the load is reduced on the wings. In order to select the aerofoils, several factors have been considered. Based on literature studies the following aerofoils were shortlisted for analysis.

Some of the aerofoils which are analysed below are as follows:

- Eppler Aero foil
- NACA aero foil
- NASA aero foil
- Wortmann aero foil

All the above aerofoils have been designed for delayed flow separation. The minimum pressure is in forward and the thickest part of the aero foil making it to generate a high lift coefficient for the aircraft. Some of the aerofoils like HS 522 exhibited a drag bucket region.

The required aircraft cruise lift coefficient is given by (49):

$$C_{L_C} = \frac{2W}{\rho\left(V_C{}^2\right)S} \tag{26}$$

Cruise Lift coefficient = 0.124

The required maximum lift coefficient is given by (49):

$$C_{L_{MAX}} = \frac{2W_{TO}}{\rho V_S{}^2 S} \tag{27}$$

The maximum lift coefficient = 0.828

From constrain analysis the required lift coefficient to achieve stall speed of 31.4 m/s is 0.9. From the studies made, a series of similar aero foils are considered for the analysis and the appropriate aero foil are used for chose for various sections of the aircraft.

6.1. Centre body aero foil analysis in XFLR5:

Generally, aerofoils having (t/c) ratio between 16-18% are suggested (38). The below listed aero foils were found to be used and suggested by various publication for the centre body of the aircraft during the trade studies (38).

1. Eppler 417
2. NACA 23112 (Reflex)
3. NASA SC (2)-0518
4. NASA SC (2)-0410
5. NACA 0015

In order to analyse the above aero foils, XFLR software has been incorporated, it has been very widely suggested for basic preliminary aerofoil analysis. The analysis of the aerofoils is done through batch analysis. This helps to compare the results and obtain an average value of the various aerodynamic coefficients which can used for the design in later stages.

The following are details of analysis done:

- Aerofoil coordinates used: Selig format dat file from reference (51)
- Type of analysis: Multi-Threaded Batch analysis using 4 cores.
- Number of iterations: 1000
- Sequential analysis with 1° increment and AOA ranging from -20 to +20
- Reynolds number range from $5e10^5$ to $21e10^6$
- Type of polar analysis: Fixed Speed with Mach number 0.24

6.1.1. Polar curve of Batch Analysis for different aerofoils considered.

Since the aircraft is expected to operate at high Reynolds number. The below polar are for AOA=0, Re= $21e10^6$ and for a cruise condition of Mach number 0.24 or 81 m/s

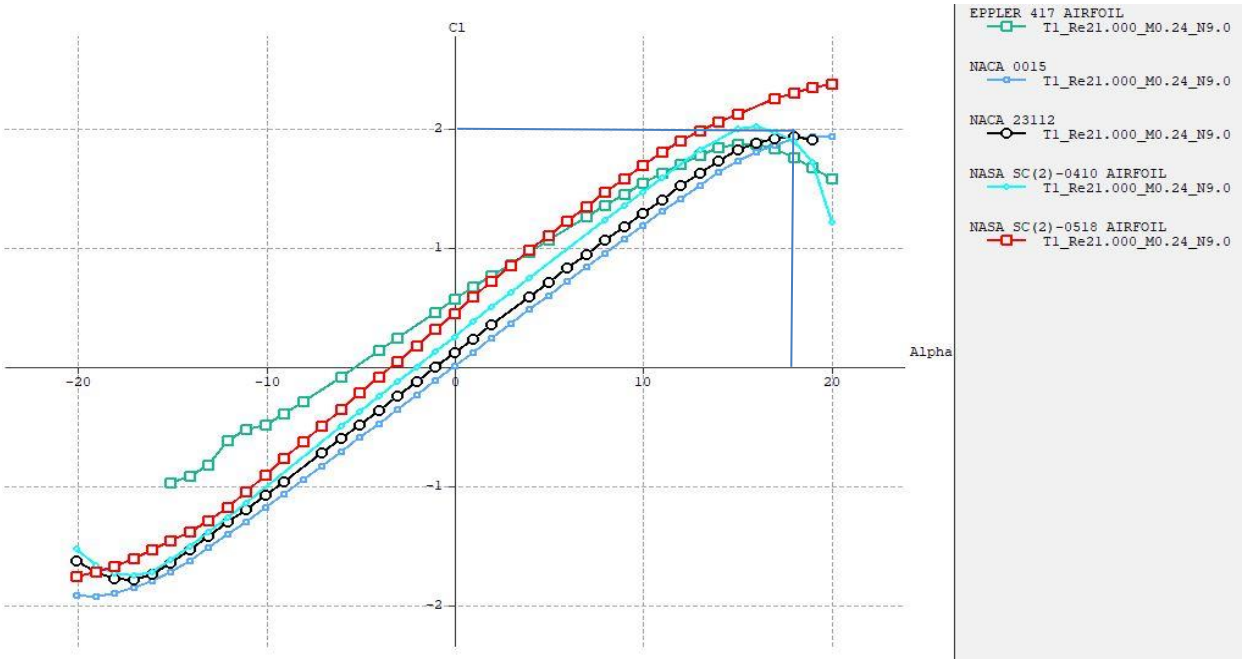

Fig. 39. Coefficient of lift vs AOA

From the above graph it can be clearly observed that, the aerofoil NASA SC (2)-0518 has the highest coefficient of lift for different angle of attack compared to other aerofoils. But in figure 40 we can observe that the highest L/D ratio is found in NACA 23112.

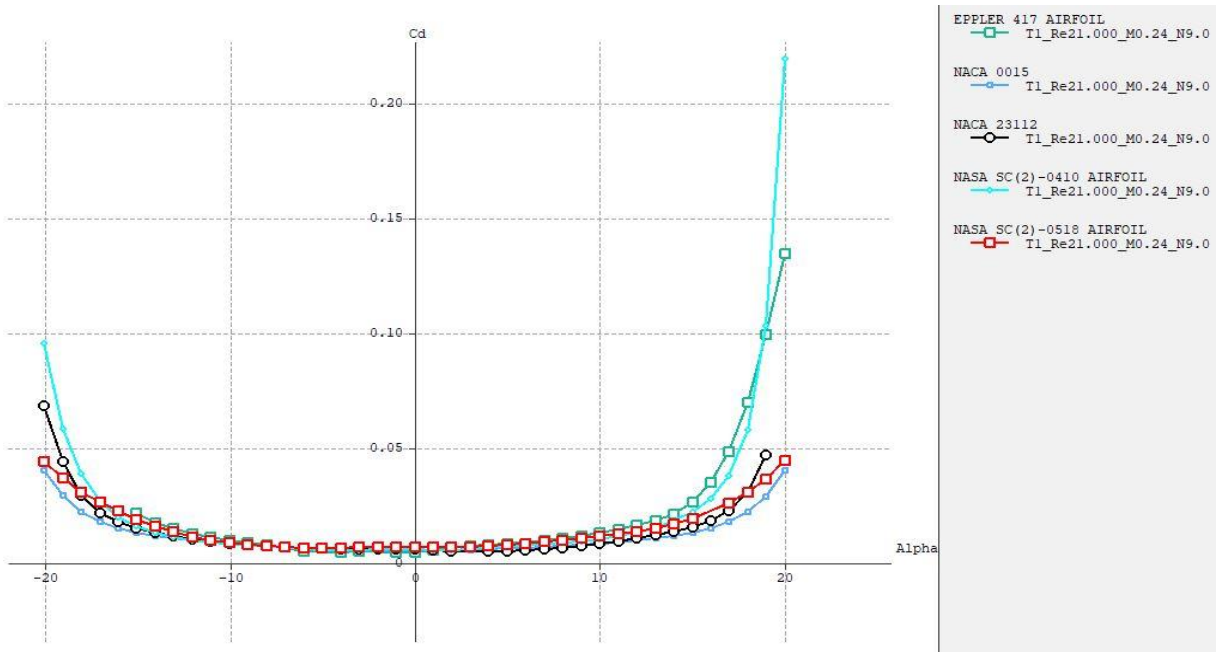

Fig. 40. Drag coefficient vs AOA

Almost all the aerofoils exhibited low drag properties between the AOA range of -10 to 10. There is a tendency in increase of drag at high AOAs. This is due high flow separations at high AOAs.

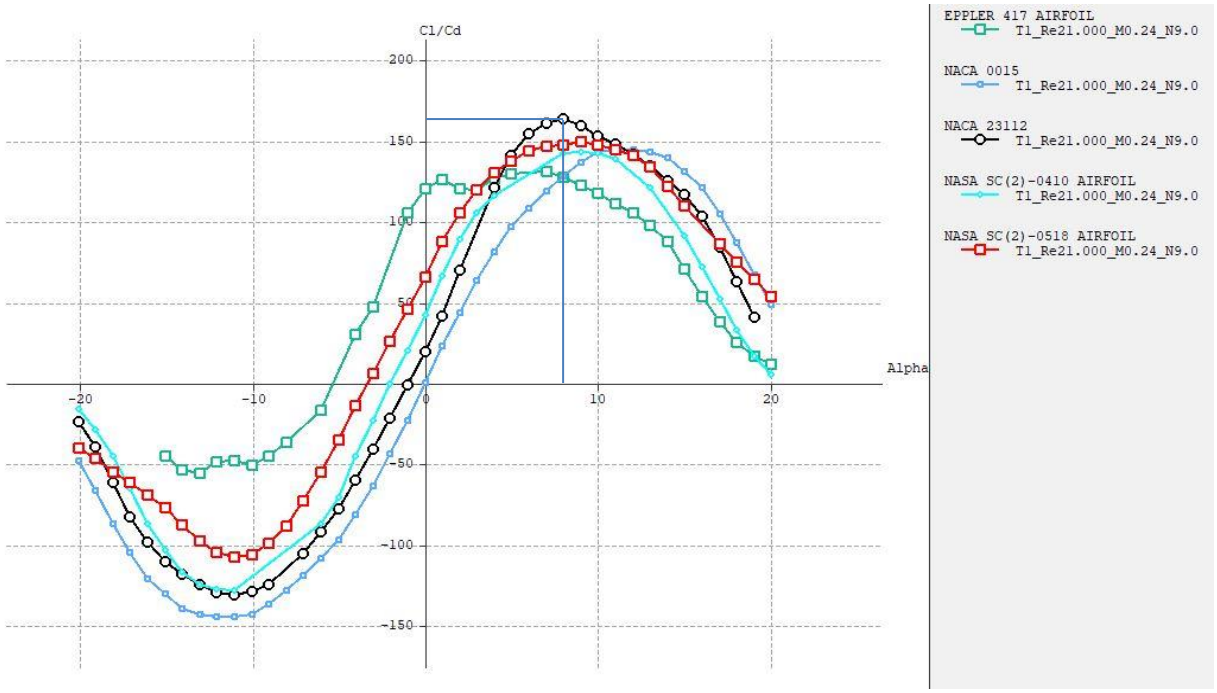

Fig. 41. C_l/C_d ratio at various angle of attack

Although NASA SC (2)-0518 has a higher coefficient of lift, but from the above figure we can see that the coefficient of lift to drag ratio is highest for NACA 23112 aerofoil at an AOA about 8°. The aerofoil NASA SC (2)-01518 is having slightly lower L/D ratio at an AOA about 9°.

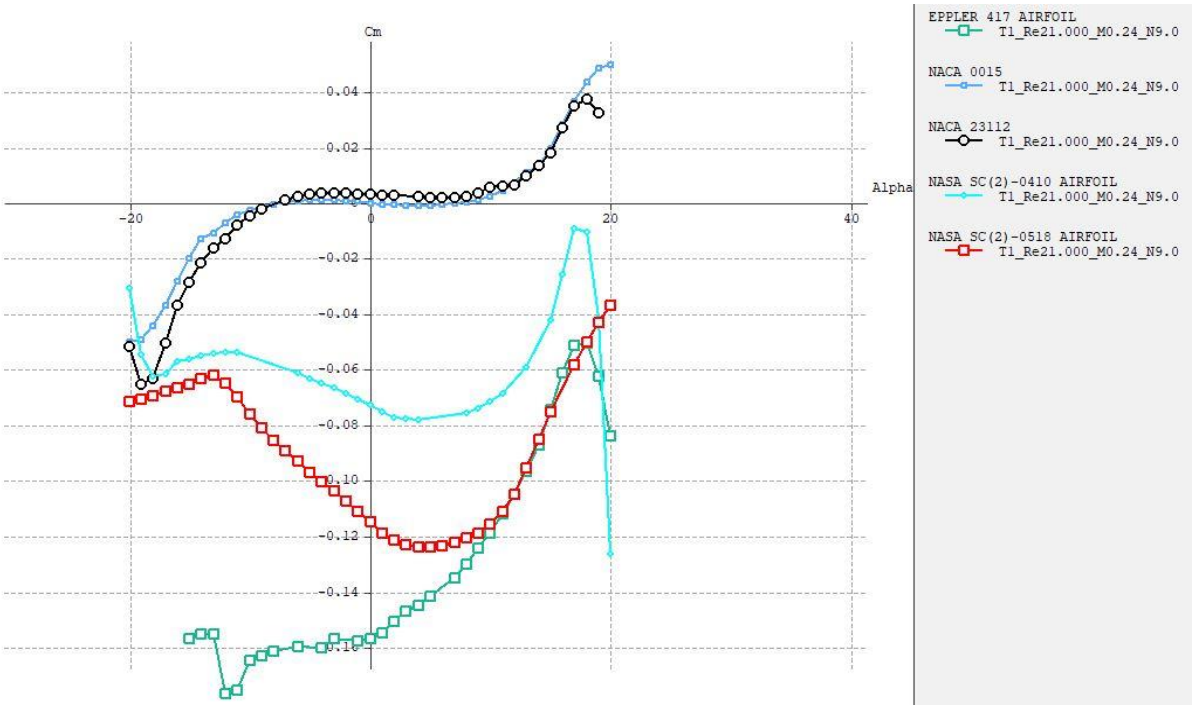

Fig. 42. Pitching moment vs AOA for different aerofoils used

The pitching moment for NACA 23112 is nearly zero for a range of AOA from-10 to 10 approximately. Aerofoil with such characteristics are best suited for the central section of the aircraft where lift generation is high. Although NASA SC (2)-0518 has very good lift coefficient, it lacks other aerodynamic properties which are best found in NACA 23112.

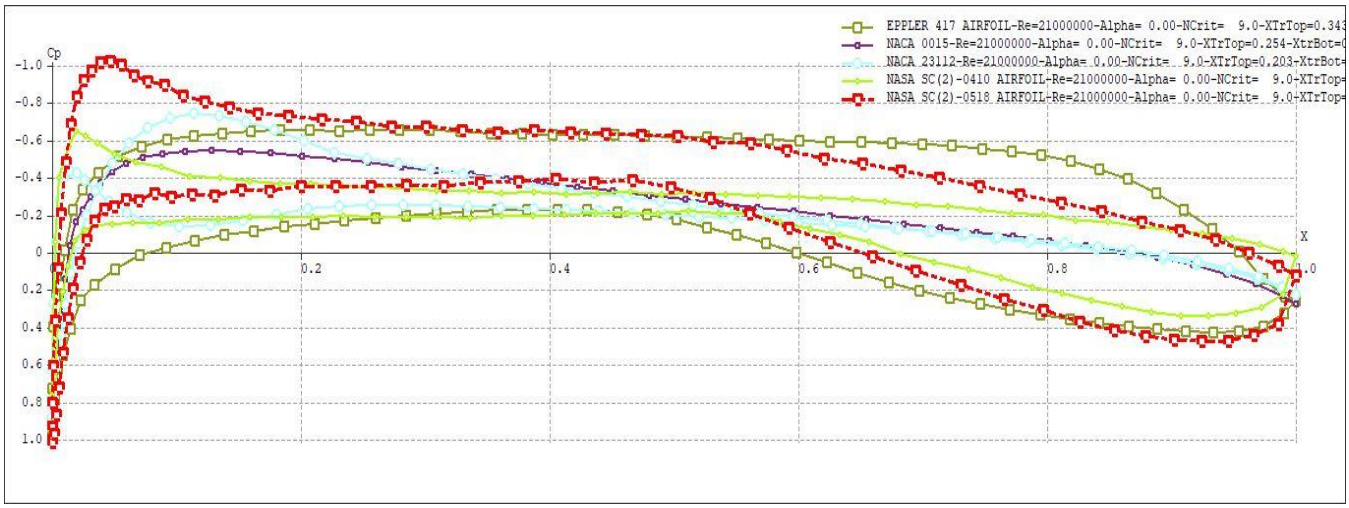

Fig. 43. Pressure coefficient across chord length.

The above figure gives a clear representation of pressure coefficient of each air foil across the chord length. All air foils exhibited similar characteristics except the symmetrical NACA 0015 as the flow on upper and lower surface is equal. Due to the profile, the pressure coefficient s high towards the leading edge. NACA 23112 has an ideal Pressure coefficient for the design configuration.

6.2. Wing Aerofoil analysis in XFLR5

Since the centre body generates maximum lift for the aircraft in BWB design, an aerofoil with high lift coefficient is used which generates high lift also has a high amount of camber and with increase in camber there is significantly more negative pitching moment of the aerofoil. In conventional cases a tail is used to make the aircraft longitudinally stable. But in this case, the tail is absent. The only way to counter the negative pitching moment is to use an aerofoil with positive pitching moment. During the trade studies the following aerofoils were found to be used in BWB large aircraft designs and the same have been analysed here.

1. HS 522 (14%)
2. FX 60-126
3. HS 522
4. MH 78 (14%)

The following are details of analysis done:

- Type of method used: panel
- Number of panels used: 100
- Aerofoil coordinates used: Selig format dat file from reference (51)
- Type of analysis: Multi-Threaded Batch analysis
- Number of iterations: 1000
- Sequential analysis with 1° increment and AOA ranging from -20 to +20
- Reynolds number range from 2.8e10^6 the wing tip just before stall to 24e10^6 at the wing root during cruise
- Type of polar analysis: Fixed Speed with Mach number 0.24

6.2.1. Polar curve of Batch Analysis for different aerofoils considered

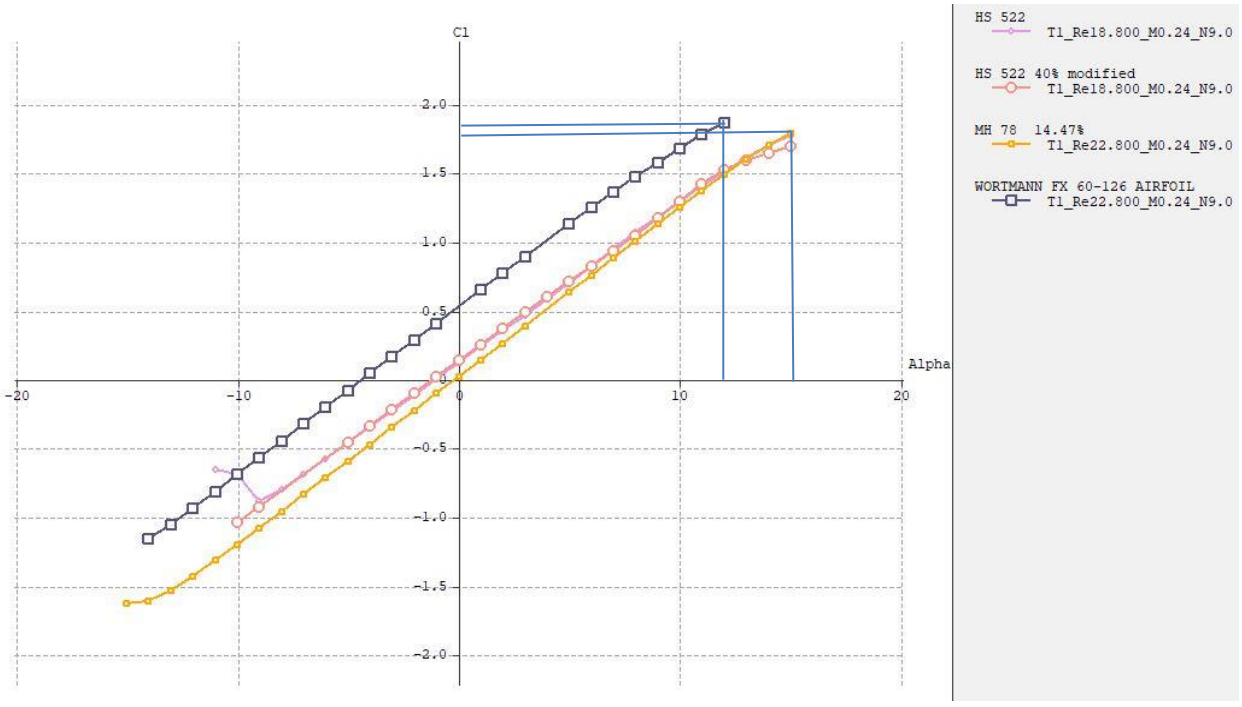

Fig. 44. Wing root and tip aerofoil C_l vs AOA

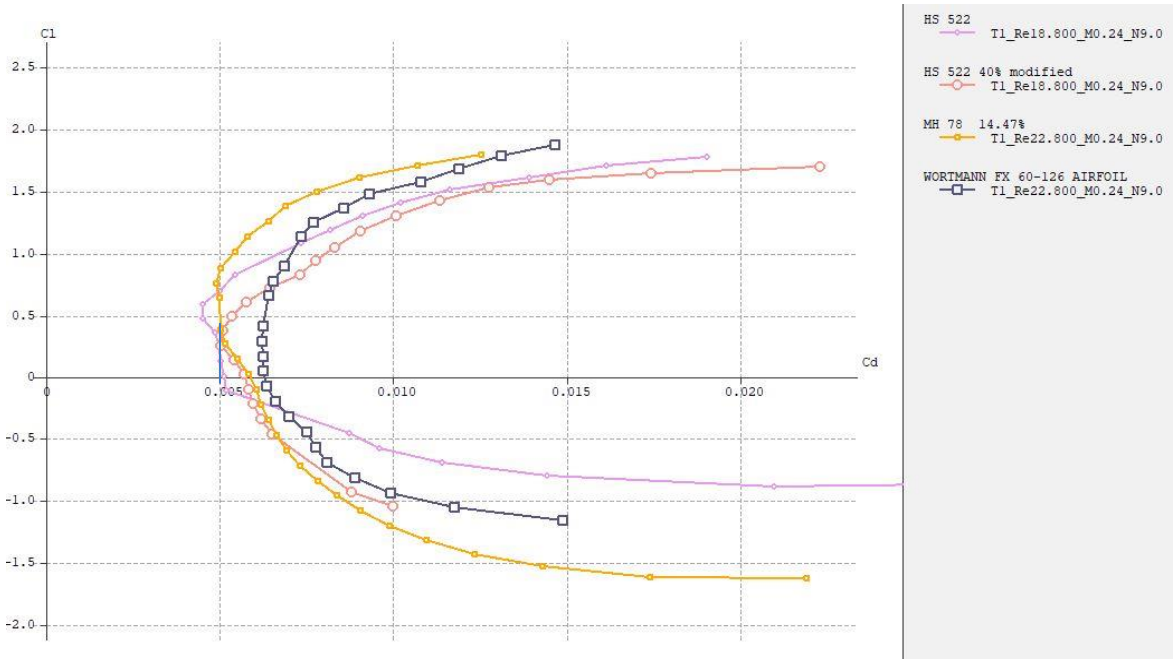

Fig. 45. Wing aerofoil analysis plot for C_l vs C_d

From figure 44 we see that the lift characteristics of MH 78 has higher stall angles which is very import for low speed aircrafts. From the above graph in figure 45 we can observe that; MH 78 has low C_{dmin}. Although the HS 522 has the lowest C_{dmin} out of all the aerofoils considered, the drag bucket region which is also seen on 40% modified HS 522 makes it unfavourable for the use.

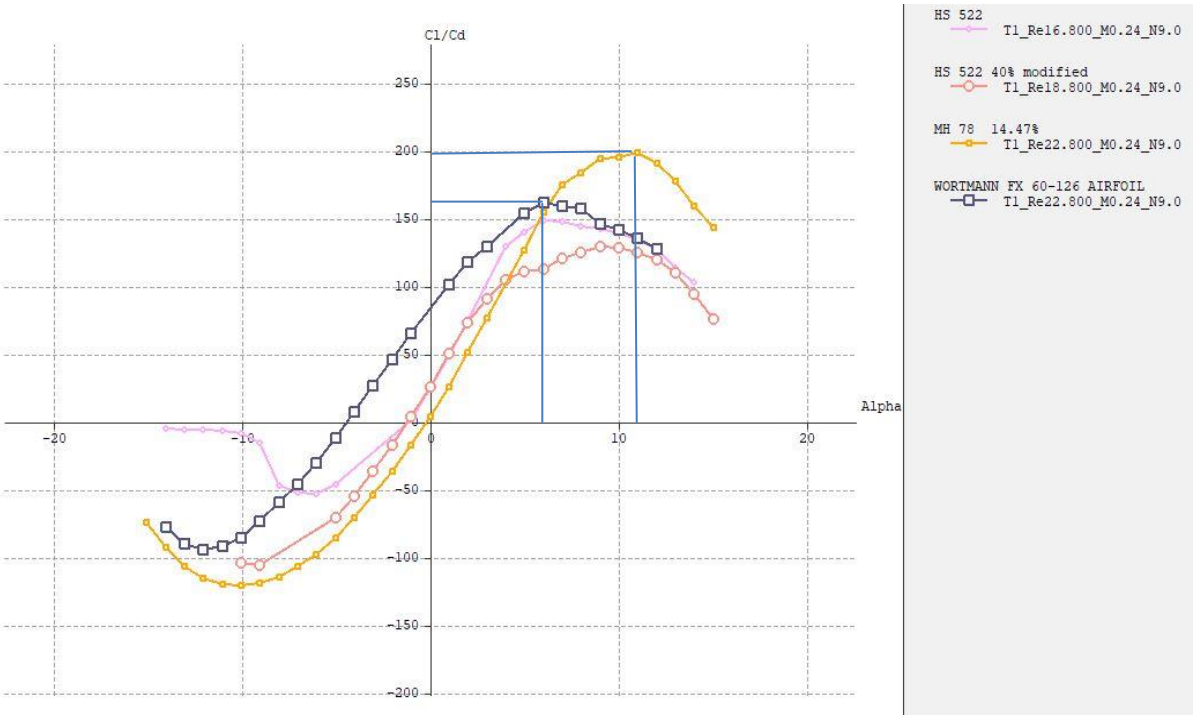

Fig. 46. Wing aerofoil cl/cd ratio vs AOA

Higher L/D ratio is seen in MH 78. From the above graph we can observe that although MH 78 has a high l/d ratio, the FX 60-126 aerofoil achieves its L/D max in a significantly lower angle of attack making it feasible to be used in wing tips. The aircraft is designed to fly in cruise condition with lowest drag generated which is achieved in the Maximum C_l/C_d point.

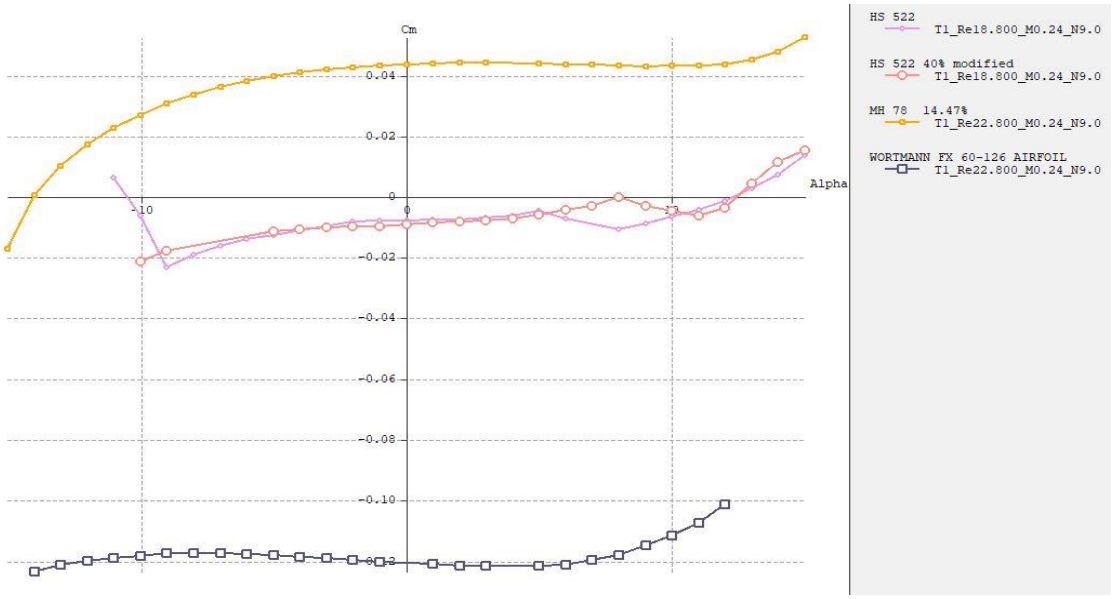

Fig. 47. Pitching moment variation vs AOA

From the above graphs we can observe that the aerofoil MH 78 modified for 14% thickness has positive pitching moment while the FX 60-126 has a highly negative pitching moment. Using MH 78 for the root section and FX 60-126 for the wing tip the, the longitudinal stability is established which has been studied in aircraft polar graphs.

6.3. Final Aerofoil selection for the aircraft

In the above 2 sections, few aerofoils were found to have excellent characteristics for BWB configuration. After analysing the aerodynamic properties, the following aero foils were used for the Aircraft analysis. The aerofoils range from +ve to -ve pitching moment characteristic.

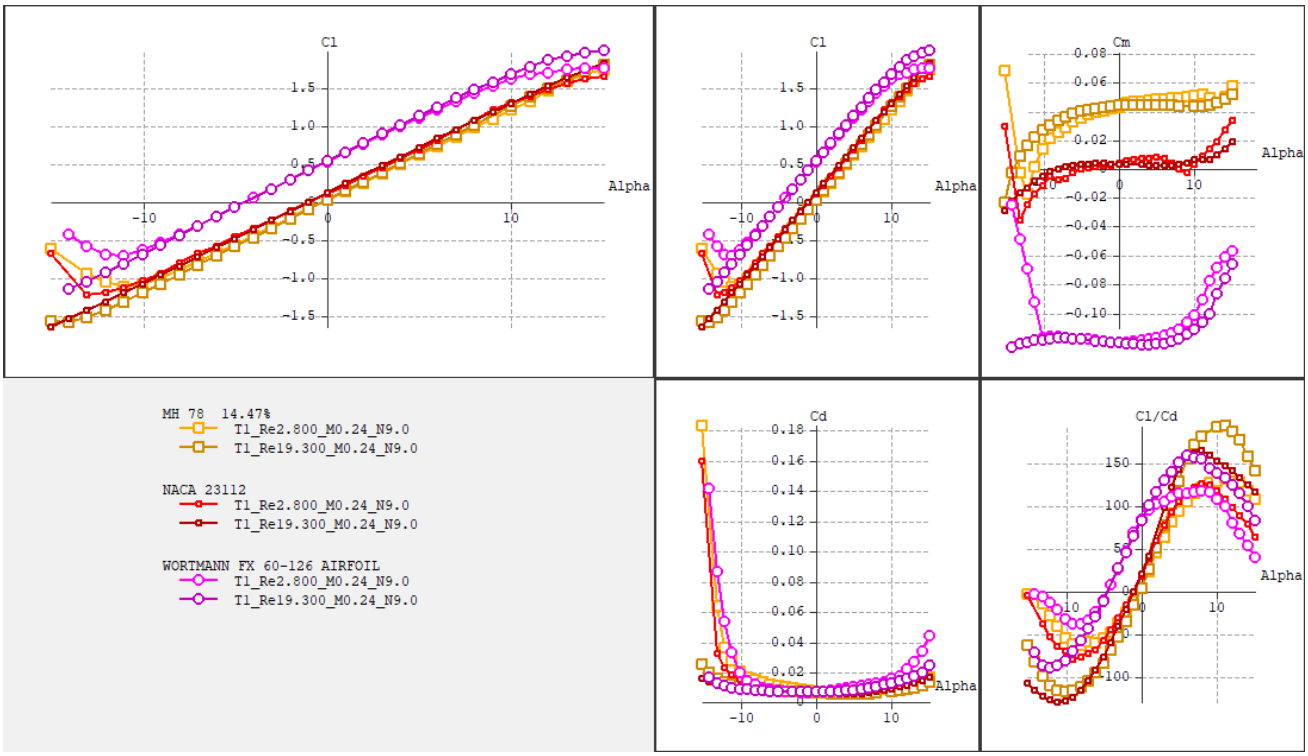

Fig. 48. Low and high operating Reynolds number properties of aerofoils used in the plane.

7. Aircraft Aerodynamic Analysis

7.1. Modelling in XLFR5

The aircraft was modelled in XFLR5 software using wing and plane design option. Vortex Lattice method (VLM) and 3D panel methods were used for the CFD analysis.

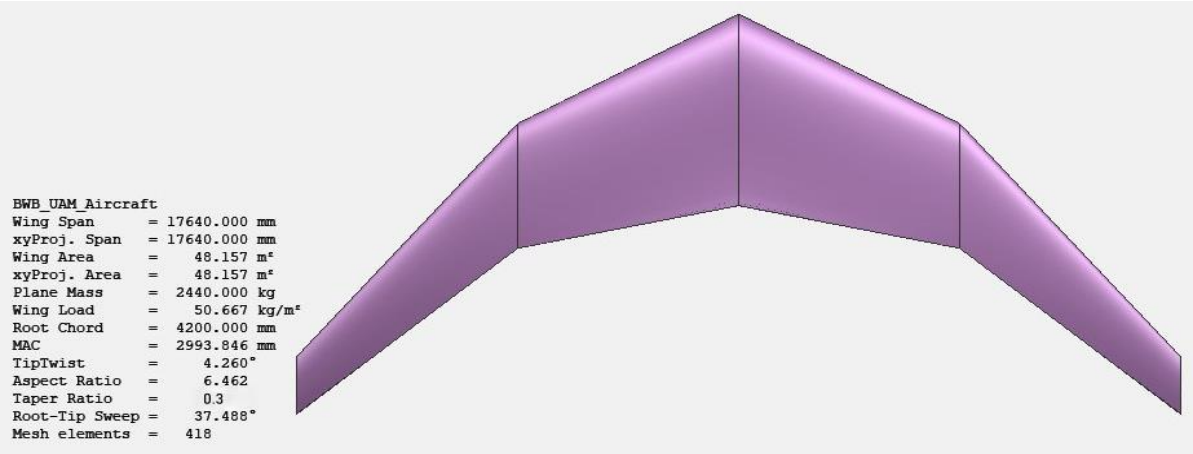

Fig. 49. Aircraft modelled according to dimensions in XFLR5

Based on polar graphs of Figure 46, the aerofoils have been placed across various sections in order to perform various analysis of lift.

Fig. 50. Different aerofoils used across various cross sections

The following are the details of the Aerodynamic analysis done for the aircraft.

- Number of VLM panels used: 418
- Number of panels used: 858
- Analysis methods: Ring vortex (VLM2)
- Viscous medium
- Aircraft Mass: 2440 Kg
- Cruise Velocity: 81 m/s
- Reynold's number range: $6.456 \cdot 10^6$ to $21.52 \cdot 10^6$

7.2. Aerodynamic results:

7.2.1. Change in pressure coefficient with variation of AOA.

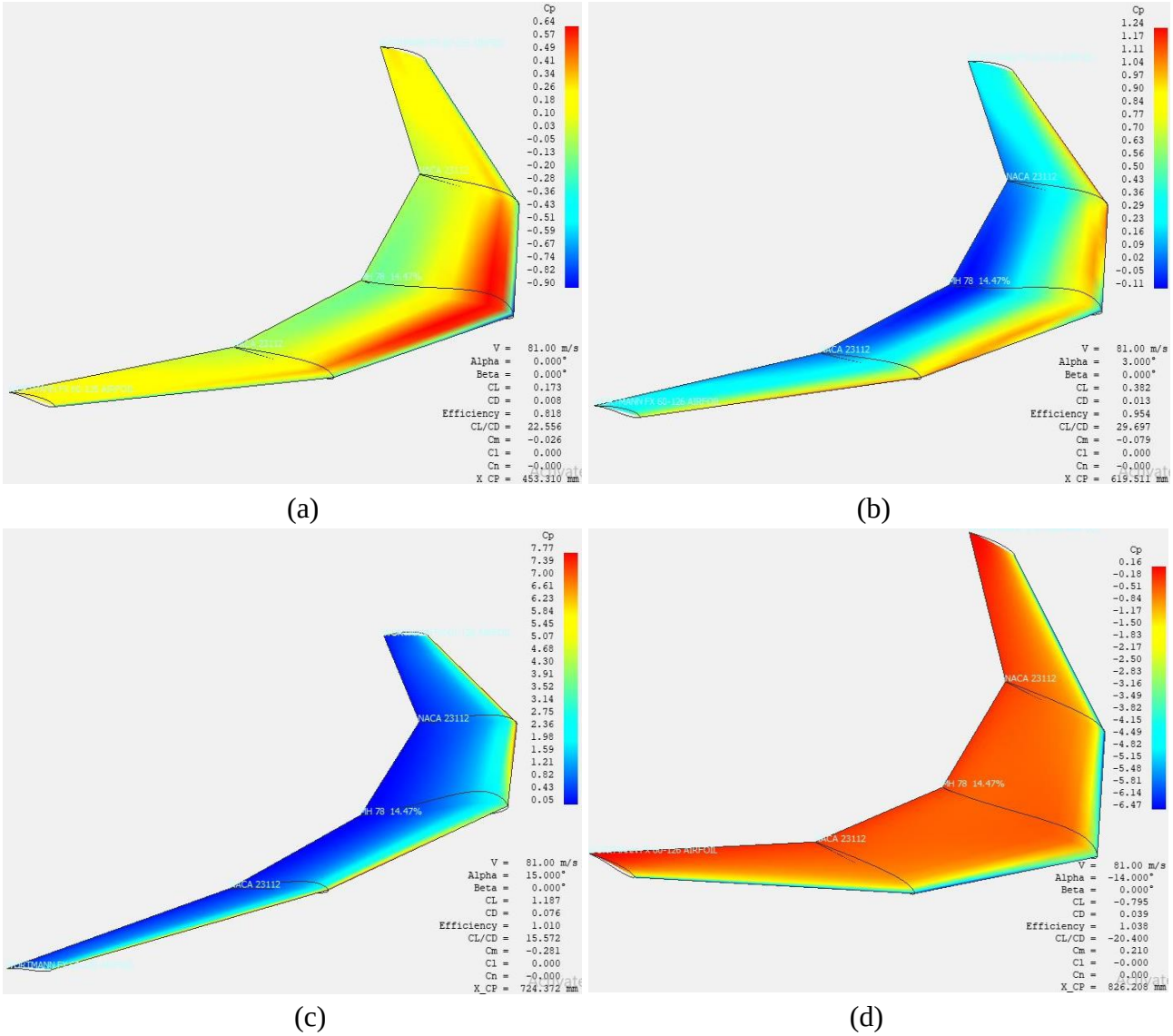

Fig. 51. (a) *Cp* at 0° AOA, (b) *Cp* at 3° AOA, (c) *Cp* at 15° AOA, (d) *Cp* at -14°AOA

The centre of pressure always acts in the thickest cross section of the air foil. In the above figure we can see the variation of pressure coefficient across the aircraft surface. The analysis was done was different angle of attacks. The following observations were made from the analysis:

- At 0 angle of attack, the pressure coefficient is concentrated at the thickest section of the Wing. The high-pressure region is due to the profile thickness of the air foil creating drag at low AOA.
- At 3-degree angle of attack, we see that the high-pressure region is shifted towards the leading edge of the wing surface. the pressure distribution is optimum to achieve high L/D ratio
- At a Positive high angle of attack of 15 degrees, we find that over the aircraft wing there is a very low-pressure region. This is the result of flow separation over the wings at high AOA.
- At a high negative angle of attack, the aircraft has a very high-pressure region over the wing surface. This is due to the high airflow over the wings caused due to high velocities.

7.2.2. Local Lift distribution

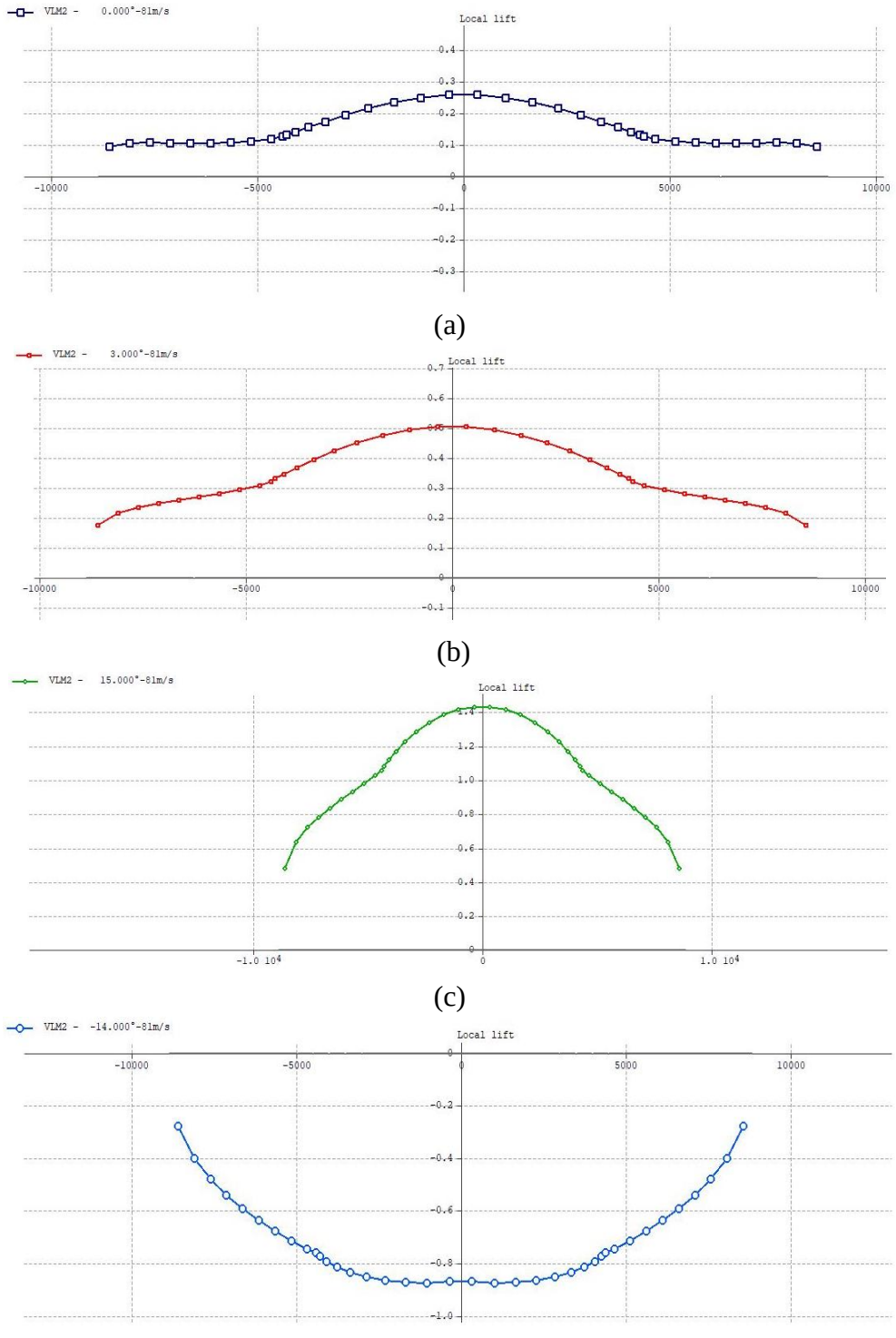

Fig. 52. Local lift distribution across the aircraft span for α=0°, 3°, 15° and -14°

From the above picture the following characteristics of the aircraft was observed for different AOA.

- Majority of the lift is produced by the centre body
- Unlike classical configuration, lift dependency is reduced on the outer main wings.
- Highest lift distribution was found at 15° AOA.
- At negative higher AOA the lift generated is not a contributing factor for aircraft

7.2.3. Aircraft Polar graphs:

The below polar graphs were generated for the aircraft at cruise condition for a velocity of 81 m/s. A fixed speed analysis was done in XFLR5 to analyse the cruise condition parameters achieved to meet the constrain analysis done in earlier section.

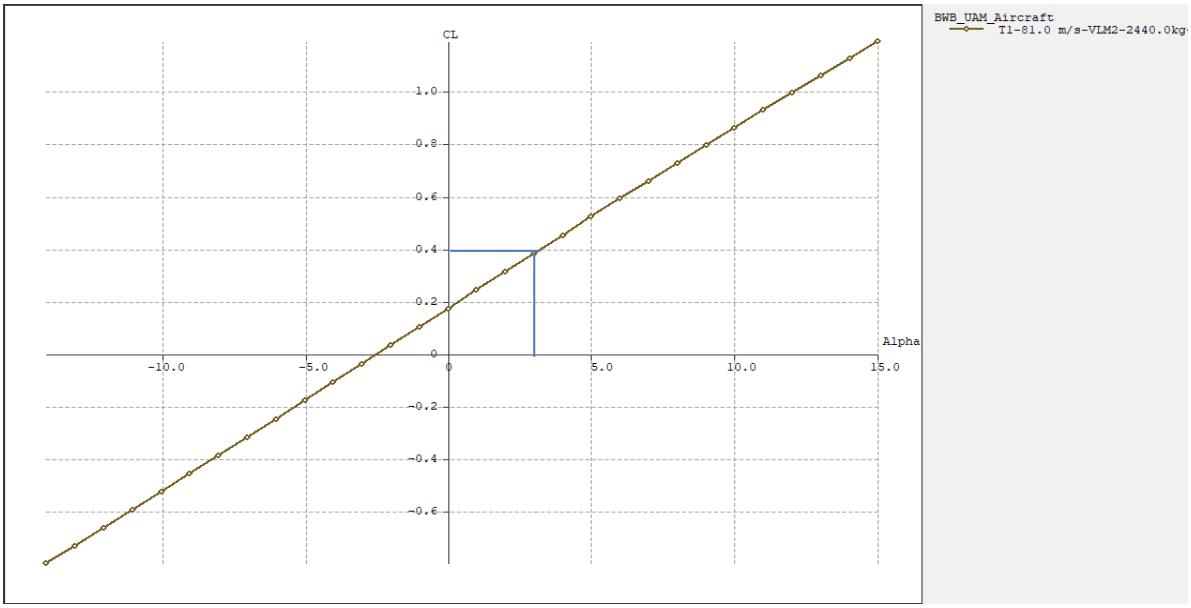

Fig. 53. Aircraft C_L vs Alpha

According to constrain analysis the requirement of lift coefficient for cruise condition was 0.215. The above graph clearly indicates that the lift generated by the aircraft is 0.4. More than required, this provides a FOS in case of additional requirements.

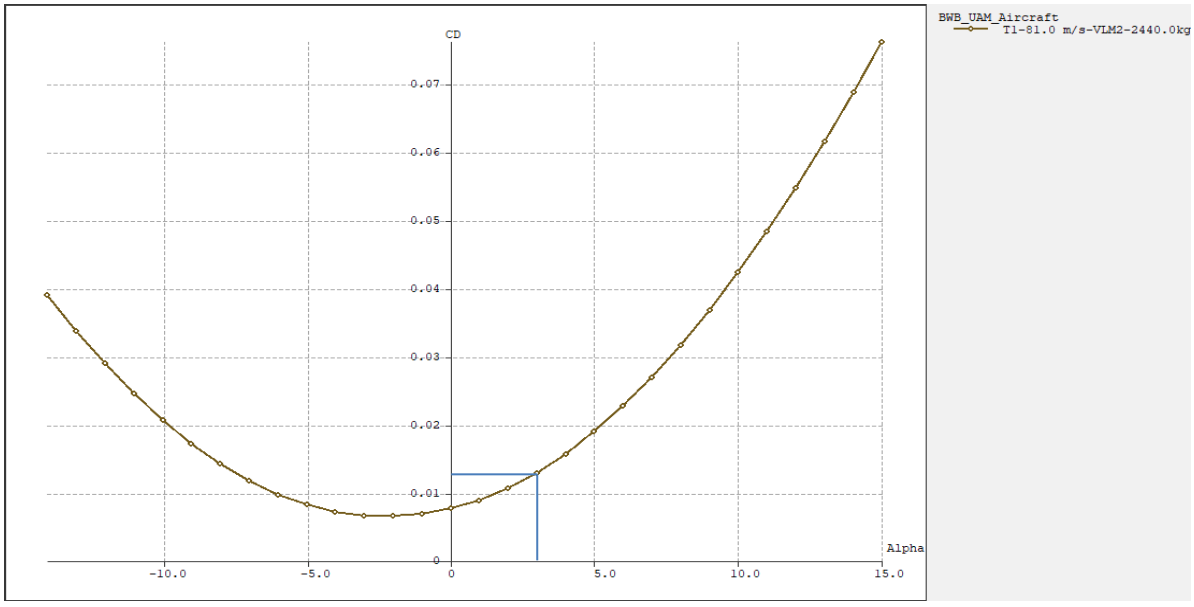

Fig. 54. Aircraft C_D vs Alpha

From the above graph we can estimate the drag coefficient for 3-degree AOA which is the cruise condition. The corresponding cruise drag coefficient was found to be 0.013. It is clear from the graph that the drag coefficient increases exponentially at high positive and negative AOAs.

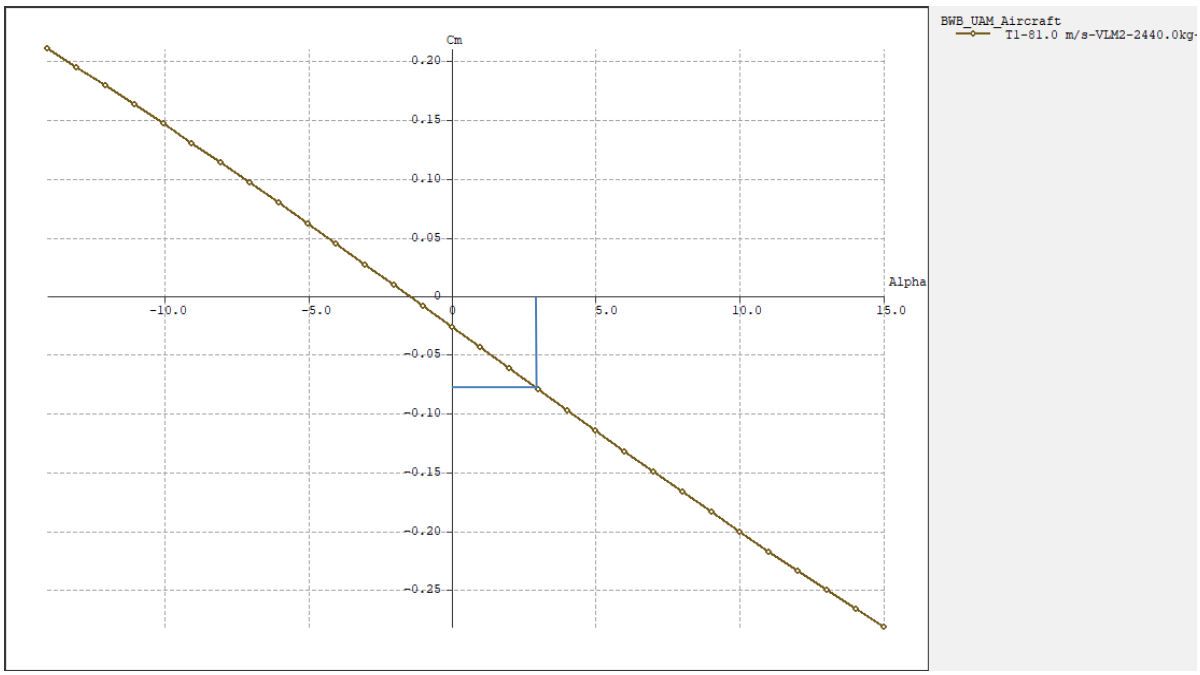

Fig. 55. Aircraft pitching moment vs Alpha

The above graph estimates the aircraft pitching moment for change in AOA. At a 3-degree angle of attack the aircraft has a negative pitching moment of -0.079. The negative pitching moment in cruise condition is considered favourable for this aircraft as it has very high lifting characteristic. The negative pitching moment will help the aircraft nose down in case of gusts or turbulence which tends the aircraft to pitch up movement.

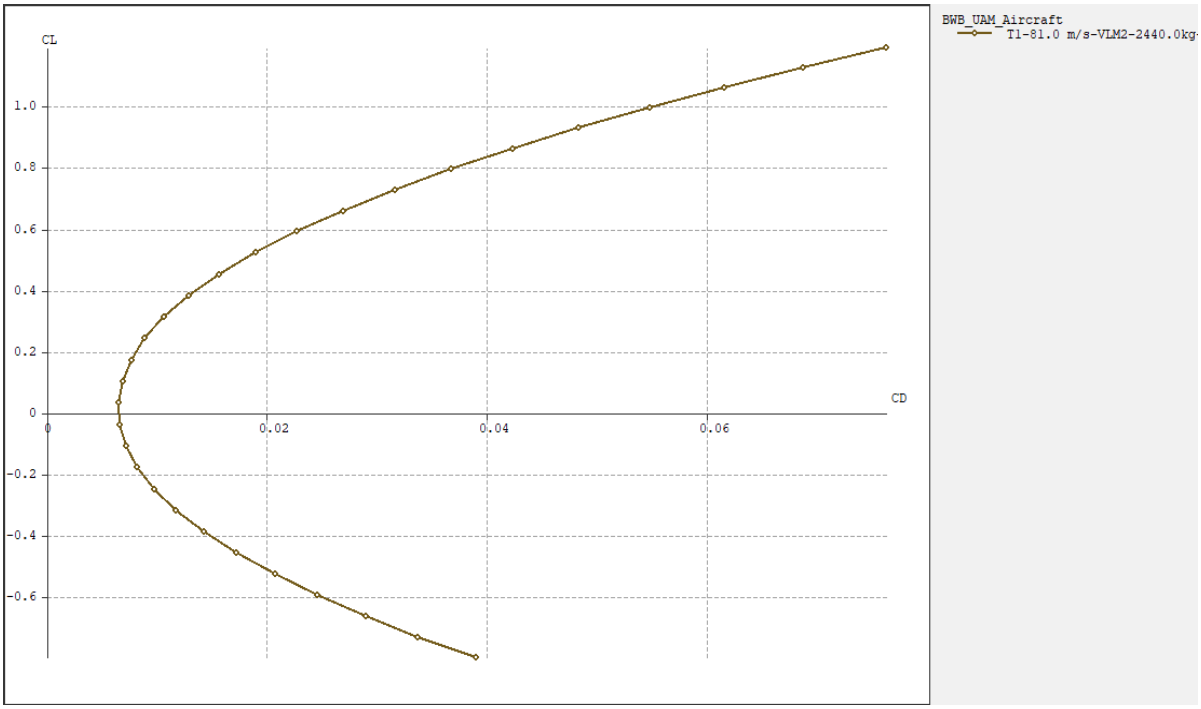

Fig. 56. Aircraft C_L vs C_D

In the constrain analysis the initial value of C_{dmin} used based on statistical data was 0.009. From the above graph we can see That the designed aircraft's C_{dmin} is close to 0 with a C_{dmin} being equal to 0.065.

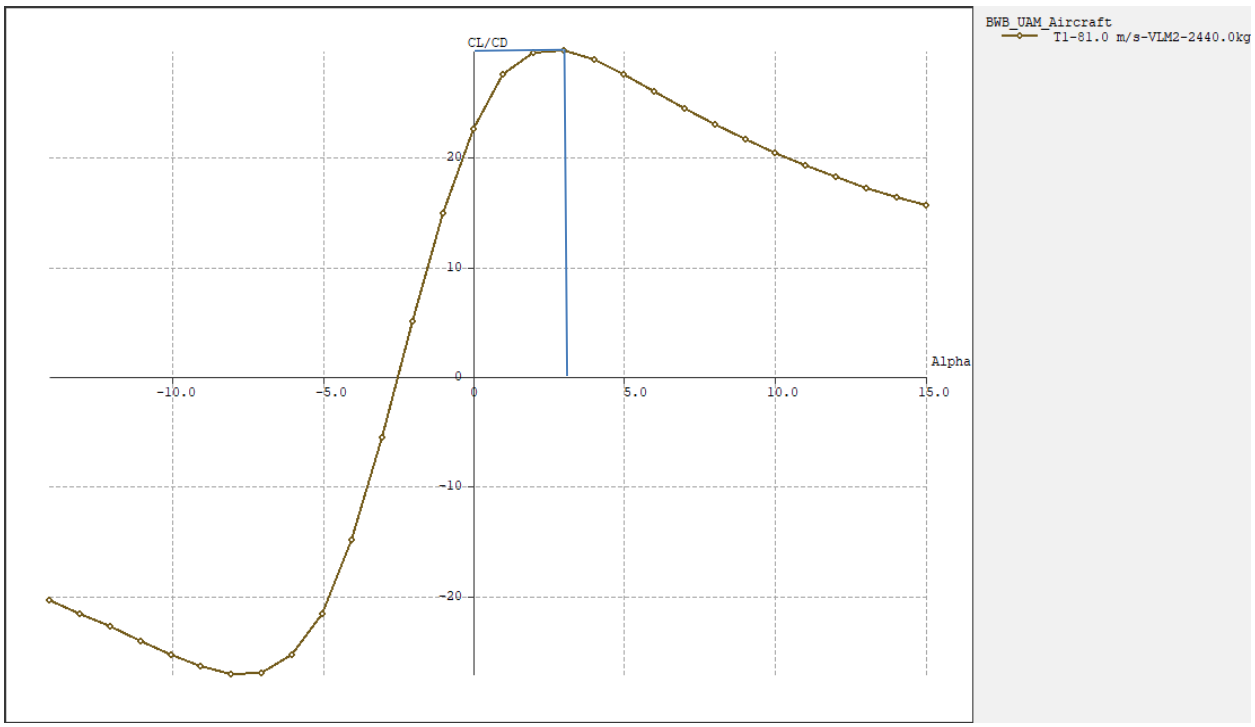

Fig. 57. Aircraft C_L/C_D ratio vs Alpha

The C_l/C_d ratios of various air foils were analysed earlier and in the above figure we can see the C_L/C_D ratio of the aircraft. At 3-degree AOA, the aircraft achieves the highest L/D ratio which is equal to 29.697. The higher C_L/C_D is preferred for cruise in order to enhance the efficiency of flight.

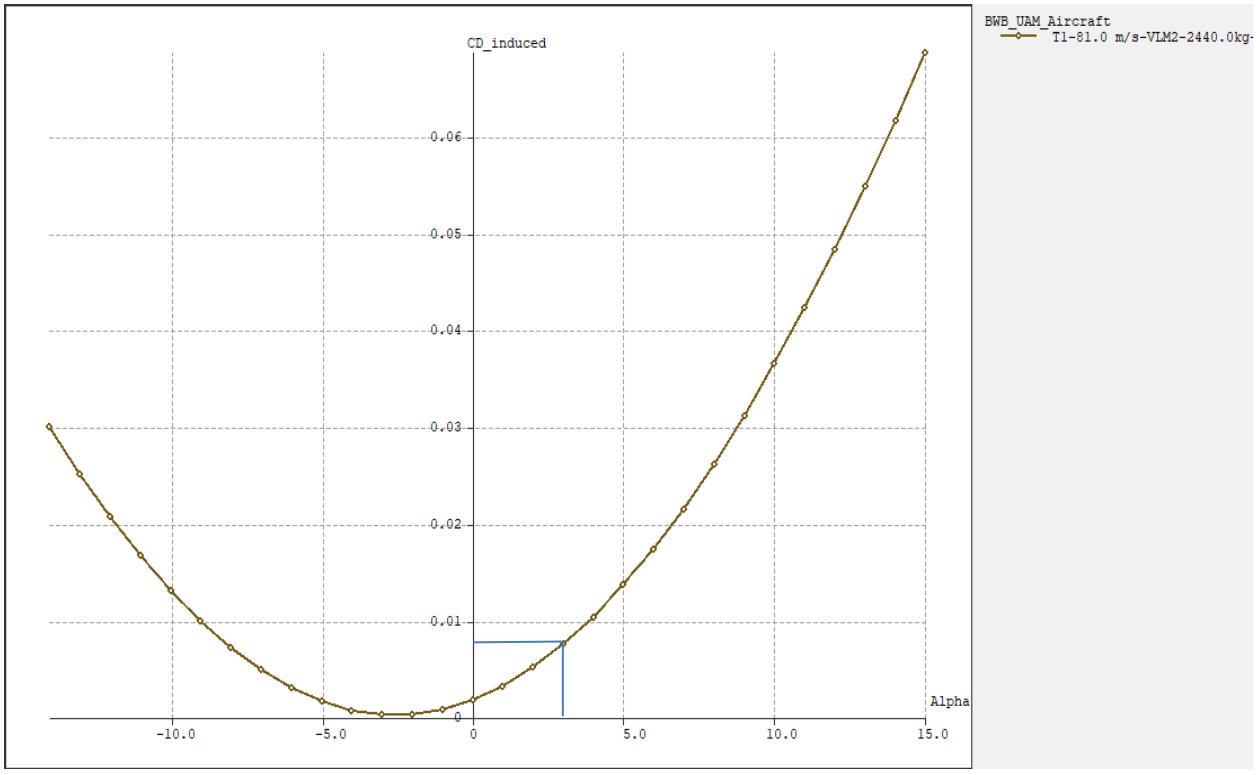

Fig. 58. Aircraft Induced drag vs Alpha

The main goal of a Blended wing design is to reduce the induced drag and increase the L/D ratio. In the above aircraft it is it evident that the Induced drag is about 0.0077 for the cruise.

8. Aircraft modelling and CFD

8.1. Modelling

Sledworks software was used to model the aircraft for this project. 2 aircrafts were modelled, One as a model for CFD analysis with complete solid part and the other for Concept representation with structural parameters. The CFD model was made by importing the air foil coordinates from reference (51) and using the loft command to arrive at the geometry with required dimensions.

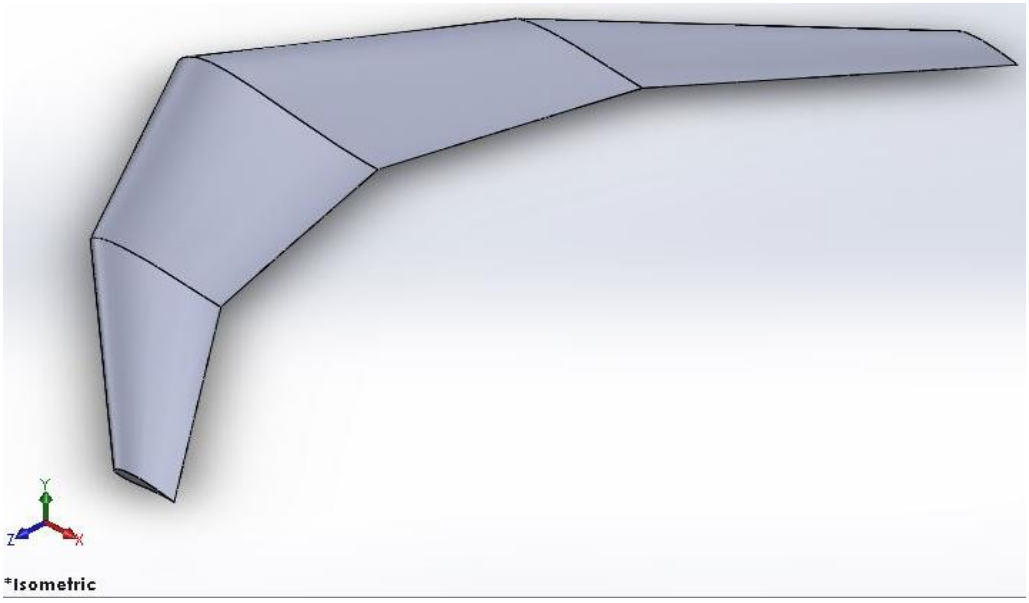

Fig. 59. Aircraft CAD model for CFD analysis

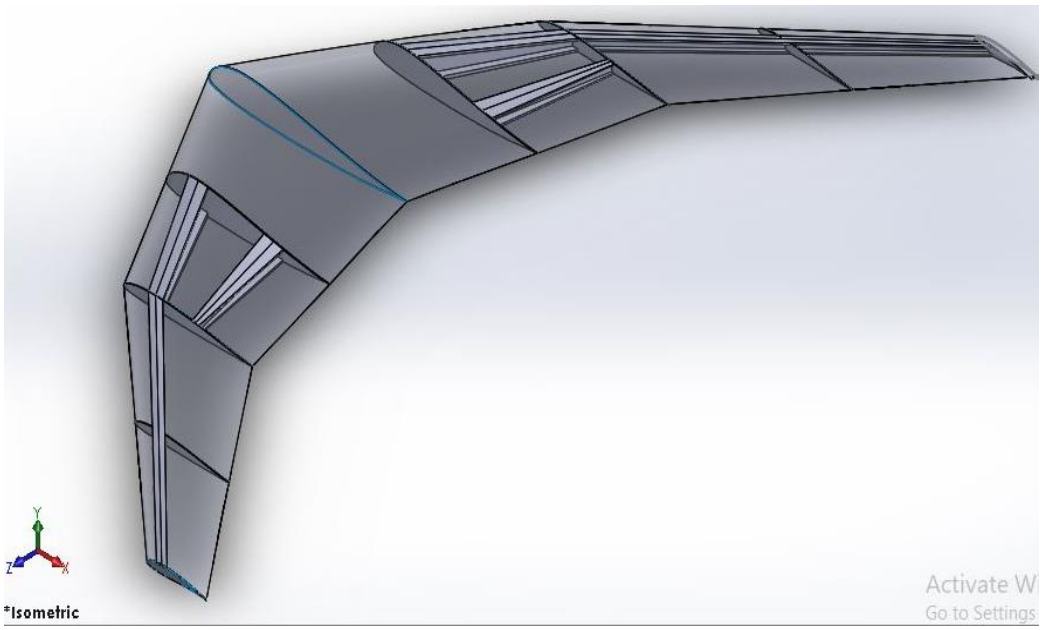

Fig. 60. Aircraft CAD model for Concept representation

The above figure 60 represents the internal structure with the main spar placed at 25% chord. The spars used in the modelling are for representation of the concept. The centre section is left blank to represent the payload carrying section. The model in figure 59 was used for CFD analysis in the Solid works flow simulation software.

8.2. Meshing:

Once the model was successfully built in solid work it was imported into flow simulation add in option. The initial parameters were set for the cruise condition of the aircraft with velocity in X direction to 81 m/s. The fluid domain 3D is used and the domain values are entered in x,y,z directions. Once the domain values are entered the mesh options are used to generate the required mesh settings for the Aircraft model.

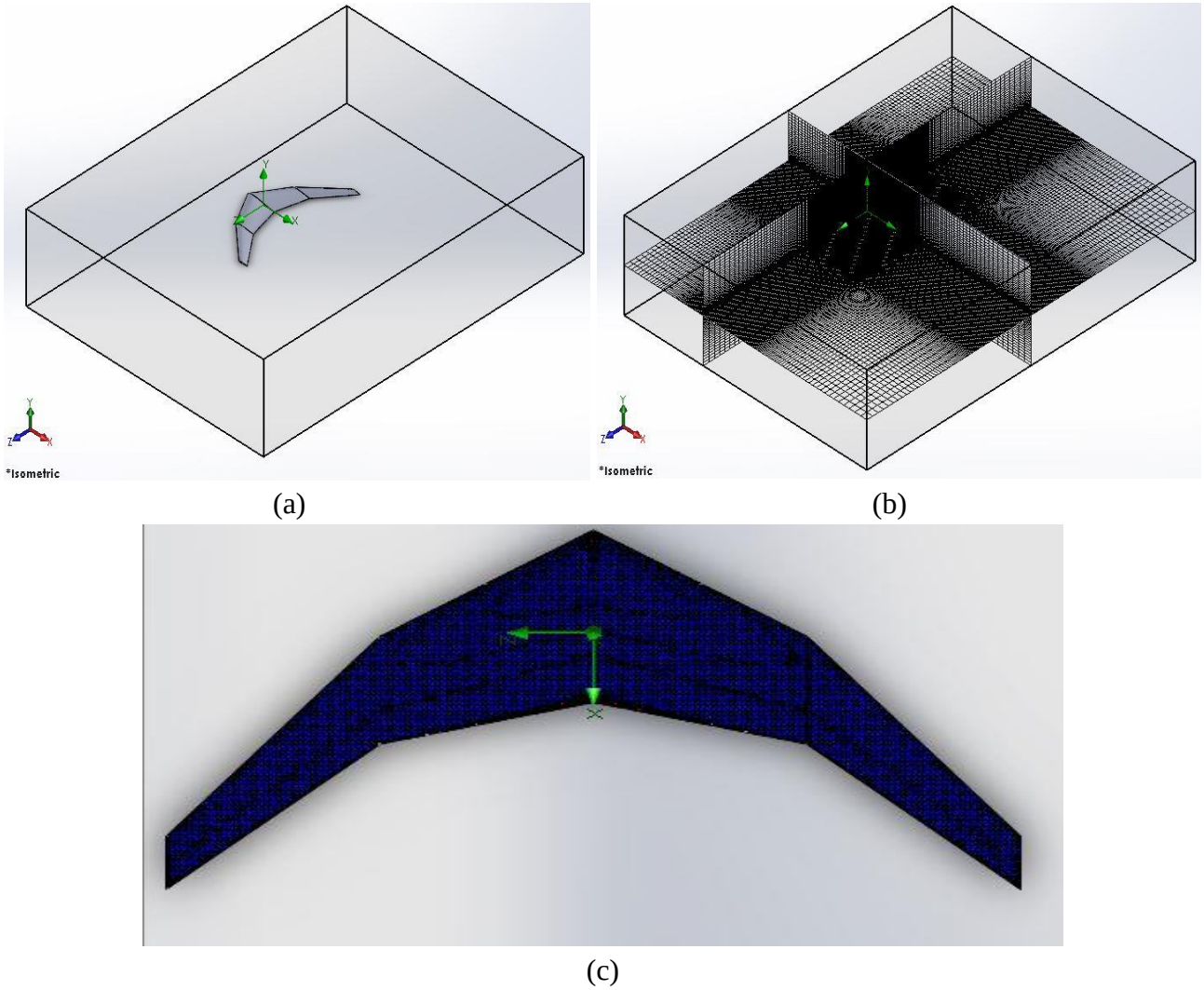

(a) (b)

(c)

Fig. 61. (a) Computational Domain used, (b) initial meshing, (c) Generated Mesh for analysis

An initial mesh level of 3 was used with mesh refinements in the leading edges and trailing edges of the model. The number of solid cells and fluid cells generated had an impact on the computational time as more cells were analysed. After the meshing was applied, the goal plots are applied to find out pressure and velocity variations on the aircraft and analyse the flow trajectory. This is done with the help of multiple goals inserted with appropriate selection

- domain size: X_{max} = 25 m, X_{min} = -12 m, Y_{max} = 6 m, Y_{min} = -6 m, Z_{max} = 25 m, Z_{min} = -25 m.
- Total cells: 2149366
- Total Fluid cells: 2137055
- Total Solid cells: 12311
- Meshing minimum gap size and ratio factor: 0.6 m and 1respectively

8.3. CFD results

The simulation was run for 2 intervals with 100 iterations. It was found that the static pressure centre on the surface of the aircraft at about 25% of the chord from root to tip exhibited low pressure region varying between 98790 – 100025 pascals. This confirms the earlier result obtained from XFLR5 in figure 51.

- Turbulence model: K-epsilon, Inlet velocity: 81 m/s, Turbulence intensity: 0.25 %

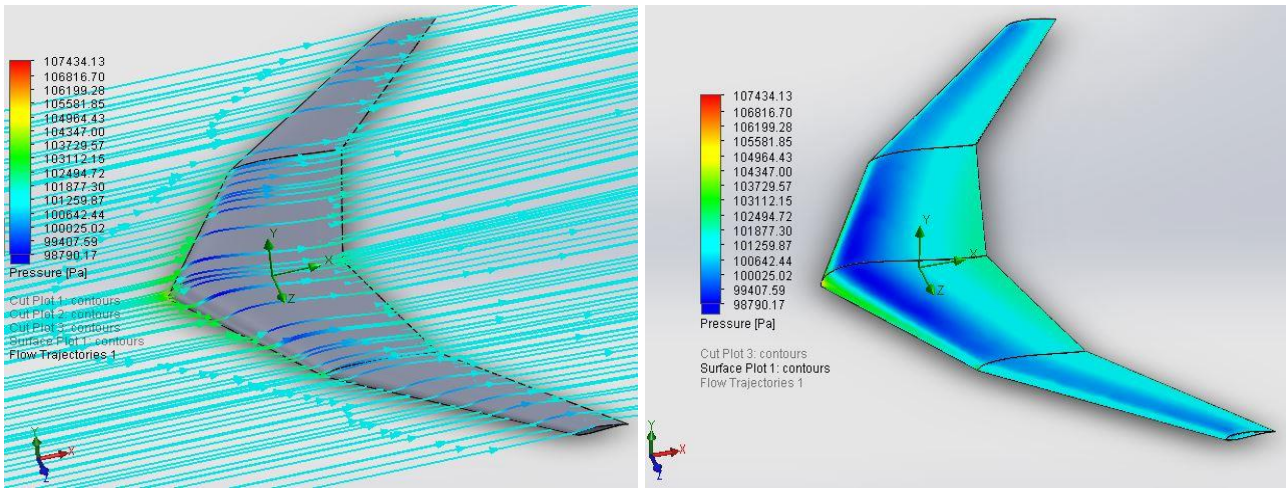

Fig. 62. Flow trajectory and static pressure plot

In the above figure we can see that the reduced static pressure on the upper surface of the aircraft favours lifting characteristics. The pressure is found to be comparatively high in the leading-edge nose section point due to the stagnation behaviour of the flow. The trailing edge and near TE regions have comparatively increasing high pressure region due to the flow separation.

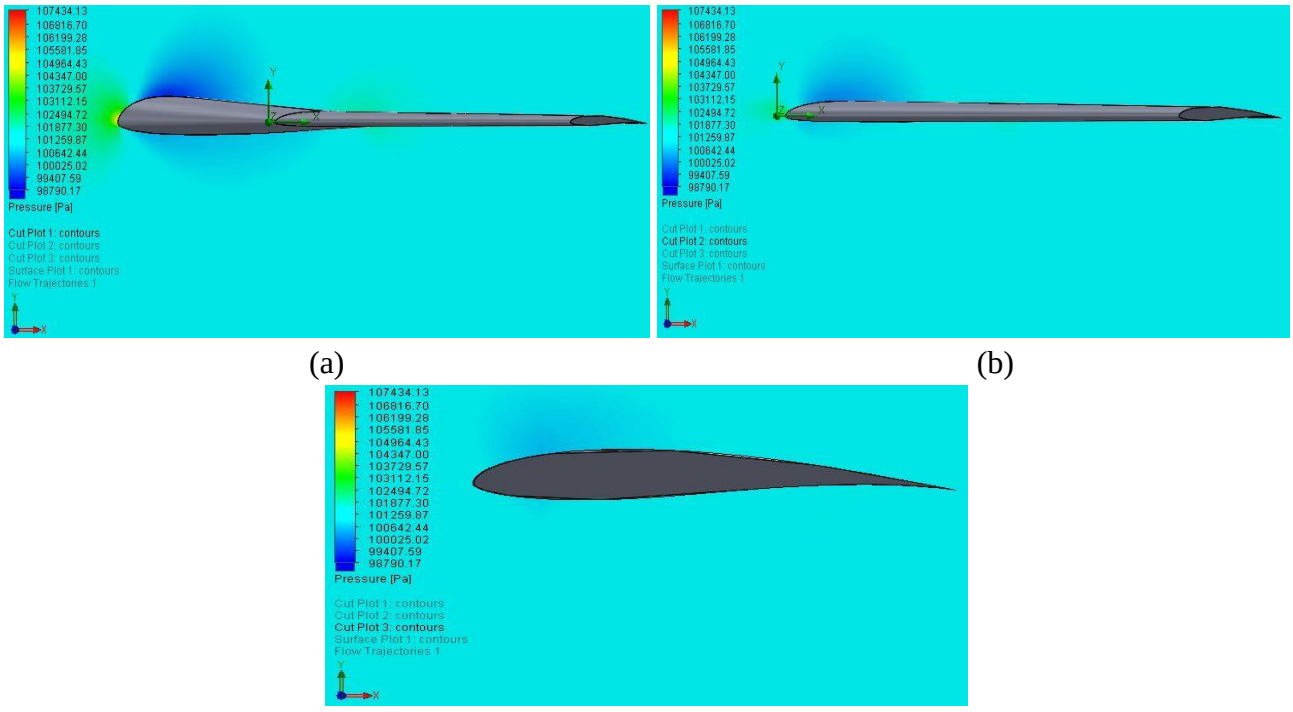

(a) (b)

(c)

Fig. 63. Pressure around the body at cruise condition (a) wing root, (b) mid-section, (c) wing tip

From the above figure we can see that for the cruise condition the aircrafts pressure distribution varies from the root to tip chord. It is found that the pressure region is low in in the 25%chord for the centre section as there are changes in static and dynamic pressure regions. This is mainly due to the aero foil profile characteristics. At the mid-section and wing tips we can observe a comparatively high-pressure region which suggests that there is a reduced lift distribution towards the wing tips. The following conditions were used for the analysis.

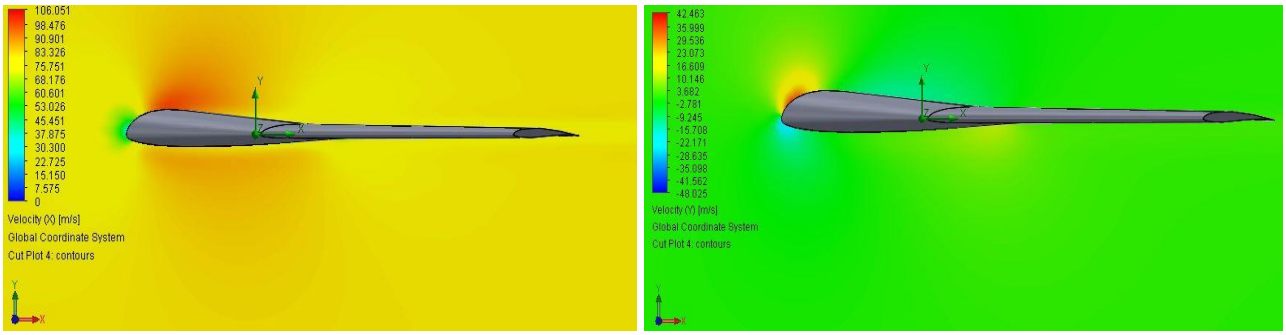

(a) (b)

Fig. 64. (a) Flow velocity in X direction, (b) Flow velocity in Y direction

In the above figure, compare to the free stream velocity, the surface velocity of the aircraft wing is high. This indicates a smooth and a dedicated and intended aerofoil around the aircraft wing favouring positive aerodynamic characteristics. In the figure (b), a sharp increase in the velocity flow is seen at the leading edge. This is due to the profile deflecting some amount of flow particles in the direction of lift. This creates a small drag characteristic which can be further optimised if required. For the intend project, the designed aircraft has exhibited good aerodynamic feasibility characterises which can be a potential design consideration for UAM operations.

Conclusions

1. The initial sizing of the aircraft based on statistical data and design approximations resulted in the following values:
   a) The maximum take-off weight was calculated to be 23936.4 N. The wing loading of the aircraft was found to be 500 N/m^2 at the design point in the constrain analysis which lead to the thrust to weight ratio equivalent of 0.24 at a lift coefficient of 0.72
   b) The aircraft required a maximum lift coefficient of 0.9 in order to achieve the stall speed requirements of 31.40 m/s.
2. From the aircraft geometric calculations, the required wing area was found to be 47.872 m^2 to lift the MTOW. The blended wing root chord was found to be 4.2 m with a maximum Reynolds number range of $24 \cdot 10^6$ million for cruise velocity of 81 m/s and a Wing outboard Tip with 1.26 m with the lowest Reynolds number at $2.8 \cdot 10^6$ million for stall speed of 31 m/s. The total span of the aircraft was determined to be 17.64 m.
3. To meet the aerodynamic necessities of the airplane, certain aero foils were selected for different cross section based on their aerodynamic characteristics. It was found that the following aero foils were best suited for the aircrafts operating Reynolds number range:
   a) For Centre Section MH 78 (14.47%) aero foil was selected with C_{Lmax} = 1.75 at 15° AOA, Highest C_l/C_d = 200 at 11° AOA, a positive pitching moment.
   b) For Mid Wing Section NACA 23112 was selected with C_{Lmax} = 1.95 at 17.5° AOA, Highest C_l/C_d = 160 at 7.5° AOA and the Lowest C_m close to zero between +10° to -10° AOA
   c) For Outboard wing Section Wortman FX 60-126 was selected with C_{Lmax} = 1.88 at 12.5° AOA, Highest C_l/C_d = 165 at 5.5°AOA and a High Negative pitching moment for all AOAs.
4. Initial Aircraft geometric modelling and analysis for cruise condition was done in XFLR5 software with selected aero foils placed across various cross sections and the following results were obtained:
   a) Low pressure distribution on the aircraft surface indicated good lift generation capabilities
   b) At 0° AOA high pressure region was found at aerodynamic centre, an optimum low-pressure region was found on the surface at 3° AOA and at high AOAs low pressure regions close to stall were observed. At high negative AOAs, high pressure region was found on the surface
   c) It was found that the lift distribution was according to the intended design with maximum lift generation at the centre body with reduced lift on the outboard section.
5. Polar graphs were generated for the Aircraft and the following results were obtained for the cruise condition:
   a) 3° AOA was found to have the highest C_L/C_D ratio of 29.697 with $C_{Lcruise}$ being equal to 0.39 and corresponding drag coefficient is 0.013
   b) The aircraft has a small negative pitching moment about -0.079 which is favourable for a full lifting body aircraft with high Coefficient of lift
   c) The minimum drag coefficient was found to be 0.065 and the induced drag C_{Di} = 0.0075
6. It was found that the aircraft had better aerodynamic characteristics compares to the initial sizing operations considered.
   a) The Lift coefficient requirement obtained from the initial diagram was 0.215
   b) The lift coefficient at 3 Degree AOA of the aircraft was found be around 0.394
7. For the same MTOW the BWB exhibited lower wing loading compared to the classical design configuration.

References

1. **ROSTEC, Peter.** Sunjet Project. *Sustainable Network for Japan-Europe aerospace research and Technology cooperation.* [Online] 26 March 2015. [Cited: 25 November 2018.] https://sunjet-project.eu/sites/default/files/Airbus%20-%20Delhaye.pdf.

2. **Hepperle, Martin.** German Aerospace Center (DLR). *Electric Flight – Potential and Limitations.* [Online] 10 August 2012. [Cited: 25 November 2018.] https://elib.dlr.de/78726/1/MP-AVT-209-09.pdf. DOI: 10.14339/STO-MP-AVT-209.

3. **Economics, Oxford.** Oxford Economics Ltd. *Executive Summary: Future trends and market opportunities in the world's largest 750 cities, How the global urban landscape will look in 2030.* [Online] 22 September 2014. [Cited: 25 december 2018.] https://www.oxfordeconomics.com/Media/Default/landing-pages/cities/OE-cities-summary.pdf.

4. **Inc, Booz Allen Hamilton.** National Aeronautics and Space Administration (NASA). *EXECUTIVE BRIEFING: Urban Air Mobility (UAM), Market Study.* [Online] 5 october 2018. [Cited: 22 december 2018.] https://www.nasa.gov/sites/default/files/atoms/files/bah-uam-executive-briefing-to-post.pdf.

5. **GMBH, ROLAND BERGER.** ROLAND BERGER GMBH. *Roland Berger Focus, Urban Air Mobility: The rise of the new mode of transportation.* [Online] November 2018. https://www.rolandberger.com/fr/Publications/Passenger-drones-ready-for-take-off.html.

6. **Inc, Uber Technologies.** Uber Elevate. *Fast-Forwarding to a Future of On-demand Urban Air Transportation.* [Online] 27 October 2016. https://www.uber.com/elevate.pdf/.

7. **Holt, Richard.** Oxford Economics. *Global Cities: Which cities will be leading the global economy in 2035?* [Online] November 2018. https://www.oxfordeconomics.com/recent-releases/7fa5c39e-6603-433c-9e59-9dd928fa2415.

8. **GmbH, Porsche Consulting.** A Porsche Consulting study. *The Future of Vertical Mobility: Sizing the market for passenger,inspection, and goods services until 2035.* [Online] 20 March 2018. https://www.porsche-consulting.com/fileadmin/docs/04_Medien/Publikationen/TT1371_The_Future_of_Vertical_Mobility/The_Future_of_Vertical_Mobility_A_Porsche_Consulting_study__C_2018.pdf.

9. **Agency, European Aviation Safety.** European Aviation Safety Agency. *Certification Specifications For Normal, Utility, Aerobatic, and Commuter Category Aeroplanes, CS-23.* [Online] 14 November 2003. https://www.easa.europa.eu/sites/default/files/dfu/decision_ED_2003_14_RM.pdf.

10. **Kundu, Ajoy Kumar.** *Aircraft Design.* [eBook] New York : Cambridge University Press, Cambridge University Press, 2010. ISBN-13 978-0-511-67785-4.

11. **GUDMUNDSSON, SNORRI.** *General Aviation Aircraft Design: Applied Methods and Procedures* . s.l. : Elsevier Inc, 2014. ISBN: 978-0-12-397308-5.

12. **Torenbeek, Egbert.** *Advanced Aircraft Design.* s.l. : John Wiley & Sons Ltd, 2013. ISBN 978-1-118-56811-8.

13. **Moore, Mark D.** National Aeronautics and Space Administration (NASA). *Distributed Electric Propulsion (DEP) Aircraft.* [Online] https://aero.larc.nasa.gov/files/2012/11/Distributed-Electric-Propulsion-Aircraft.pdf.

14. *Computational Analysis of a Wing Designed for the X-57 Distributed Electric Propulsion Aircraft.* **Deere, Karen A., et al.** Denver : American Institute of Aeronautics and Astronautics (AIAA), 2017. ISBN: 978-1-5108-4375-2.

15. *Design and Performance of the NASA SCEPTOR Distributed Electric Propulsion Flight Demonstrator.* **Borer, Nicholas K., et al.** Washington, .D.C : American Institute of Aeronautics and Astronautics, 2016. 16th AIAA Aviation Technology, Integration, and Operations Conference.

16. *Drag Reduction Through Distributed Electric Propulsion.* **Stoll, Alex M., et al.** Atlanta, Georgia : American Institute of Aeronautics and Astronautics (AIAA), 2014. Aviation Technology, Integration, and Operations Conference. DOI: 10.2514/6.2014-2851.

17. **GmbH, Lilium.** Lilium GmbH. *Press Kit.* [Online] https://lilium.com/press/.

18. —. Lilium GmbH. [Online] https://lilium.com/technology/.

19. **Begari, Vishakh.** Dynamic Stability of a Manned VTOL Jet. *STAR Global conference.* [Online] 2017. https://www.star-global-conference.com/sites/default/files/public_pdf_presentation/SGC2017%20Lilium%20Vishakh%20Begari%20Prakash.pdf.

20. *The Aerodynamics of Three-Surface Airplanes.* **R., Kendall E.** San Diego, California : American Institute of Aeronautics and Astronautics (AIAA), 1984. Aircraft Design Systems and Operations Meeting. DOI: 10.2514/6.1984-2508.

21. **sciences, Aurora Flight.** *OUR FIRST FLIGHT: Passenger Air Vehicle (Video).* [Online] Aurora Flight sciences, 23 January 2019. https://www.youtube.com/watch?v=yS2t8aInfIM.

22. *Aerodynamic Tradeoff Study of Conventional, Canard, and Trisurface Aircraft Systems.* **Bruce P Selberg, Kamran Rokhsaz.** s.l. : American Institute of Aeronautics and Astronautics (AIAA), 1986, Journal of Aircraft. DOI: 10.2514/3.45379.

23. *Linear and Non-Linear aerodynamics of 3 surface aircraft concepts.* **Agnew, J. W, Lyerla, G. W and Grafton, S. B.** Danvers : American Institute of Aeronautics and Astronautics (AIAA), 1980. 6th Atmospheric Flight Mechanics. DOI: 10.2514/3.57586.

24. **Inc, Opener.** *Press Kit.* [Online] Opener Inc. https://www.opener.aero/press/.

25. *Energy Optimal Speed Profile for Arrival of Tandem Tilt-Wing eVTOL Aircraft with RTA Constraint.* **Pradeep, Priyank & Wei, Peng.** 2018 (Unpublished). DOI: 10.13140/RG.2.2.19438.87367.

26. *The effect of Design Parameters on Tandem-Airfoil Configuration Aerodynamics.* **Fu, Jinbin, Ji, Simei and Huang, Xing.** Toyama : s.n., 2016. 2016 Asia-Pacific International Symposium on Aerospace Technology.

27. *Dual-wing systems with decalage angle optimization.* **K. Rokhsaz, B.P. Selberg.** 5, s.l. : American Institute of Aeronautics and Astronautics (AIAA), 2012, Vol. 23. DOI: 10.2514/3.45327.

28. *The Effect of Wing Spacing on Tandem Wing Aerodynamics.* **Timothy M Broering, Yongsheng Lian.** Chicago, Illinois : American Institute of Aeronautics and Astronautics (AIAA), 2010. 28th AIAA Applied Aerodynamics Conference. DOI: 10.2514/6.2010-4385.

29. *Understanding Box Wing Aircraft: Essential Technology to Improve Sustainability in the aviation industry.* **SOMERVIllE, Alexander, et al.** s.l. : Taylor and Francis Group, 2016, Vol. 20 (3). eISSN 1822–4180.

30. **Oy, Flynano.** [Online] Flynano Oy. http://flynano.com/.

31. *Aerodynamic Optimization of Box Wing – A Case Study.* **Khalid, Adeel and Kumar, Parth.** 4, s.l. : Embry-Riddle Aeronautical University, 2014, International Journal of Aviation, Aeronautics and Aerospace , Vol. 1.

32. *CFD Analysis of Box Wing Configuration.* **Sahana D S and Abdul Aabid.** 4, 2016, International Journal of Science and Research (IJSR), Vol. 5. ISSN (Online): 2319-7064.

33. **Schiktanz, Daniel.** *Master Thesis: Conceptual design of Medium range Box wing aircraft.* Hamburg : Hamburg University of Applied Sciences, 2011.

34. **Beijing Yi-Hang Creation Science & Technology Co., Ltd.** *Ehang 184.* [Online] Beijing Yi-Hang Creation Science & Technology Co., Ltd. http://www.ehang.com/ehang184/gallery/.

35. **GmbH, Volocopter.** *Volocopter 2X.* [Online] Volocopter GmbH. https://www.volocopter.com/en/urban-mobility/.

36. *Computational Analysis of Multi-Rotor Flows.* **Yoon, Seokkwan, Lee, Henry C. and Pulliam, Thomas H.** San diego : American Institute of Aeronautics and Astronautics (AIAA), 2016. SciTech Fourm, 54th AIAA Aerospace Sciences Meeting. DOI: 10.2514/6.2016-0812.

37. **Inc., Bell Helicopter Textron.** *Bell Nexus.* [Online] Bell Helicopter Textron Inc. https://www.bellflight.com/company/innovation/nexus.

38. **kozek, Martin and Schirrer, Alexander.** *Modelling and Control of a Blended Wing Body Aircraft, A Case Study.* s.l. : Springer. ISBN 978-3-319-10792-9 (eBook).

39. **d.o.o., PIPISTREL vertical Solutions.** [Online] PIPISTREL vertical Solutions d.o.o., 2019. https://www.pipistrel-aircraft.com/pipistrel-and-honeywell-collaborate-on-aircraft-technologies-for-urban-air-mobility/.

40. *Aerodynamic Design Optimization Studies of a Blended-Wing-Body Aircraft.* **Lyu, Zhoujie and Martins, Joaquim R. R. A.** 5, s.l. : American Institute of Aeronautics and Astronautics (AIAA), 2014, Journal of Aircraft, Vol. 51. DOI: 10.2514/1.C032491.

41. *Benefits of the Blended Wing Body Aircraft Compared to Current Airlines.* **Marino, Matthew, Siddique, Obaid and Sabatini, Roberto.** Istanbul : s.n., 2015. International Symposium on Sustainable Aviation. ISSA-2015-000.

42. *Design of the Blended Wing Body Subsonic Transport.* **Liebeck, R. H.** 1, s.l. : American Institute of Aeronautics and Astronautics (AIAA), 2004, Journal of Aircraft, Vol. 41. DOI: 10.2514/1.9084.

43. **Torenbeek, Egbert.** European Workshop on Aircraft Design Education (EWADE). *Blended Wing Body and All-Wing Airlines.* [Online] 2007. https://www.fzt.haw-hamburg.de/pers/Scholz/ewade/2007/EWADE2007_Torenbeek.pdf.

44. *Distributed electric propulsion for small business aircraft a concept-plane for key-technologies investigations.* **Hermetz, Jean, Ridel, Michael and Doll, Carsten.** DAEJEON, South Korea : HAL, 2016. ICAS 2016. hal-01408988.

45. **Welles, Andrew V. and Dang, Prof. Thong.** College of Engineering & Computer Science - Syracuse University. *CFD Analysis of Distributed Propulsion Systems for Vertical Takeoff and Landing.* [Online] http://eng-cs.syr.edu/wp-content/uploads/2017/10/CFD-Analysis-of-Distributed-Propulsion-Systems-for-Vertical-Takeoff-and-Landing.pdf.

46. *Development of A Fixed-Wing mini UAV with Transitioning Flight Capability.* **Bronz, Murat, et al.** Denver : American institute of aeronautics and astronautics (AIAA), 2017. 35th AIAA Applied Aerodynamics. hal-01534809.

47. *Design of Separate Lift and Thrust Hybrid Unmanned Aerial Vehicle.* **Dewi, Puspita Triana, et al.** s.l. : UNSYS digital, 2015, The Journal of Instrumentation, Automation and Systems. DOI: 10.13140/RG.2.1.4900.9681.

48. **Nagpurwala, Prof Q H.** *Ducted Fans and Propellers.* [Online] http://164.100.133.129:81/eCONTENT/Uploads/09-%20Ducted%20Fans%20and%20Propellers%20%5BCompatibility%20Mode%5D.pdf. PEMP RMD 2501.

49. **Sadraey, Mohammad H.** *Aircraft Design: A system Engineerning Approach.* s.l. : John Wiley & Sons Ltd, 2013. ISBN: 9781119953401.

50. *Pipistrel Taurus G4: on Creation and Evolution of the Winning Aeroplane of NASA Green Flight Challenge 2011.* **Tomažič, Tine, et al.** 2011, Journal of Mechanical Engineering. DOI:10.5545/sv-jme.2011.212.

51. **tools, Airfoil.** Airfoil Tools. *http://airfoiltools.com/.* [Online]

52. **Roskam, Dr. Jan.** *Airplane Design Part III: Layout Design of Cockpit, Fuselage, Wing and Empennage: Cutaways and Inboard Profile.* s.l. : DAR Corporation . Vol. 3. ISBN-13: 978-1884885563.

Appendices

Appendix 1. MATLAB code for constrain diagram

```
function Final_Thesis_UAM_BWB_Aircraft
clear;
close all;
clc;
                %Units=S.I%
AR = 6.5;
% W_g = 23936.4;          %N MTOW
V_turn = 81;              %m/sec Turn Velocity
H_turn = 1000;            %m Turn Altitude
V_v = 7.5;                %m/sec Rate of climb (ROC)
V = 40;                   %m/sec Climb Velocity
CDmin = 0.009;            %Coefficient Minimum Drag
W_S = 60:1250;            %N/m^2 Wing Loading
V_lof = 37;               %m/sec Lift off Velocity
g = 9.81;                 %m/sec^2 Acceleration due to gravity
S_g = 400;                %m Ground Run Distance
C_dto = 0.04;             %Drag Coefficient Take off
C_lto = 1.6;              %Lift Coefficient Take off
Mu = 0.04;                %Drag Coefficient Rolling
n = 2;                    %Turn Load Factor
H_climb = 0;
V_c = 81;                 %m/sec Cruise Velocity
H_c = 1000;               %m Cruise Altitude
C = 3048;                 %m Service Ceiling
v_stall= 20:40;           %m/sec Stall Velocity

%step 1; Oslwalds Span Efficiency
e = 1.78*(1-0.045*AR^0.68)-0.64;

%step 2; Calculating lift induced drag constant k
k = 1/(pi*AR*e);

%step 3; Calculating density 'rho' and dynamic pressure 'q' at Turn condition
rho1 = 1.225*(1-0.0000068756*H_c).^4.2561;
q1 = 0.5*rho1*(V_turn)^2 ;
T_W1 = q1*(CDmin./W_S+k*(n/q1)^2.*W_S);

%step 4; Calculating T/W at Climb condition
q2 = 0.5*1.225*(V)^2;
T_W2 = (V_v/V)+q2./(W_S)*CDmin+k/q2.*(W_S);

%step 5; Calculating T/W at Take off Condition
q3 = 0.5*1.225*((V_lof)/sqrt(2))^2;
T_W3 = (V_lof)^2/(2*g*S_g)+q3*C_dto./(W_S)+Mu*(1-q3*C_lto./W_S);

%step 6; calculating T/W at cruise condition
T_W4 = q1*CDmin*(1./W_S)+k*(1/q1).*W_S;

%step 7; dynamic pressure and T/W at Ceiling condition
rho2 = 1.225*(1-0.0000068756*C)^4.2561;
T_W5 = 0.508./(sqrt((2/rho2).*(W_S)*sqrt(k/(3*CDmin))))+4*(sqrt((k*CDmin)/3));

title('Constraint Diagram (Units: m, m/s, N/m^2)','FontSize',12,'FontWeight','Bold');

%step 8 ;plotting T_W for W_S
hold on; grid on;
```

```
plot(W_S,T_W1,'b-','LineWidth',4);
plot(W_S,T_W2,'r--','LineWidth',4);
plot(W_S,T_W3,'m--','LineWidth',4);
plot(W_S,T_W4,'k-','LineWidth',4);
plot(W_S,T_W5,'k-.','LineWidth',4);

xlabel('Wing Loading, W/S, N/m^2','FontSize',11,'FontWeight','Bold');
ylabel('Thrust Loading, T/W','FontSize',11,'FontWeight','Bold');

%V_Stall%
v_stall_min = min(v_stall); v_stall_max=max(v_stall);
v_stall = v_stall_min:(v_stall_max-v_stall_min)/4:v_stall_max;
rho = 1.225;  %Kg/m^3
q = rho*(v_stall).^2/2;
for i=1:length(v_stall)
 C_L_stall(i,:) = 1/q(i).* W_S;
end

%plot C_L_Stall
[ax,p1,p2]=plotyy(0,0,W_S,C_L_stall);
set(get(ax(2),'YLabel'),'String','C_L_s_t_a_l_l','FontSize',10,'FontWeight','Bold');
set(ax(2),'XLim',xlim,'YLim',[0,3],'YTick',[0 1 1.5 2 2.5 3]); set(ax(1),'XLim',xlim);
set(p2,'LineWidth',1.5); set(p1,'LineStyle','none','Marker','.');
legend({['Turn: v=' num2str(V_turn) ', n=' num2str(n) ', h=' num2str(H_turn)];...
        ['Climb: v_v=' num2str(V_v)  ', v=' num2str(V) ', h=' num2str(H_climb)];...
        ['T-O: L=' num2str(S_g) ', v=' num2str(V_lof)];...
        ['Cruise: v=' num2str(V_c) ', h=' num2str(H_c)];...
        ['Ceiling: h=' num2str(C)];'';...
        ['v_s_t=' num2str(v_stall(1))];['v_s_t=' num2str(v_stall(2))];...
        ['v_s_t=' num2str(v_stall(3))];['v_s_t=' num2str(v_stall(4))];...
        ['v_s_t=' num2str(v_stall(5))]},'Location','NorthWest');

end
```

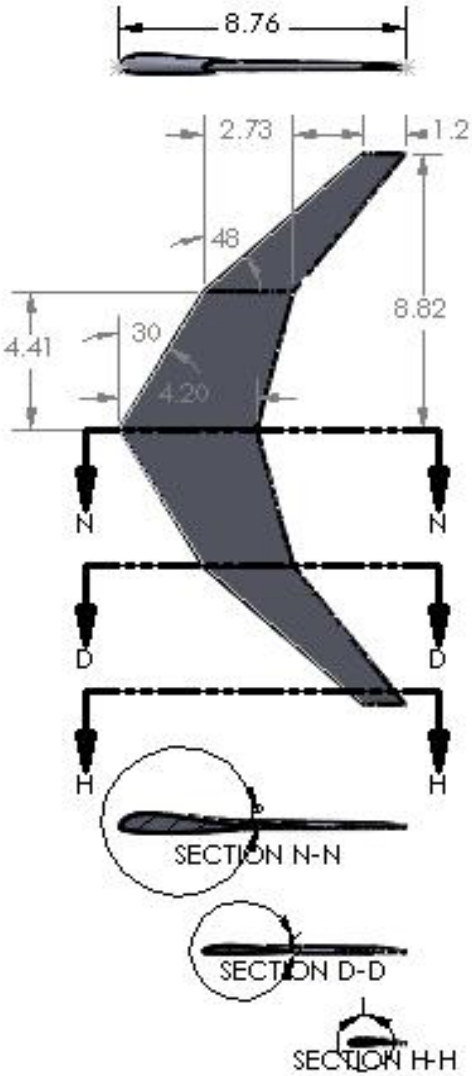

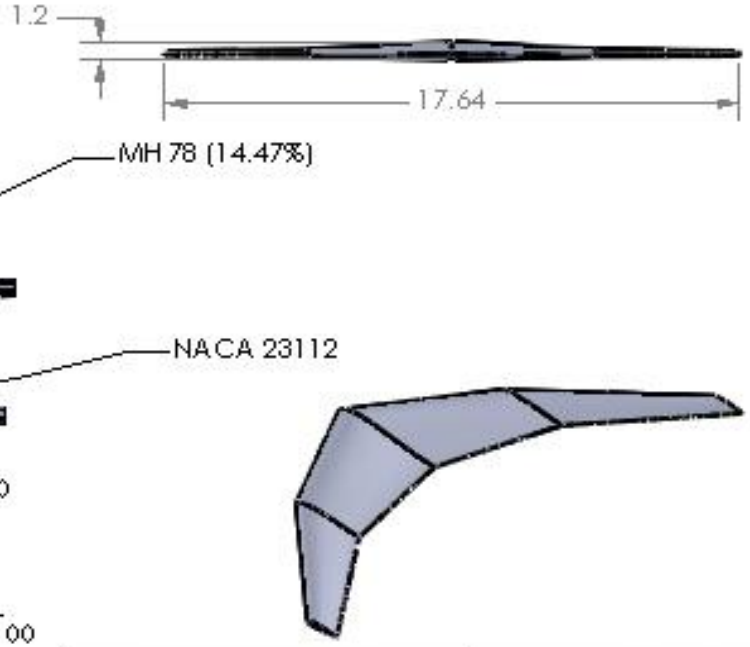

Aircraft Parameter	Value
Wing Loading	500 N/m^2
MTOW	23936.4 N
Wing Area	47.87 m^2
T/W ratio	0.24

Owner	Author	Supervisor	Scale
KTU	Sathvik S Rao	V. Lukoševičius	1:200

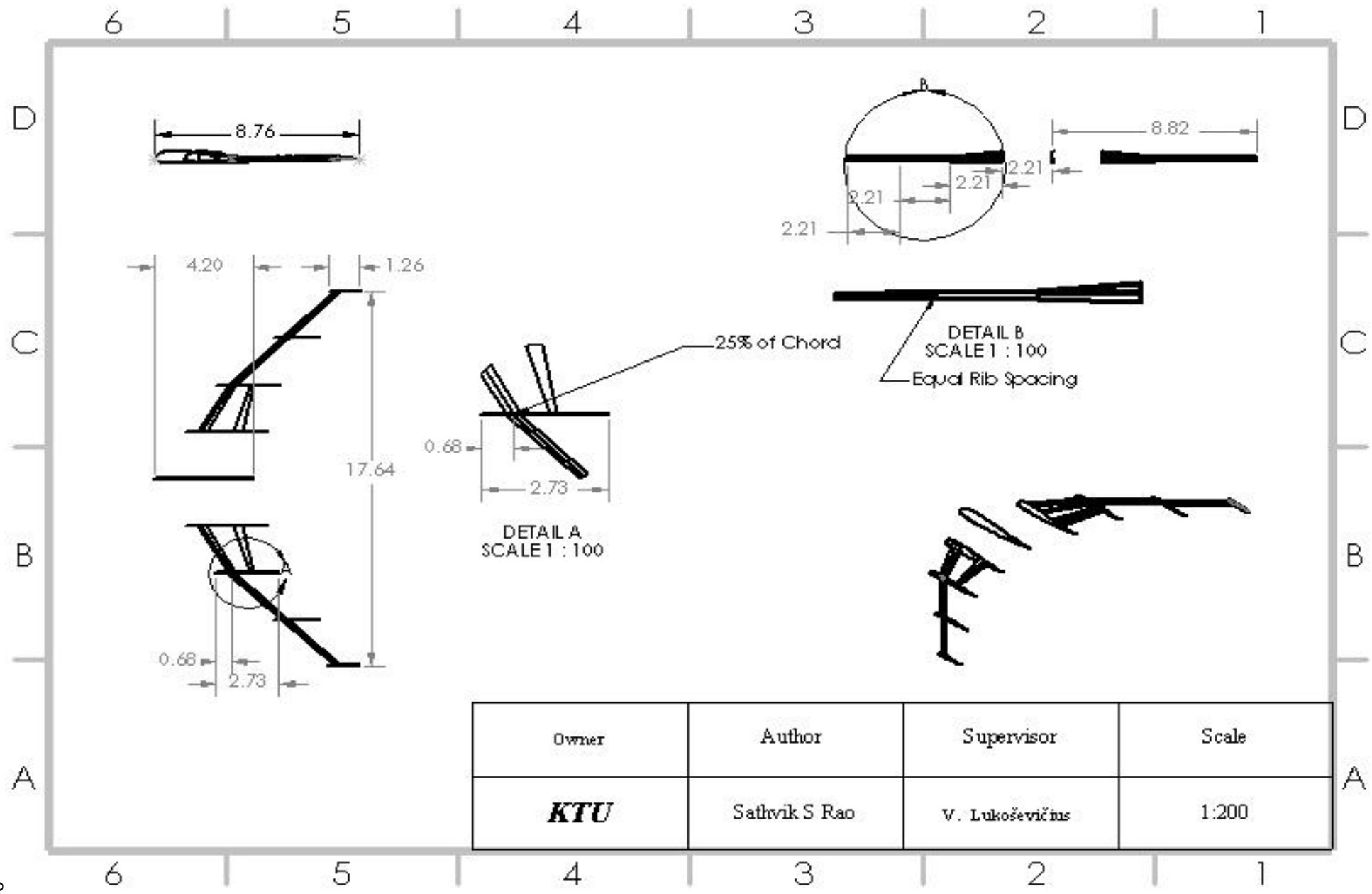

Owner	Author	Supervisor	Scale
KTU	Sathvik S Rao	V. Lukoševičius	1:200

Appendix 4: Aircraft operational concept representation with payloads.

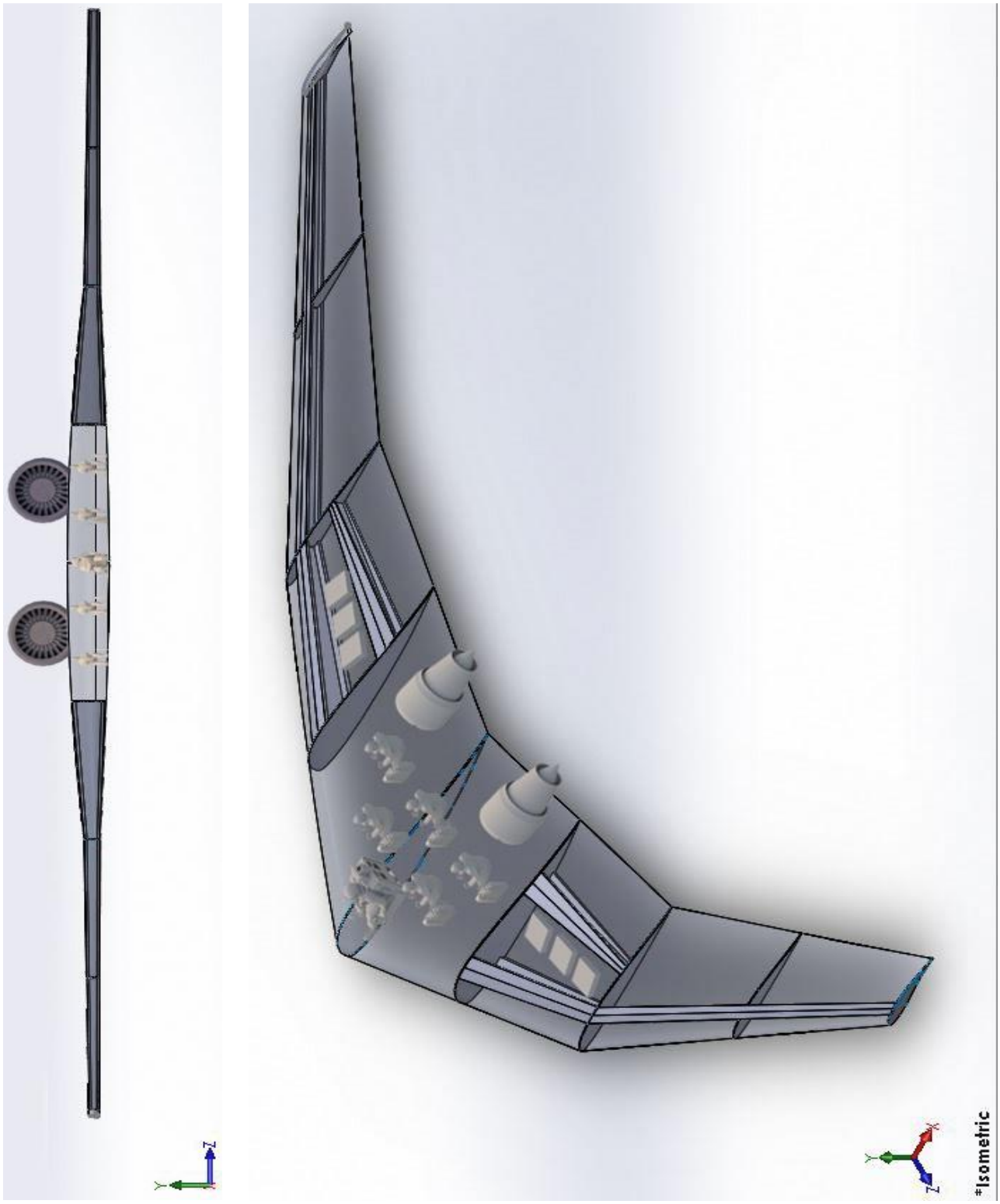

Photo editing tools were used to represent Crew, Passengers, engine, batteries and Passenger baggage.